Water Resources Research Institute
of The University of North Carolina

Report No. 480

PREDICTING WATER QUALITY IMPACTS OF REROUTING DRAINAGE WATER FROM THE PAMLICO SOUND TO RESTORED WETLANDS

By
Tiffany Messer[1], Michael Burchell[2], Francois Birgand[2] and Steven Broome[3]

[1]Nicholas School of the Environment
Duke University
Durham, NC 27708

[2]Dept. of Biological and Agricultural Engineering
North Carolina State University
Raleigh, NC 27695

[3]Dept. of Soil Science
North Carolina State University
Raleigh, NC 27695

UNC-WRRI-480

The research on which this report is based was supported by funds provided by the North Carolina General Assembly and/or the US Geological Survey through the NC Water Resources Research Institute.

This report fulfills the requirements for a project completion report of the Water Resources Research Institute of The University of North Carolina. The authors are solely responsible for the content and completeness of the report.

WRRI Project No. 13-03-W
November 2016

Table of Contents

List of Figures

List of Tables

Predicting Water Quality Impacts of Rerouting Drainage Water from the Pamlico Sound to Restored Wetlands

1. Introduction

Agriculture production is vital to the economy in coastal regions, but its successes continue to place environmental pressures on nearby shellfishing waters and wetland ecosystems. Water drained from agricultural croplands often contains nutrients, sediment, and fecal bacteria. Drainage water from croplands routed directly into coastal rivers and estuaries can contribute to lower quality of shellfishing waters, while the hydrologic alterations can also lower water tables in surrounding wetland ecosystems, resulting in degraded ecosystem structures and increased potential for peat fires (Ardón *et al.,* 2010; Chescheir *et al.,* 1991). Furthermore, N rich drainage water routed into nutrient sensitive terrestrial, freshwater, and marine ecosystems has been found to negatively influence their functionality (Carnicer, *et al.*, 2015; Ribaudo *et al.*, 2011; US EPA, 2010; Matson *et al.,* 1997; Vitousek *et al.*, 1997).

Strategically placed wetland restorations in coastal landscapes have been reported to effectively store water and reduce nutrients, sediment, and fecal bacteria of incoming agricultural drainage water. Restored forested wetlands are one type of wetland that has been found to provide additional water treatment, flood abatement, biodiversity, and carbon storage in coastal regions (Adame *et al.,* 2015). Chescheir *et al.* (1991) investigated the effectiveness of two forested wetlands receiving nutrient rich drainage water in the Albemarle Peninsula of North Carolina. Nitrate-nitrogen (NO_3-N) concentrations were reduced by as much as 97%. Ardón *et al.* (2010) reported that after restoring wetland hydrology and rerouting agricultural drainage water into a formally drained 440 ha forested wetland area in the Albemarle Peninsula of North Carolina, yearly NO_3-N removal rates were 5.98 kg N ha^{-1} yr^{-1}. Therefore, conservation programs that invest resources into strategically positioned wetland restoration projects in agricultural areas could lead to a reversal in both declining wetland ecosystem structure and water quality trends in coastal estuaries.

In the U.S. achieving jurisdictional wetland hydrology is often the primary parameter for wetland restoration projects because of its legal importance for mitigation banking credits and its critical impact on establishing at least some acceptable level of wetland vegetation, saturated soils, and internal plant and microbial processes such as denitrification and carbon sequestration common in natural wetlands (Mitsch, and Gosselink, 2007; Caldwell, 2007). Traditional Natural Resource Conservation Service (NRCS) wetland restoration designs in coastal regions of North Carolina typically include plugging of drainage ditches, constructing berms to impound water, installing water control structures (e.g., flashboard risers), and surface topography manipulations to help restore minimal jurisdictional wetland hydrology (Jarzemsky *et al.,* 2013; Tweedy *et al.,* 2001). Additional techniques in wetland restoration projects (e.g., berm construction, surface topography manipulations, substrate nutrient and chemical modifications, native plants reestablishment) are often employed to help natural processes that once existed develop quickly to speed the rate of recovery in degraded ecosystems (Dobson *et al.*, 1997). While this can be an effective practice for restoring the wetland hydroperiod and habitat, this type of design does not always maximize the potential of the restoration to improve water quality of downstream ecosystems.

Natural, restored, or enhanced wetlands have been used to treat agricultural drainage water with significant concentrations of NO_3-N with varied success. Nitrate-nitrogen (NO_3-N) removal rates in restored wetlands receiving NO_3-N rich waters are variable. Beutel *et al.* (2009) observed NO_3-N removal rates in a surface-flow constructed wetland receiving agricultural runoff to range from 139 to 146 mg N m^{-2} d^{-1} with inflow NO_3-N concentrations of 1 to 3 mg L^{-1}. Karpuzcu and Stringfellow observed removal rates as high as 350 mg N m^{-2} d^{-1} in a study of NO_3-N reduction in wetlands receiving agricultural drainage water. However, Bachand and Horne (1999) observed NO_3-N removal rates as high as 2800 mg N m^{-2} d^{-1} in a macrocosm constructed free-water surface wetland study receiving NO_3-N concentrations of 8 NO_3-N mg L^{-1}.

Nitrogen cycling in wetlands involve complex physical and microbial processes. Variability of wetland nutrient removal effectiveness depends on factors such as wetland to watershed ratio, soil type, wetland ecosystem type, residence time, and hydraulic and nutrient loading rates (Arheimer and Wittgren, 2002; Zedler, 2003; Woltermade, 2000). Primary NO_3-N removal processes in wetland systems include denitrification and plant uptake. Denitrification, a microbially mediated transformation of NO_3-N to nitrogen gas (Hunter *et al.,* 2001; Reddy *et al.,* 1989), has been identified as the primary NO_3-N removal pathway within wetland systems. However, removal through denitrification is limited if the soil/water interface does not provide ideal conditions such as low soil redox, carbon availability, and suitable pH and temperatures. Plant uptake has generally been assumed the second most important removal mechanism for NO_3-N reduction in wetlands, because as plants die, mineralization of the tissues can reintroduce sources of N to the wetland and downstream (Tanner *et al.,* 2002).

Ideally, wetland performance evaluations should be conducted prior to the development of water management plans for wetland systems receiving N rich water. However, several researchers have attempted to establish nutrient management plans at the field scale after pumping to those areas began., often leading to challenges in evaluating the maximum nutrient removal potential and tracing NO_3-N transformations occurring within these systems (Bruland *et al.,* 2006; Chescheir *et al.,* 1991). Results of these studies indicated the need to use a controlled mass balance approach to improve predictions of NO_3-N transformations within full-scale wetland systems (Kangas and Adey, 1996), prior to initiating loading. Additionally, further research to determine the impact of the varying conditions that affect NO_3-N removal rates within wetland systems is critical to develop more efficient wetland management strategies.

Mesocosms are useful tools to accomplish this. The allow researchers to examine nutrient transformations within a controlled system and several studies have found mesocosms to adequately model full-scale wetlands for NO_3-N reduction. Ahn and Mitsch (2002) did not observe significant differences in the degree of mixing and effects on water quality improvement in a study comparing mesocosms to full-scale wetland evaluations on a 1:10,000 scale. Additionally, Bachand and Horne (2000) concluded that wetlands could be adequately modeled with macrocosms to determine NO_3^--N reductions compared to full-scale wetlands and found no significant differences on a 1:1,000 scale. The few discrepancies observed between coupled mesocosm to full-scale studies have found them to underestimate NO_3^-N reductions (Ahn and Mitsch, 2002; Bachand and Horne, 2000). Therefore, mesocosms may actually provide conservative estimates of NO_3-N treatment due the spatial heterogeneity (e.g.,

light penetration, plant density, hydraulic conductivity) in full-scale wetlands that often provide additional NO_3-N removal potential (Bírgand *et al.*, 2007).

NO_3-N removal potential of two wetland restoration projects in eastern North Carolina that could be used to treat agricultural drainage water were evaluated in this study. These sites have two distinct soil types in terms of nutrients, carbon, texture, and pH, all of which have been shown to influence NO_3-N removal via microbial processes or plant uptake (Puckett *et al.*, 2004; Engles and Marschner, 1995). At one of the sites situated in Hyde County, NC, the restoration plan called for pumped NO_3-N rich drainage water to enter a degraded wetland ecosystem to reduce the volume of NO_3-N rich water pumped to the nutrient sensitive Pamlico Sound. Stakeholders requested predictions of NO_3-N removal rates within the future restored wetlands. The second site was situated downstream from a major agricultural facility in Carteret County, NC and buffers the North River Estuary. It was in a landscape position that could be ideal for drainage water treatment, so a clearer understanding of the NO_3-N removal potential of this site will help those stakeholders determine if water treatment should be a goal of the restoration plan.

1.1 Objectives

A laboratory study was conducted to identify nitrogen removal potential (particularly NO_3-N) for two distinct wetland restoration sites with different soils. The wetland mesocosms were loaded with soils from both sites, planted, and allowed to establish. The impact of the soils (nutrients, bulk density, pH) along with season, N load, water temperature, and antecedent soil moisture conditions on NO_3^-N removal rates were investigated. We hypothesized that removal in the Scuppernong (organic soil) wetlands would perform better than the Deloss (mineral soil) wetlands because of its significantly higher carbon availability (α=0.05), which is often the primary limiting agent for microbial removal of NO_3-N in restored and constructed wetland systems (Warneke *et al.*, 2011; Burchell *et al.*, 2007). Primary objectives of the study included:

1. Utilize mesocosm-scale wetlands with restoration site soils receiving NO_3^-N rich drainage water to quantify the NO_3^-N removal rates under varying seasonal, N loading, and antecedent soil moisture conditions.
2. Compare NO_3^-N removal rates between two distinct wetland soil types and explore if differences do exist.
3. Determine potential causes for differences between treatments if they exist.
4. Improve our understanding of hourly nitrogen and carbon cycling within these systems with advanced analytical techniques using real time UV-Vis spectrometry.
5. Create a dataset of NO_3-N removal observations over varying season, N loading, and antecedent conditions for two wetland environments at the mesocosm scale,
6. Evaluate the fit of five NO_3-N removal models (the zero order, first order, efficiency loss, tanks in series, and Monod) with observed NO_3-N removal observations
7. Quantify the impact of plant and microbial assimilation (temporary removal) and denitrification (complete removal) on NO_3-N removal rates in two distinct wetland environments.
8. Provide predictions for the maximum drainage water volumes that can be pumped into the restored wetlands based on the kinetic model that best fit observed NO_3-N removal datasets

The goal of this report is to summarize the major results and impacts of this study. Additional details can be found in the Ph.D. dissertation of Messer (2015) available on-line at http://www.lib.ncsu.edu/resolver/1840.16/10634.

2. Materials and Methods

2.1 Wetland Mesocosm Setup for Batch Study Experiments

Six large wetland mesocosms (3.5 m long X 0.9 m wide X 0.75 m deep) were constructed in a greenhouse near North Carolina State University 16 months prior to the initial experiment (Figure 1). Three randomized mesocosm replicates were loaded with Deloss soil from Carteret Couty, a poorly drained, mineral soil typically associated with marine terraces (fine-loamy, mixed, semiactive, thermic Typic Umbraquults), while three more were loaded with Scuppernong soil from Hyde County, a poorly drained, organic soil typically associated with Pocosin wetlands (loamy, mixed, dysic, thermic Terric Haplosaprists). Three smaller mesocosms that did not have soil served as controls for the experiments.

The climax forested wetland ecosystems expected at each restoration site was impossible to replicate at the mesocosm scale. Therefore, in early May 2011, the wetland mesocosms, with the exception of the controls, were planted with a monoculture of soft-stemmed bulrush (*Schoenoplectus tabernaemontani*) obtained from a greenhouse (Mellow Marsh Farms, Siler City, NC). Soft-stemmed bulrush was chosen because other researchers have successfully utilized this plant to simulate wetland nutrient dynamics at the mesocosm scale (Burchell *et al.*, 2007; Kadlec *et al.*, 2005). Additionally, the above and below ground biomass of *S. tabernaemontani* can establish quickly with careful attention to the plant requirements. The bulrush was planted on 15 cm centers, or approximately 125 plants per mesocosm. During the remainder of 2011 and into the fall of 2012, the plants were allowed to establish under saturated to inundated conditions.

A recirculation system was installed in each mesocosm to simulate the conditions of drainage water slowly moving through the wetland. The systems consisted of 13 mm Schedule 40 PVC distribution system connected to a Rio Plus 180 mini head pump (TAAM Inc.,CA), which was adjusted to allow drainage water to turnover once a day. To determine if soil redox values were at levels conducive for denitrification, platinum-tipped probes were constructed as described by Wafer *et al.* (2004), and installed in replicates of 5 at soil depths of 5 and 15 cm within each mesocosm.

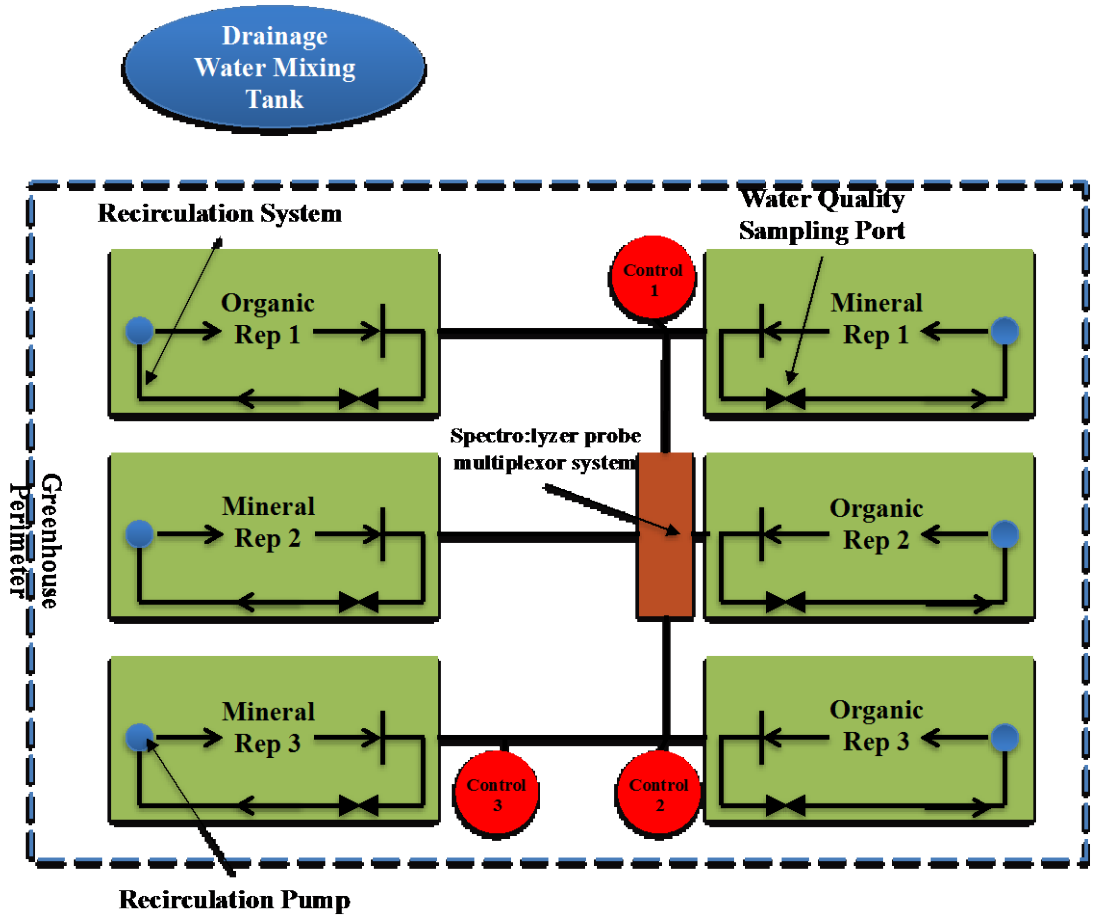

Figure 1: Wetland mesocosm experimental setup.

Few water quality studies collected continuous measurements of water chemistry due to budget limitations or logistics. Continuous measurements can be important in minimizing errors, and can provide insightful information on fluctuations of pollutant concentrations that may occur between infrequent sampling events. Bírgand *et al.* (2010) demonstrated that daily or weekly sampling can lead to large calculation errors (20% or more) in mass transport of chemicals such as NO_3-N, and limits the understanding of the biogeochemical factors that govern changes in chemical concentrations at the watershed outlet. Likewise, Jollymore *et al.* (2012) found that weekly measurements underestimated exports of dissolved organic carbon (DOC) by 30% compared to continuous measurements at the watershed outlet. To evaluate the importance of frequent measurements in this study and to advance the techniques typically used in mesocosm experiments, a Spectro::Lyzer automatic UV-Vis spectrometer probe (S::CAN company-Vienna, Austria) was connected to a multiplexor pumping system and controlled with a Arduino programmable logic controller (PLC) (Ivrea, Italy) that allowed measurements of NO_3-N and DOC to be made in all mesocosms at hourly intervals.

2.1.1 Wetland Mesocosm Batch Experiments

Eighteen experiments were conducted between September 2012 to September 2014 to evaluate NO_3-N removal across season and at variable loading rates. The experiments were conducted as batch studies, with each mesocosm loaded at constant hydraulic and nutrient loading rates (Table 1). Initial NO_3-N concentrations were varied throughout the batch studies,

with target concentrations based on those commonly observed in agricultural drainage water near the two restoration sites (2.5-10 mg L^{-1}). A base target load of 0.6 g NO_3-N m^{-2} which corresponded to an 18 cm water depth and 2.5 mg L^{-1} NO_3-N concentration was chosen because observations at the future restoration sites suggested the restored wetland loadings will be most frequently near this level. Additional batch runs were completed with target loads varying between of 0.9 g NO_3-N m^{-2} and of 3.6 g NO_3-N m^{-2} and water depths of 18 to 30 cm. Each batch study lasted 7 to 10 days.

Table 1: Summary of wetland mesocosm batch studies.

Season	Date	Experiment Period	Water Depth Prior to Loading	Water Depth After Loading	Target NO_3—N	Target NO_3—N Load
		Days	cm		mg L^{-1}	g N m^{-2}
Fall	9/25-10/4/12	10	4	30	2.5	0.9
Fall	10/16-10/26/12	10	4	18	5	0.9
Fall	11/5-11/15/12	10	18	30	10	2.2
Fall	9/24-10/4/13	10	4	30	10	3.6
Fall	10/15-10/25/13	10	4	18	2.5	0.6
Fall	9/2-9/9/14	7	-5†	20	2.5	0.9
Winter	1/22-2/1/13	10	4	15	2.5	0.6
Winter	2/11-2/21/13	10	4	18	5	0.9
Spring	5/28-6/7/13	10	4	18	2.5	0.6
Spring	4/8-4/18/14	10	4	18	5	0.9
Spring	4/21-5/1/14	10	4	30	10	3.6
Spring	5/27-6/6/14	10	4	30	2.5	0.9
Summer	7/2-7/12/13	10	4	30	2.5	0.9
Summer	8/6-8/16/13	10	4	30	5	2.0
Summer	8/20-8/27/13	7	4	30	2.5	0.9
Summer	6/13-6/20/14	7	4	18	2.5	0.6
Summer	7/22-8/1/14	10	4	30	10	3.6
Summer	8/12-8/19/14	7	4	18	5	0.9

† - Negative value indicates water level below wetland surface

Artificial agricultural drainage water was mixed onsite in a 3,785 L tank using technical grade calcium nitrate decahydrate. After the tank was filled with water, the chemical was added and thoroughly mixed for 5-10 minutes to evenly distribute the NO_3-N. Following mixing, a grab sample was taken from the tank for water quality analysis. Simulated drainage water was then pumped into each mesocosm using a gasoline powered pump. An in-line flow meter measured the exact volume applied to each mesocosm to precisely determine NO_3-N loads applied to individual mesocosms.

2.1.2 Water Quality Sampling and Analysis

Grab water quality samples were collected from the recirculation system on days 0, 1, 2, 3, 5, 7, and in 14 of 18 batches, day 10. Samples were analyzed for NO_3-N, dissolved organic carbon (DOC), Total Kjeldahl Nitrogen (TKN), ammonium-N (NH_4-N) and chloride (Cl^-). Organic-N (ON) was determined as the difference in measured TKN and NH_4-N values. All water quality samples were filtered through 0.45 μm filters. NO_3-N and NH_4-N water grab samples were evaluated at the Soil Science Environmental and Agricultural Testing Laboratory (SSC-EATS Lab) in Raleigh, NC with a Quikchem 8000 (Lachat, Milwaukee, WI). Measurements of NO_3-N concentrations were made using the cadmium reduction method.

DOC, TKN, and Cl^- grab samples were evaluated by the North Carolina State University Biological and Agricultural Engineering Environmental Analysis Test Service Laboratory (BAE EAL) in Raleigh, NC using the High-Temperature Combustion Method (Van Hall *et al.*, 1963) and a Teledyne Techmar Apollo 9000 (Mason, OH), the acid digestion and ammonia salicylate method for automated analysis (EPA Method 351.2, 1979), and the ferricyanide method for automated analysis (EPA Method 325.2, 1979), respectively.

While these parameters were needed to study the fate of N within the wetland systems, NO_3-N, and DOC samples were also used to calibrate the UV-Vis spectrometer. NO_3-N and DOC concentrations were measured hourly from the six wetland mesocosms and three controls using the UV-Vis spectrometer accompanied with a PLC system (Figure 2). Each mesocosm had 0.3175 cm plastic tubing in the water column that was connected to the multiplexor system. A program uploaded onto the PLC controller was developed to switch on a peristaltic pump and open one dedicated solenoid valve at a time for water quality sampling of each mesocosm. Samples were sent to a 4 mm quartz cuvette positioned between the measurement window of the spectrometer for analysis. The entire system was flushed with the new incoming sample 15 seconds prior to the reading. Once the spectrometer reading was completed, the peristaltic pump would reverse pumping direction and route water back into the mesocosm. Each sample period took approximately 3 minutes from start to finish. The cuvette was serviced at maximum intervals of every 48 hr to prevent loss of data from fouling. During the service the cuvette was soaked in oxalic acid solution for up to 10 min before being rinsed with deionized (DI) water. Data stored on the spectrometer was also offloaded onto a field computer (Acer Inc., Taiwan) on regular intervals.

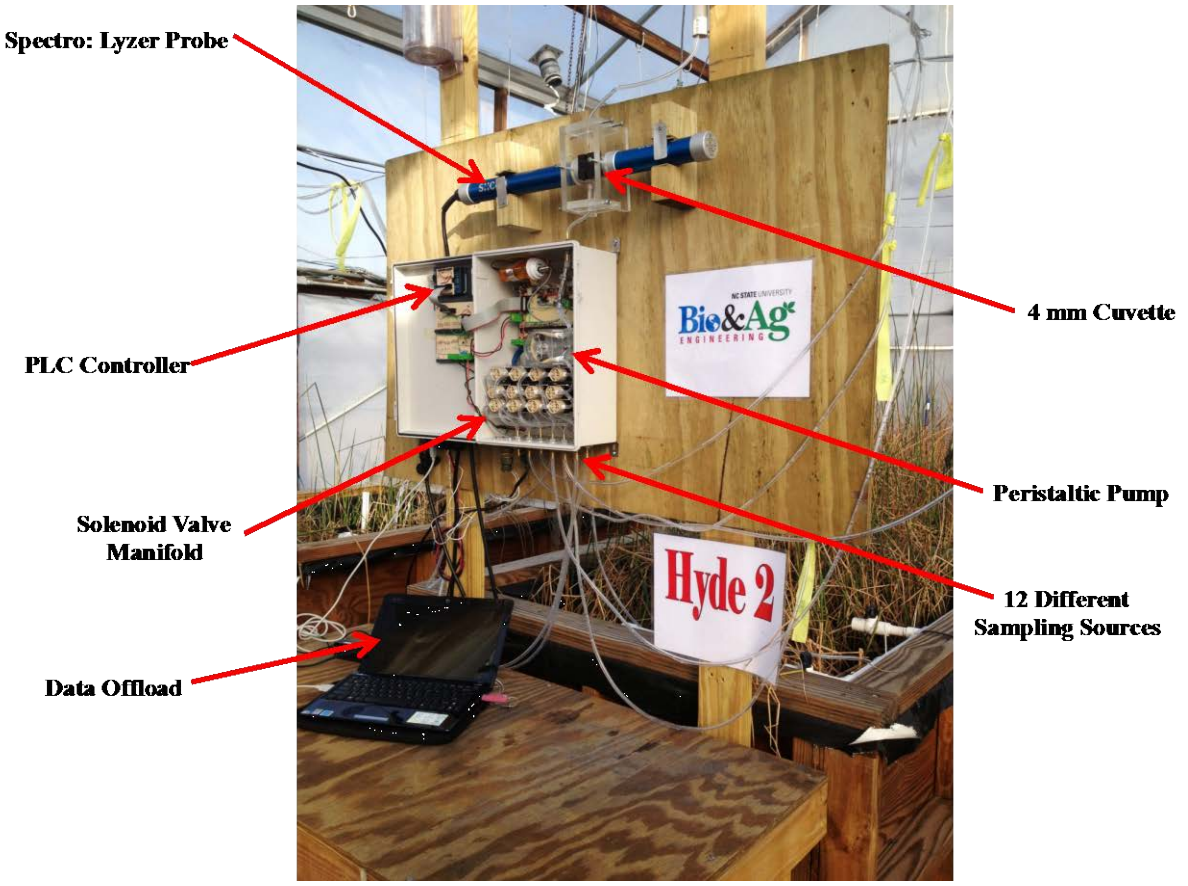

Figure 2: Spectro::Lyzer automatic UV-Vis spectrometer probe field setup.

pH and dissolved oxygen (DO) were measured within the water column on grab sample days to evaluate daily changes. A Y60500 YSI® Professional Plus Multiparameter Instrument connected with a Y6124C YSI® Dual ISE/Dissolved Oxygen/Temp Cable with a Y6203 YSI® Polarographic Dissolved Oxygen Probe (Yellow Spring, OH) attached was used to measure dissolved oxygen (DO). pH was measured with a Mettler Toledo™ SevenGo™ pH portable field meter (Columbus, OH). Additionally, water temperature in the wetland mesocosms were monitored hourly using 8k HOBO pendant temperature sensors (Onset Computer Corporation, Bourne, MA).

The impact of evapotranspiration on water chemistry was taken into account based on the changes in the water depth measured on a stage gage in each mesocosm and Cl^- concentrations over the course of each experiment. N species and DOC concentrations were then adjusted to account for water loss through evapotranspiration.

NO_3-N and NH_4-N concentration profiles above and below the sediment-water interface were evaluated at 1 cm intervals within the water and soil column of the wetland mesocosms two days after a NO_3-N loading event during one experiment (Batch 18) in the summer of 2014 using two dialysis porewater samplers (Bírgand, 2000; Hesslein, 1976). Samplers allowed concentration profiles to be assessed by establishing equilibrium between surrounding water and the water in the sampler using a dialysis membrane. The samplers were installed in the mesocosm systems for 120 hours. Following removal from the mesocosms, each slot was sampled through the membranes using a hypodermic needle and syringe and transferred into 5 mL glass vials. A total of 60 samples were analyzed (30 from one mineral

and 30 from one organic wetland mesocosm) at the Soil Science Environmental and Agricultural Testing Laboratory with a Quikchem 8000 (Lachat, Milwaukee, WI).

2.1.3 Wetland Substrate and Biomass Sampling and Analysis

Analyses of wetland plant biomass and soils in each mesocosm were completed to determine average nitrogen and carbon content in these pools. Samples were taken at the beginning and completion of each growing season. Above ground and below ground biomass were collected from a 30 cm x 30 cm clip plot within each mesocosm, and were washed, oven dried, and ground for analysis at the end of each growing season. Biomass was analyzed for %N, %C, and residual moisture content by the BAE-EAL and SSC-EATS Lab to estimate these nutrient pools in the emergent macrophytes. Soil cores were collected at 0-15 cm and 15-30 cm depths at the beginning and end of each growing season and were oven dried, ground, and passed through a 1 mm sieve. Soil cores were analyzed for %N, %C, residual moisture content, and other critical nutrients at the NCDA Soil Test Lab (Raleigh, NC) and SSC-EATS Lab.

Soil conditions in the field-scale restored wetlands will be variable prior to receiving pumped drainage water, which will impact N removal rates. Therefore, antecedent soil moisture conditions/redox status was measured prior to each batch study. Additionally, soil redox readings were measured in each mesocosm on grab water quality sampling days during batch studies using an Accumet AP63 portable pH/mV meter (Fisher Scientific ®, Pittsburgh, Pa) attached to the redox lead and a portable KCl-saturated Ag/AgCl reference electrode (Jensen Instruments, Tacoma, WA) inserted in the wetland soil. Five readings at each depth were averaged to represent the redox condition at each depth within the mesocosms. Measurements were then adjusted using a correction factor of 204 mV (Richardson and Vepraskas, 2001).

2.1.4 NO_3-N Removal Rates (J_{NN})

NO_3-N removal rates over the 7 to 10 day experiment periods were determined based on initial and final NO_3-N concentrations and volume of simulated agricultural drainage water applied and remaining at the completion of the experiment (Eq. 1).

$$J_{NN} = \frac{(N_{Applied} - N_{Remaining})}{A * t} \quad \textbf{Eq. 1}$$

where, $N_{Applied}$ was the applied NO_3-N load (mg), $N_{Remaining}$ was the NO_3-N remaining in the mesocosm water column at the completion of the experiment (mg), A was the surface area of the wetland mesocosm (m^2), and t was the time period of the experiment (d).

Equation 3.1 assumed a zero order removal rate. Therefore, to identify a range in NO_3-N removal rates throughout the batch studies, removal rates were evaluated between each grab sampling day (Days 1 to 2, 2 to 3, 3 to 5, 5 to 7, and 7 to 10) with Eq. 2.

$$J_{NN} = \frac{(N_{Sample1} - N_{Sample2})}{A * t} \quad \textbf{Eq. 2}$$

where, $N_{Sample1}$ was the NO_3-N load at previous sampling point (mg), $N_{Sample2}$ was the NO_3-N remaining in the mesocosm water column at the following sampling point of the experiment (mg), A was the surface area of the wetland mesocosm (m^2), and t was the time period (d) in between successive sampling periods, and varied for 1 to 3 days.

2. 1.5 Statistical Data Analysis

Multivariate statistical analyses were completed to determine differences in NO_3-N reductions between the two-wetland soil treatments and the controls over time using linear mixed effects model in SAS glimmix® (SAS Institute, Cary, NC):

$$Y_{ijk}=\mu+\alpha_i+\beta_j+\alpha\beta_{ij}+\varepsilon_{ijk} \quad \textbf{Eq. 3}$$

where, μ is the overall mean response, α_i is the fixed effects, β_j are the random effects, $\alpha\beta_{ij}$ are the random effects due to interactions, and ε_{ijk} is the error unaccounted for by the effects. *i* was the treatment type (Mineral, Organic, Control), *j* was time, and *k* was the replication (1, 2, 3). Variability in NO_3-N concentrations between treatments was adjusted using the following equation to allow for comparisons to be made between replicates and treatments with slightly different initial NO_3-N concentrations:

$$y'(t)=\frac{y(0)}{y(t)} \quad \textbf{Eq. 4}$$

where y'(t) was the ratio of the analyte concentration at time t (y(t)) and the initial analyte concentration (y(0)). The overall mean response of each analyte was then evaluated. The effects of treatment, season, and N loading, were assessed utilizing Tukey honest significance tests in SAS glimmix®. All statistical tests were considered significant at α=0.05.

2.2 Evaluation of Appropriate Models to Predict NO_3-N Removal

Five models were considered to predict NO_3-N removal (Figures 3 and 4): zero order (ZO), first order (FO), efficiency loss (EL), tanks in series (TIS), and Monod (M). Observations from nine of the eighteen completed batch run studies were used to determine removal rate coefficients. Coefficients were calculated using NO_3-N concentrations 24 hours following NO_3-N loading (t_1, to allow initial concentrations to stabilize in each mesocosm) and final NO_3-N concentrations (t_f) for each model. The kinetic model fits were then evaluated (validated) using the remaining nine experimental datasets from the batch run studies (Bowie *et al.* 1985).

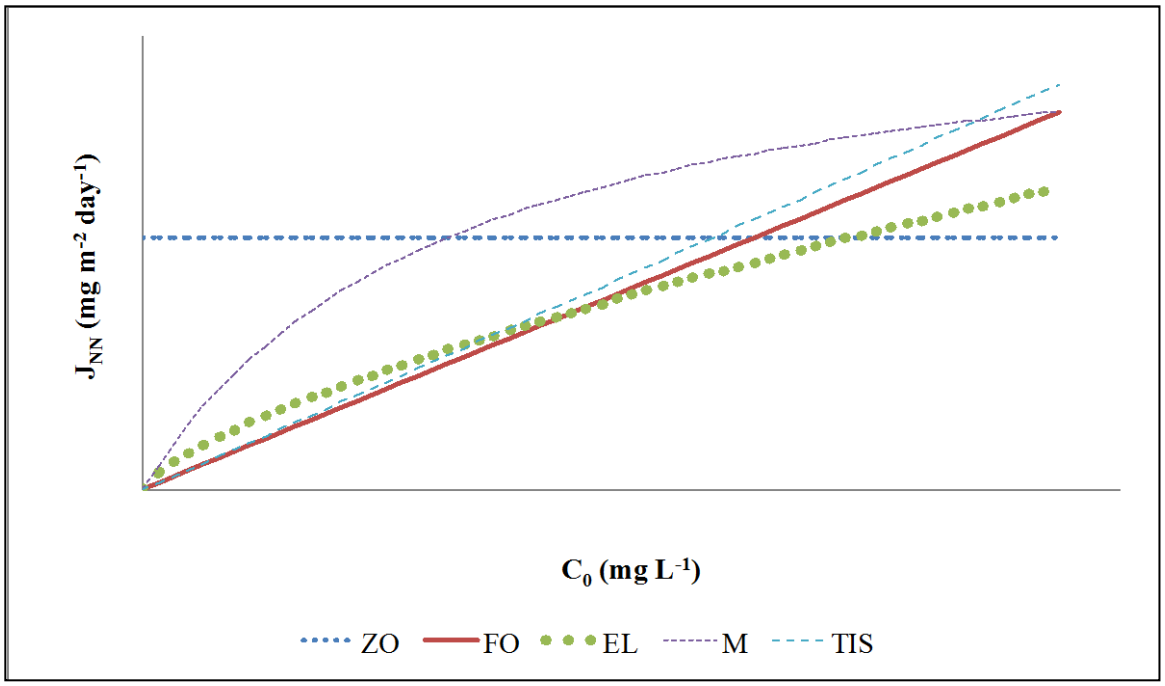

Figure 3: Comparison of the five evaluated models relationship with NO_3-N removal rate (J_{NN}) and initial NO_3-N concentration over time (C_o). Scales are linear. Values presented are theoretical and not meant to represent observed NO_3-N removal in this study.

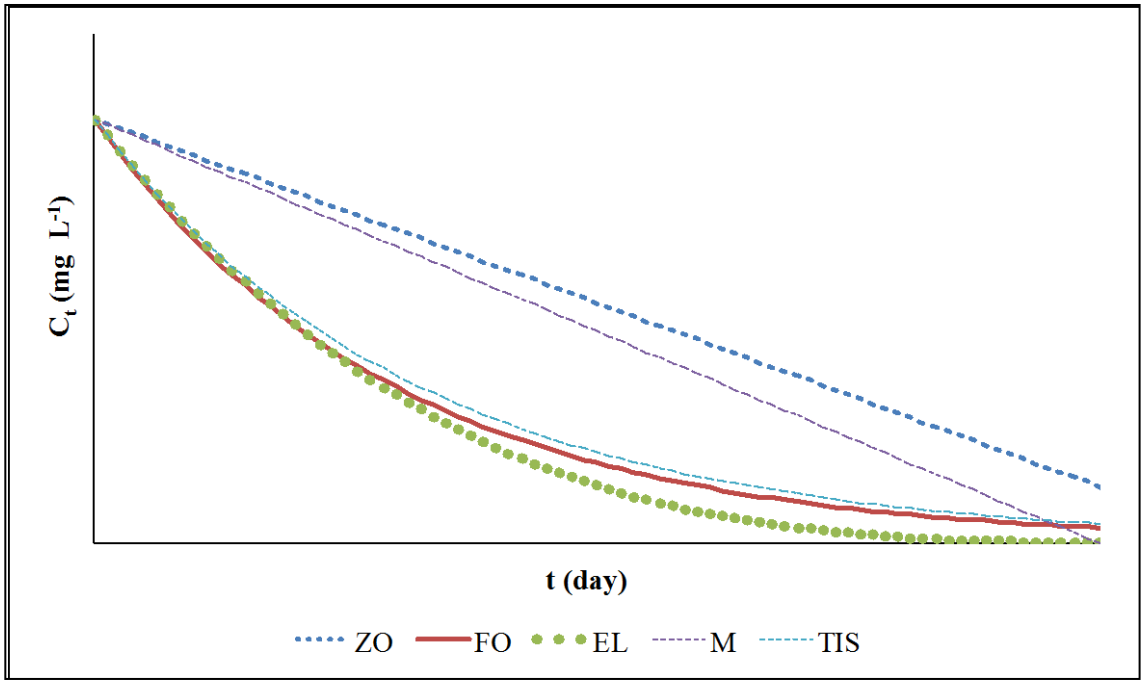

Figure 4: Comparison of the five evaluated models relationship with the NO_3-N concentration over time (C_t) and hydraulic retention time (t). Values presented are theoretical and are not meant to represent observed NO_3-N removal in this study.

Table 2: NO_3-N Removal Kinetic Model Overview. Descriptions of models can be found in Appendix 1.

Acronym	Model	Equation	Variables
ZO	Zero Order	$J_{ZO} = \frac{(C_1 - C_t) * D}{t}$	C_1 was the NO_3-N concentration in the wetland mesocosm 24 hours after simulated drainage was added to allow the system to be well mixed (mg L^{-1}) C_t was the NO_3-N concentration at end of the analysis (mg L^{-1}) t was the residence time from 24 hours after simulated drainage water was added to the system (Day 1) to the final sampling day (Day 10 or the last sampling day where C_t>0.05) D was water depth (m)
FO	First Order	$\rho_{FO} = -\left(\frac{D * ln\frac{C_t}{C_1}}{t}\right)$	ρ_{FO}, the mass transfer coefficient (cm d^{-1}) C_1 was the NO_3-N concentration in the wetland mesocosm 24 hours after simulated drainage was added to allow the system to be well mixed (mg L^{-1}) C_t was the NO_3-N concentration at end of the analysis (mg L^{-1}) t was the hydraulic retention time from 24 hours after simulated drainage water was added to the system (Day 1) to the final sampling day (Day 10 or the last sampling day where C_t>0.05) D was water depth (m)
EL	Efficiency Loss	$\rho_{EL} = \left(\frac{(C_t)^{1-\alpha} - C_1^{1-\alpha}}{t}\right)^{\left(\frac{1}{\alpha-1}\right)} D$	ρ_{EL} was the mass transfer coefficient (cm d^{-1}) α was a unitless constant that varies between 0 and 1, D was water depth (cm) C_1 was the NO_3-N concentration in the wetland mesocosm 24 hours after simulated drainage was added to allow the system to be well mixed (mg L^{-1}) C_t was the NO_3-N concentration at end of the analysis (mg L^{-1}) t was the hydraulic retention time from 24 hours after simulated drainage water was added to the system (Day 1) to the final sampling day (Day 10 or the last sampling day where C_t>0.05)
TIS	Tanks in Series	$\rho_{TIS} = \frac{\left(\left(\frac{C_t}{C_1}\right)^{-\frac{1}{N}} - 1\right) ND}{t}$	ρ_{TIS} was the mass transfer coefficient (cm d^{-1}) C_1 was the NO_3-N concentration in the wetland mesocosm 24 hours after simulated drainage was added to allow the system to be well mixed (mg L^{-1}) C_t was the NO_3-N concentration at end of the analysis (mg L^{-1}) t was the hydraulic retention time from 24 hours after simulated drainage water was added to the system (Day 1) to the final sampling day (Day 10 or the last sampling day where C_t>0.05) N was the number of tanks D (cm) is the water depth

Table 2cont.: NO_3-N Removal Kinetic Model Overview. Descriptions of models can be found in Appendix 1.

M	Monod	$J_M = \frac{J_{max} * C_o}{K_s + C_o}$	J_M was the area based NO_3-N loss rate (mg m^{-2} d^{-1}) J_{max} was the maximum removal rate achieved by the system (mg m^{-2} d^{-1}) C_o (mg L^{-1}) was the initial NO_3-N concentration K_s (mg L^{-1}) was the half saturation constant

2.2.2 Temperature Adjustment of Removal Rate Coefficients

The effect of temperature on the estimated removal coefficients of each batch run (J or ρ) was determined using a modified Arrhenius relationship (Dzakpasu *et al.,* 2011):

$$X = X_{20}\theta^{(T-20)} \qquad \textbf{Eq. 5a}$$

where, X was either J, the area based NO_3-N loss (mg m^{-2} d^{-1}) at temperature T (°C), or ρ, the mass transfer coefficient (cm d^{-1}) at temperature T (°C), X_{20} was either J_{20}, the area based NO_3-N loss (mg m^{-2} d^{-1}) at 20°C, or ρ_{20}, the mass transfer coefficient (cm d^{-1}) at 20°C, and θ was an empirical temperature coefficient. A linear form was used to estimate J_{20} and ρ_{20} for each treatment using first 9 of the 18 batch run datasets:

$$\log(X) = \theta\log(T - 20) + \log(X_{20}) \qquad \textbf{Eq. 5b}$$

values of log(X) versus (T-20) were plotted and fit with a linear regression, where the slope and intercept were log θ and log (X_{20}), respectively.

2.2.3 Statistical Evaluation of Model Fit

The accuracy and the reliability of the five models for predicting NO_3-N removal rates, were compared utilizing six statistical parameters that are described in Table 3 (Naz *et al.*, 2009; Youseff *et al.,* 2006): coefficient of determination (R^2), relative root mean square error (RRMSE), model efficiency (MEF), mean error (ME), mean absolute error (MAE), and the normalized percent error (NPE). The statistical parameters were used to evaluate the correlation, differences, variations, and forecast error between the predicted and measured NO_3-N removal rates only in the 9 batch studies that were used to validate the removal rate models.

Table 3: Statistical parameters evaluated for each kinetic model (Saeed and Sun, 2012; Janssen and Heuberger, 1995).

Acronym	Parameter	Definition	Range	Increased strength as approaches:	Equation
R^2	Coefficient of determination:	Measures the extent of linear correlation between two datasets.	0-1	1	$\frac{\lvert\sum_{i=1}^{n}(P_i-\bar{P})^2(O_i-\bar{O})^2\rvert}{\sum_{i=1}^{n}(P_i-\bar{P})^2\sum_{i=1}^{n}(O_i-\bar{O})^2}$
RRMSE	Relative root mean square error:	Measures the differences between the predicted and the measured values.	0 - ∞	0	$\frac{\sqrt{\frac{1}{n}\sum_{i=1}^{n}(P_i-O_i)^2}}{\bar{P}}$
MEF	Model efficiency:	Measures the variations accounted for by the model.	-∞ to 1	1	$1-\frac{\sum_{i=1}^{n}(P_i-O_i)^2}{\sum_{i=1}^{n}(P_i-\bar{P})^2}$
ME	Mean error:	Measures bias in the average values of the model to predictions and observations.	-∞ - ∞	0	$\frac{\sum_{i=1}^{n}(P_i-O_i)}{n}$
MAE	Mean absolute error:	Measures the forecast error in a time series.	0 - ∞	0	$\frac{\sum_{i=1}^{n}\lvert P_i-O_i\rvert}{n}$
NPE	Normalized Percent Error:	Measures the percent ratio of the observed value to the predicted value	-100-100	0	$100\,X\frac{\bar{P}-\bar{O}}{\bar{P}}$
P_i = predicted dataset; O_i = observed dataset; $\bar{P}$, $\bar{O}$= mean values of P,O datasets, n = # of evaluated batch runs					

2.3 Nitrogen Tracer Study Experimental Setup

The tracer studies were a subset of the 2-year series of NO_3-N removal experiments. Two separate studies were conducted. One mesocosm with Deloss soil and one with Scuppernong soil were used in the first study, while a second mesocosm with Deloss soil and a second with Scuppernong soil were used in the second study.

2.3.1 Wetland Mesocosm Ar and Br^- Solute Tracer Studies

Each wetland mesocosm was outfitted with a recirculation system to replicate the conditions of drainage water moving through the wetland. The systems consisted of 13 mm Schedule 40 PVC and a Rio Plus 600 mini head pump (TAAM Inc.,CA), which allowed for drainage water to turnover once a day and assisted in mixing the tracers in the mesocosms homogeneously. A coupled Ar gas tracer and Br^- solute tracer study was completed in July 2013 and July 2014 to determine the aeration coefficients within the mineral and organic wetland systems, to account for movement of gases during each experiment (Tobias, *et al.*, 2009). The aeration coefficient was essential for adequately estimating the N_2 production from denitrification in the wetland mesocosms by approximating the transport time of N gases from the sediment/water interface to the water/air interface. Values were estimated by incorporating both the diffusivity of gas in water and the physical processes within the air/water interface

(e.g., wind, biomass density). The Br^- solute tracer was added to the mesocosms to evaluate mixing and evapotranspiration. Four 66 L containers were filled with 50 L of water and sparged for 2 hours with Ar gas using a 13 cm diffuser (Pentair, Apopka, FL) at 10 psi. 3.5 g of NaBr was added to the containers during the final 30 minutes of the sparging to achieve a concentration of 6 mg L^{-1} Br^- in each mesocosm. Following the sparging, the Ar and Br^- saturated water was pumped into the two mesocosms as a single dose utilizing 12-V low flow submersible pumps (Waterra, WSP-12-5).

During the aeration coefficient evaluation, duplicate samples were collected at 0 min, 30 min, 1 hr, 2 hr, 4 hr, 8 hr, 12 hr, 16 hr, 20 hr, 24 hr, 30 hr, and 48 hr following the introduction of the Ar and Br^-. Ar samples were taken utilizing a lab grade peristaltic pump (Cole Palmer, 57160) at approximately 15 cm into the water column at 0.9 m and 2.7 m along the length of the mesocosm. Samples were pumped for 3 minutes into 30 mL exetainers (Labco, Lampeter, UK), filling them the equivalent of 3 times. A bead of water was allowed to form along the top of the exetainer. They were then capped, and placed upside down in 1 L Nalgene bottles prefilled with distilled water to minimize gas loss during shipping. Samples were analyzed at the MSTC Analytical Instrumentation Laboratory at the University of Connecticut using a membrane inlet mass spectrometer (Bay Instruments, Easton, MD). Duplicate Br^- samples were taken at the same time of each Ar sampling event. The samples were filtered with 0.45 µm filters and were evaluated at the Environmental and Agricultural Testing Service Laboratory at NCSU using a Quikchem 8000 (Lachat, Loveland, CO).

2.3.2 Wetland ^{15}N Enrichment Tracer Study

^{15}N enrichment tracers were utilized to trace applied $^{15}NO_3$-N transformations through the entire wetland (Figure 5). N pool sizes in each mesocosm were estimated prior to enrichment to determine appropriate ^{15}N mass required for each study. The water N_{pool} (g) was calculated by multiplying NO_3-N (g L^{-1}), the initial mean NO_3-N concentration in the water, by V_{Added} (L), the volume of water added into each mesocosm.

$$Water\ N_{Pool} = NO_3^- - N \times V_{Added} \qquad \textbf{Eq. 6}$$

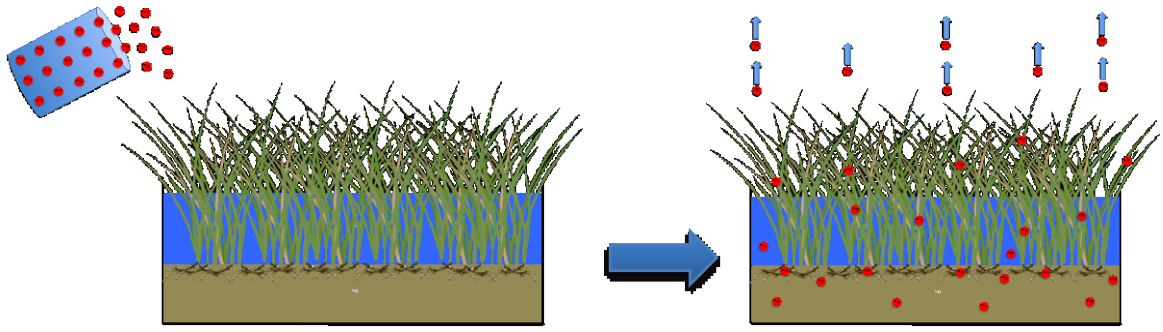

Figure 5: ^{15}N enrichment to wetland mesocosm to determine the pools (soil, gas, water, and biomass) N species reside.

The total nitrogen pool in the above and belowground biomass (g) was calculated as:

$$Plant\ Biomass\ N_{Pool} = NC \times M_{Total} \times \frac{A_{Mesocosm}}{A_{Sample}} \quad \textbf{Eq. 7}$$

where the plant biomass N_{Pool} was the total N in the biomass (g), NC was the fractional N content in the biomass pool examined (i.e., %N/100), M_{Total} was plant mass in the pool evaluated in the mesocosms, $A_{Mesocosm}$ was the total area of the mesocosm (3.15 m^2), and A_{Sample} was the plant biomass sampling area (0.09 m^2).

The total nitrogen pool in the sediment was calculated using the following equation:

$$Sediment\ \ N_{Pool} = A \times D \times p_b \times NC \quad \textbf{Eq. 8}$$

where the sediment N_{Pool} was the total N in the sediment (g), NC was the fractional N content in the sediment pool evaluated (i.e., %N/100), A was the total mesocosm area (3.15 m^2), p_b was the bulk density (g m^{-3}), and D was the soil sample depth (0.15 m). Bulk densities were 1.06 and 0.49 g cm^{-3} for the mineral and organic soils, respectively.

The first wetland mesocosm-scale ^{15}N enrichment study began in August 2013. The target overall NO_3-N load for the experiment was 0.9 g m^{-2}; a load observed in agricultural drainage water at the future wetland restoration sites. Treatment time was predetermined to last 7 days with water depths of 30 cm. The second wetland mesocosm-scale ^{15}N enrichment study began in July 2014 with overall target NO_3-N load of 3.6 g m^{-2}. Treatment time was extended to 10 days since previous non-tracer experiments indicated higher NO_3-N loads required longer residence times (see Chapter 3). Each mesocosm was also enriched with 3.5 g of NaBr to achieve a concentration of 6 mg L^{-1} Br^-, that was used as a conservative tracer to adjust NO_3-N removal calculations for evapotranspiration.

Based on N pools in each wetland mesocosm, drainage water was enriched with 15% and 29% ^{15}N in the mineral and organic wetland mesocosms, respectively, in the ^{15}N enrichment study with a target NO_3-N load of 0.9 g m^{-2}. Enrichment in the organic wetland mesocosm was larger because the total N pool in the mesocosm was twice that of the mineral wetland mesocosm. The enrichment solution of $K^{15}NO_3$ was prepared based on the mesocosm volume (L) and ambient NO_3-N (mg L^{-1}) concentrations. 9 g of $K^{15}NO_3$ and 4 g $K^{15}NO_3$ were added to the organic and mineral mesocosms, respectively. The solution was released as a single dose into each mesocosm while being filled with simulated NO_3-N rich agricultural drainage water to achieve a 0.9 g m^{-2} NO_3-$^{14+15}N$ load.

The second enrichment study was completed in the two other wetland mesocosms that had not received ^{15}N applications in the previous study. Mineral and organic wetland mesocosms were enriched with 15% and 19%, respectively, in the ^{15}N enrichment study with a target NO_3-N load of 3.6 g m^{-2}. Therefore, 16 g of $K^{15}NO_3$ and 18 g $K^{15}NO_3$ were added to the organic and mineral mesocosms, respectively. The solution was again released as a single dose into each mesocosm while being filled with simulated agricultural drainage water to achieve a 3.6 g m^{-2} NO_3-$^{14+15}N$ load.

Duplicate water samples were collected to ensure the system was well mixed using a lab grade peristaltic pump (Cole Palmer, 57160) at approximately 15 cm below the water surface at 0.9 m and 2.7 m along the length of the mesocosm. NO_3-^{15}N and N_2-^{15}N samples were taken on days 1, 2, 3, 5, 7, and 10 (only in the 3.6 g m^{-2} experiment). Additional samples were taken 5 cm from the soil/water interface and 5 cm from the water/air interface during the

second experiment to evaluate possible differences in N_2-^{15}N, N_2O-^{15}N, and NO_3-^{15}N in the water column. During NO_3-^{15}N sampling, 90 mL of filtered water was placed into 125 mL amber polyethylene bottles, followed by a pellet of KOH to preserve the sample. 500 mL of water was pumped into 125 mL serum bottles for the N_2-^{15}N samples. The water discharge tube was placed in the bottom of the sample bottle, filled until all bubbles were removed, and a meniscus was formed along the top of the bottle. A KOH pellet was then added and a stopper with a needle to allow air to escape was used to secure the sample in the sample bottle. Once capped, the needle was removed from the stopper. N_2-^{15}N and NO_3-^{15}N samples were then placed in the laboratory refrigerator until shipped on ice to the USGS Stable Isotope Laboratory for analysis. Samples were analyzed for N_2-^{15}N and N_2-^{14}N using a Thermo Scientific Delta V Plus continuous flow IRMS (USGS 10-C16, Reston, VA). N_2O-^{15}N was evaluated in the second ^{15}N experiment, where water was pumped for 3 minutes into the 30 mL exetainers allowing for the sample to fill the exetainer 3 times. A bead of water was allowed to form along the top of the exetainer. Samples were then capped, and placed upside down in 1 L Nalgene bottles prefilled with distilled water for shipping. Samples were analyzed at the UC Davis Stable Isotope Laboratory with a ThermoFinnigan GasBench + PreCon trace gas concentration system interfaced to a ThermoScientific Delta V Plus isotope-ratio mass spectrometer (Bremen, Germany).

Sediment and biomass samples were taken in replicates of three to five prior to enrichment and at the end of the experiments to determine ^{15}N in those pools. Biomass samples of the *S. tabernaemontani* were separated between live, dead, roots, and seeds to assess the distribution of ^{15}N throughout the plant. Additionally, emergent, herbaceous biomass other than *S. tabernaemontani* growing in the wetland mesocosms was sampled. Samples were dried, ground, and encapsulated prior to delivery to the Duke Environmental Stable Isotope Laboratory (DEVIL) and analyzed for $^{15}N/^{14}N$ using a Thermo Finnigan Delta Plus XL continuous flow mass spectrometer with a Carol Erba Elemental Analyzer and zero-blank sampler connected to a Conflo III interface (Waltham, MA) in the first experiment. Due to limitations of sample enrichment that could be measured at the DEVIL, biomass and soil samples were analyzed in the second ^{15}N enrichment study at the UC Davis Stable Isotope laboratory. Biomass samples were analyzed with a PDZ Europa ANCA-GSL elemental analyzer interfaced to a PDZ Europa 20-20 isotope ratio mass spectrometer (Sercon Ltd., Cheshire, UK), while the soil samples were analyzed with an Elementar Vario EL Cube or Micro Cube elemental analyzer (Elementar Analysensysteme GmbH, Hanau, Germany) interfaced to a PDZ Europa 20-20 isotope ratio mass spectrometer (Sercon Ltd., Cheshire, UK). Extractable NH_4-N and $^{15}NH_4$-N in the soil was also assessed in the second experiment at the MSTC Analytical Instrumentation Laboratory at the University of Connecticut using KCl extraction and a Hitachi UV/Vis spectrophotometer (Schaumburg, IL), respectively.

Additional parameters measured on days 0, 1, 2, 3, 5, 7, and 10 included NO_3-N, ammonium-N (NH_4-N), dissolved organic carbon (DOC), N_2O, dissolved oxygen (DO), redox measurements, pH, and water temperature. NO_3-N and NH_4-N water grab samples were evaluated at the Soil Science Environmental and Agricultural Testing Laboratory with a Quikchem 8000 (Lachat, Loveland, CO). DOC grab samples were evaluated by the North Carolina State University Biological and Agricultural Engineering Environmental Analysis Test Service Laboratory using the High-Temperature Combustion Method (Van Hall *et al.*, 1963) and a Teledyne Techmar Apoll 9000 (Mason, OH). N_2O samples were taken utilizing the peristaltic pump at approximately 15 cm into the water column at the 0.9 m and 2.7 m

distances along the width of the mesocosm. Helium flushed serum bottles were filled with 10 mL of water inserted with a 23G needle attached to a syringe. Samples were analyzed in the Environmental and Agricultural Testing Service Laboratory at NCSU with a Hewlett Packard Gas Chromatograph 6890 Series system (Palo Alto, CA) and gas chromatograph ChemStation software (Agilent Tech, Santa Clara, CA). The DO, pH, redox measurements, and water temperature were measured using parameter specific probes as described in Chapter 3.

2.3.3 N Removal using NO_3:Br^- Ratio

NO_3-N is a biologically active ion meaning it is predominately taken up or removed from the water column in wetland systems. Br^- is a conservative tracer, but has similar transport characteristics as NO_3-N (Sparks *et al.*, 2015). Therefore, the change in NO_3:Br^- ratios can indicate net biological removal of NO_3^- in the wetland mesocosms. Br^- concentrations also provided a baseline to account for potential evapotranspiration in the wetland, evidence that the system were well mixed, and a more accurate calculation of the NO_3^- removal in the systems.

2.3.4 ^{15}N Mass Balance Approach

A mass balance of the ^{15}N tracer added to the wetland mesocosm systems was completed to quantify the impacts of plant uptake and denitrification on NO_3-N concentration reductions observed in the wetland mesocosm systems. Isotopic mass balance measurements provide the ability to quantify routes of $^{15}NO_3$-N removal and assess the overall recovery of ^{15}N added to experimental systems.

$^{15}NO_3$-N removal into various N pools was calculated by quantifying the distribution of ^{15}N in the water, biomass, and sediment at t_o (prior to enrichment time) of the experiment and t_F (final sampling time) of the experiment. Tukey's t-tests were utilized to determine differences between mean t_o and t_f enrichment ^{15}N signatures in the water, soil, biomass, and gas pools of the two wetland mesocosms. Differences were considered significant at the α = 0.05 level.

δ^{15}N values, the measure of the ratio of ^{15}N:$^{14+15}$N, received from the analysis labs were transformed to At% (100*Atom Fraction) using Eq. 14, where the AR was the absolute ratio of mole fractions (0.0036764 for N) and δ^{15}N‰ was in permil. The conversion was necessary to determine the ^{15}N percent recovery (Eq. 15)

$$At\%^{15}N = \left(\frac{100 * AR * \left(\frac{\delta^{15}\mathrm{N}_{Sample}‰}{1000} + 1 \right)}{1 + AR * \left(\frac{\delta^{15}\mathrm{N}_{Sample}‰}{1000} + 1 \right)} \right) \quad \textbf{Eq.9}$$

The mass of ^{15}N recovered from each pool at t_f was derived using the following equation:

$$\%^{15}N_{RecoveryPool} = \frac{N_{Pool\,Size}(AF_{t_F} - AF_{t_o})}{^{15}N_T} \quad \textbf{Eq.10}$$

where, the percent recovery for each pool ($^{15}N_{Recoverypool}$) was determined by multiplying the difference between initial (AF_{t_o}) and final (AF_{t_f}) ^{15}N atom fractions in each sample by the size of the total N in each pool for individual mesocosms ($N_{PoolSize}$) and dividing by the total mass of the ^{15}N tracer added to each mesocosm ($^{15}N_T$) (Harrison *et al.*, 2012).

The rates of denitrification were determined for each mesocosm utilizing a numerical first order reaction model spreadsheet that simulated transformations of $^{15}NO_3$-N into $^{15}N_2$-N gas (Tobias, 2014; Böhkle *et al.*, 2004). Because $^{15}N_2$-N measurements in this study were not continuous, the spreadsheet was used to model the transfer of $^{15}N_2$-N into the atmosphere over a given time step (0.25 hr) by integration of $^{15}N_2$-N produced over time. The model separated NO_3-^{15}N removal into two pools: denitrification (determined through the $^{15}N_2$-N production rate) and biological uptake. The removal rates of $^{15}NO_3$-N from the water column coupled with the $^{15}N_2$-N production rates allowed the model to estimate the contribution of denitrification on the observed $^{15}NO_3$-N removal. The model was calibrated using NO_3-N, N_2-N, $^{15}NO_3$-N, and $^{15}N_2$-N values from water samples taken throughout the experiments and gas-specific aeration coefficient determined from the Ar enrichment experiments.

The gas-specific aeration coefficient for each wetland mesocosms was calculated using the following equation (Tobias *et al.*, 2009):

$$k_{N_2N_2O} = \left\{ -\ln \left[\frac{\frac{Ar}{Br} at\ t_o}{\frac{Ar}{Br} at\ t_F} \right] \times \frac{1}{t} \right\} \times Sc \qquad \textbf{Eq. 11}$$

Ar and Br^- were the dissolved Ar and Br^- concentrations at the initial (t_o) and final (t_F) sampling times, respectively, and t was the experimental period (24 hrs). Sc was a correction factor to convert the aeration coefficient derived from Ar (369) to N_2 (413) or N_2O (431) based upon the ratio of the Schmidt numbers for each gas to that of Ar (Tobias *et al.*, 2009; Wanninkhof, 1992).

Total recovered ^{15}N (%), i.e., the portion of ^{15}N accounted for in all evaluated pools (water, plant biomass, sediment, and gas), was then calculated as:

$$\%^{15}N_{Recovered} = \%^{15}N_{Gas} + \%^{15}N_{Plant\ Biomass} + \%^{15}N_{Sediment} + \%^{15}N_{Water} \qquad \textbf{Eq. 12}$$

Other protocols developed during this study for the mesocosm ^{15}N enrichment experiments can be found in Appendix 2.

3. Results and Discussion

3.1 Wetland Mesocosm Batch Runs

3.1.1 Initial Wetland Substrate Conditions

The physiochemical parameters of the two substrates are shown in Table 4. The wetlands with Scuppernong and Deloss soils will be referred to as organic and mineral wetlands, respectively, for the remainder of this article.

Table 4: Description of the wetland substrate conditions: pH, Nitrate-N (NO_3-N), Total Phosphorus (TP), Humic Matter (HM), Total Nitrogen (TN), Total Carbon (TC) and TC:TN ratios. * % represents g/100 g soil.

Wetland	Season	pH	NO_3-N ($g\ m^{-3}$)	TP ($g\ m^{-3}$)	HM ($kg\ m^{-3}$)	TN (%)	TC (%)	TC:TN	TN:TP
Organic	2011 Fall	3.5	35	18	88	0.75	22.48	29.97	44.91
	2012 Spring	3.8	< 5	18	70	0.8	25.38	31.73	47.90
	2012 Fall	-	-	-	-	0.85	23.87	28.08	-
	2013 Spring	4	< 5	18	71	0.68	21.27	31.28	40
	2013 Fall	-	-	-	-	0.91	26.85	29.51	-
	2014 Spring	4.3	< 5	18	79	0.74	22.3	35.02	42.77
	2014 Fall	-	-	-	-	0.93	27.64	34.82	-
Mineral	2011 Fall	5	21	57	25	0.16	3.50	21.88	2.66
	2012 Spring	5.4	< 5	55	21	0.18	3.96	22	3.11
	2012 Fall	-	-	-	-	0.18	3.96	22	-
	2013 Spring	5.3	< 5	41	23	0.15	3.42	22.8	3.51
	2013 Fall	-	-	-	-	0.15	3.47	23.13	-
	2014 Spring	5.7	< 5	47	19	0.19	4.59	28.56	3.8
	2014 Fall	-	-	-	-	0.14	3.36	27.52	-

Wetland soils with higher organic matter have been shown to impact microbial communities and result in higher NO_3-N removal rates (Burchell *et al.,* 2007). As expected, the organic wetland soil had a significantly higher total carbon (TC) content compared to the mineral soil ($\alpha = 0.05$). The mineral wetland soil TC values ranged from 3.36 to 4.59%, while the organic soil values ranged from 21.27 to 27.64%. Significantly higher total nitrogen (TN) was found in the organic wetland soil compared to the mineral soil ($\alpha = 0.05$), where the mineral soil TN values ranged from 0.14 to 0.19% and the organic soil values ranged from 0.68 to 0.91%. Similar findings were reported by Ewing *et al.* (2012) during an evaluation of wetland soil morphological and chemical properties following 15 to 30 years of agricultural production for organic, histic epipedons, and mineral soils. The study found that extractable nutrients from the substrates increased as the period the soils were used for crop production increased. The organic soils had TC and TN content of 29-35% and 0.7 to 0.9% in the top 30 cm, respectively, while the mineral soils had TC and TN content of 6-7% and 0.2 to 0.3% in the top 27 cm. Hunt *et al.* (2014) evaluated 28 restored wetland sites in North Carolina, Virginia Delaware, and Maryland. Soil C content was reported from the study to range from 1.8 and 2.0%, while soil N content was reported $\leq 0.2\%$ in the study, much less than the C and N content observed in the organic soil, but similar to the mineral soil evaluated in this study. Therefore, both substrates investigated in this study were considered to have a relatively high carbon content compared to other restored wetland soils, while the mineral soils had low TN content and the organic soils had high TN content.

The TC:TN ratios were also high in our study for both substrates, which is important for optimal denitrifying conditions. Li *et al.* (2011) reported wetland N removal efficiencies decreased as C:N ratio approached 5:1 in a study investigating N removal in a dominant broadleaf/conifer natural wetland system adjacent to farmland. Therefore, both wetland systems appeared to not be carbon limited. Ewing *et al.* (2012) also evaluated total extractable phosphorus (TP) in the wetland substrates to range from 19 to 55 g m^{-3} and 41 to 95 g m^{-3} in the organic and mineral soils, respectively. The organic substrate evaluated in this study had low TP (18 g m^{-3}), while the mineral soil had higher TP (41 to 57 g m^{-3}) likely since the mineral soils were recently used for agricultural production (Ewing *et al.,* 2012). Additionally, the soil pH was significantly lower in the organic wetland soil (which is commonly observed in these soils) compared to the mineral wetland soil ($\alpha = 0.05$). Soil pH values ranged from 3.5 to 4.3 in the organic soils and 5 to 5.7 in the mineral soils.

3.1.2 Wetland Mesocosm NO_3-N Removal Rates

Average N load and removal rates for each batch run study are presented in Table 4. Initial NO_3-N concentrations were within 10-20% of the initial target concentrations. Significant differences were observed between initial and final NO_3-N concentrations in the mineral and organic treatment wetland systems for all batch runs (α=0.05). Significant NO_3-N mass reduction was observed in both the mineral and organic wetland systems, with reductions as high as 98% (Table 5; Figure 6). It should be noted that the final sampling point used in each batch study was determined as either sampling day 10 or sampling day just prior to when NO_3-N concentrations reached <0.05 mg L^{-1}, since this was the NO_3-N threshold limit for the Quikchem 8000 instrument. NO_3-N removal in the controls was not significant during any batch study (α=0.05) (Figure 6).

Season	Load	Water Depth	Mean Water Temperature	Mean NO_3^-–N (Initial - Final)		Time Required to Achieve Reported % Reduction		Mean NO_3^-N % Reduction		ρ ± SD		J_{NN} ± SD (Average for Day 0 to Final Sampling Day)	
				WET-Min	WET-Org	WET-Min	WET-Org	WET-Min	WET-Org	WET-Min	WET-Org	WET-Min	WET-Org
	g m^{-2} d^{-1}	cm	°C	----------mg L^{-1}----------		----------d----------		----------%----------		----------cm d^{-1}----------		----------mg m^{-2} d^{-1}----------	
Fall 2013	0.6	18	18	3.56 – 0.22	3.56 – 0.14	7†	10	94	96	6.17 ± 0.27	5.63 ± 0.56	134 ± 4	103 ± 18
Winter 2013	0.6	15	9	2.28 – 1.02	2.28 – 1.00	10	10	55	56	1.23 ± 0.48	1.04 ± 0.57	14 ± 3	13 ± 1
Spring 2013	0.6	18	25	3.45 – 0.89	3.45 – 0.13	3†	7†	74	96	5.43 ± 0.41	7.35 ± 1.18	116 ± 21	72 ± 3
Summer 2014	0.6	18	26	3.38 – 0.13	3.38 – 0.53	3.3†	3.3†	96	84	14.31 ± 4.19	8.25 ± 1.51	183 ± 38	127 ± 6
Fall 2012	0.9	18	17	4.7 – 0.91	5.00 – 0.99	10	10	81	80	3.12 ± 0.24	3.50 ± 1.83	69 ± 13	59 ± 16
Winter 2013	0.9	18	11	6.13 – 2.63	6.13 – 2.94	10	10	57	52	1.02 ± 0.57	0.78 ± 0.30	56 ± 15	42 ± 14
Spring 2014	0.9	18	20	6.02 – 0.14	6.02 – 0.23	6.9†	6.9†	98	96	9.41 ± 2.1	7.94 ± 1.14	127 ± 28	88 ± 16
Summer 2014	0.9	18	26	6.49 – 0.35	6.49 – 0.10	3†	5†	95	98	11.68 ± 2.36	9.37 ± 3.10	322 ± 61	215 ± 34
Fall 2012	0.9	30	22	2.35 – 0.15	2.35 - .0.72	9	9	94	69	6.22 ± 0.91	2.97 ± 0.31	62 ± 9	63 ± 16
Fall 2014†	0.9	20	27	3.25 – 0.33	3.25 – 0.09	3†	4.9†	90	97	17.09 ± 5.84	14.72 ± 0.88	275 ± 23	173 ± 1
Spring 2014	0.9	30	26	3.29 – 0.11	3.29 – 0.38	5†	5†	97	89	25.70 ± 6.85	15.34 ± 3.20	216 ± 44	164 ± 5
Summer 2013	0.9	30	27	3.09 – 0.36	3.09 – 0.09	5†	10	88	97	11.68 ± 2.36	9.15 ± 1.45	137 ± 18	98 ± 9
Summer 2013	0.9	30	25	3.66 – 0.27	3.66 – 0.27	6.8†	6.8†	93	93	10.64 ± 1.97	11.36 ± 3.6	144 ± 4	144 ± 5
Fall 2012	2.2	30	11	6.44 – 3.41	6.52 – 3.17	10	10	47	51	1.99 ± 0.38	2.22 ± 0.46	45 ± 2	176 ± 12
Summer 2013	2	30	27	3.66 – 0.27	6.64- 1.01	6.9†	6.9†	95	85	12.62 ± 3.10	7.68 ± 1.89	283 ± 17	212 ± 31
Fall 2013	3.6	30	16	14.32 – 2.84	14.32 – 4.47	10.2	10.2	80	69	4.21 ± 0.02	2.92 ± 1.03	316 ± 2	260 ± 40
Spring 2014	3.6	30	25	11.88 - 1.19	11.88 – 3.19	10.1	10.1	90	73	6.52 ± 1.02	3.54 ± 0.22	288 ± 14	234 ± 5
Summer 2014	3.6	30	25	12.97 – 0.38	12.97 – 1.01	7†	9.9	97	92	17.49 ± 6.08	6.85 ± 1.86	603 ± 140	344 ± 8

Table 5: Summary of selected water quality parameters during batch studies, NO_3-N removal rate means (J_{NN}) ± standard deviations (SD), and first order mass transfer coefficient (ρ) ± standard deviations (SD).

† - % reduction was 100% at the following sampling day. *Shaded rows are experiments that had significant differences between removal rates (α = 0.05).

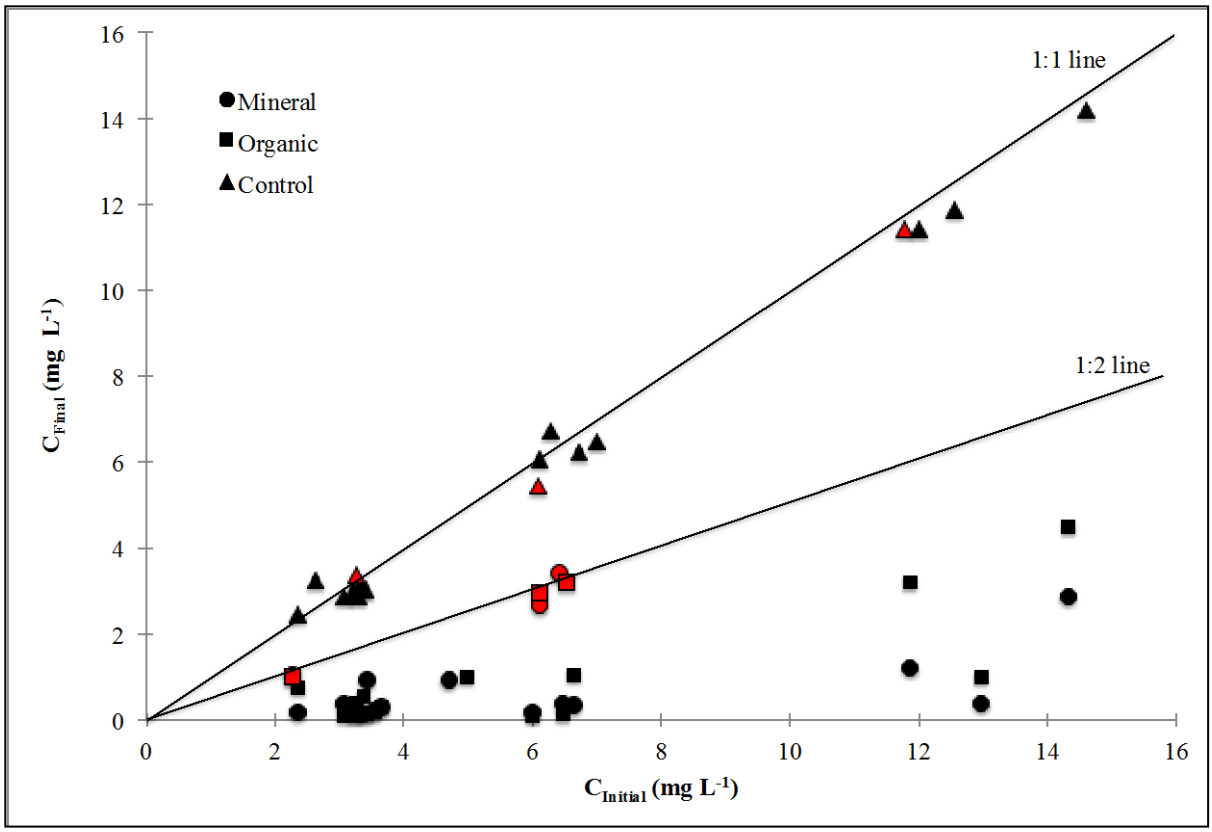

Figure 6: Average NO_3-N initial and final concentrations for all batch runs assuming zero order. *Red points are batch runs that had average water temperatures below 12° C. **The 1:2 line represents 50% NO_3-N removal at the completion of the batch study.

NO_3-N removal rates were highest in the mineral wetland mesocosms. Mineral removal rates ranged from 62 to 603 mg m^{-2} d^{-1}, while removal rates in the organic wetland systems were from 58 to 344 mg m^{-2} d^{-1} during the growing season when water temperatures were above 12° C. Both wetland system NO_3-N removal rates were similar to removal rates found in other microcosm and mesocosm wetland studies during the growing season. Gebremariaum and Beutel (2008) reported comparable NO_3-N removal rates (175-500 mg m^{-2} d^{-1}) in an evaluation of surface flow constructed treatment wetland mesocosms spiked with NO_3-N at 15 mg L^{-1} during the summer. Stringfellow *et al.* (2013) investigated three wetland restoration substrates receiving agricultural drainage water during the growing season utilizing microcosms and reported mean areal NO_3-N removal rates to range from 142 – 380 g m^{-2} d^{-1}, also consistent with the estimated wetland mesocosm NO_3-N removal rates in this study during the growing season. Removal rates in the mineral and organic wetland systems during periods the water temperature was below 12° C ranged from 16 to 40 g m^{-2} d^{-1} and 15 to 54 g m^{-2} d^{-1}, respectively. Although removal rates were low during batch studies completed when the water temperature was below 12° C, the wetland mesocosm treatment systems still provided at a minimum 51% and 47% NO_3-N removal in the mineral and organic wetland systems, respectively. A complete summary of the 18 batch studies can be found in Appendix 3.

3.1.3 Other Nitrogen Species

NO_3-N was our primary focus in this study because this is typically the dominant N species in agricultural drainage water and contributes much of the total N loads to downstream ecosystems. However, observations of other N species were conducted in this study. NH_4-N concentrations initially ranged between 0.3 to 0.6 mg L^{-1} and 0.1 to 0.4 mg L^{-1} in the organic and mineral wetland mesocosms, respectively, and decreased to below minimum detection limits (< 0.05 mg L^{-1}) within 72 hours following the beginning of each batch study. ON concentrations ranged between 1.4 to 1.7 mg L^{-1} and 0.7 to 1.5 mg L^{-1} in the organic and mineral wetland mesocosms respectively throughout the experiments. Notable changes in ON concentrations were not observed between the beginning and completion of the batch run experiments, which was expected because they were in the range of background concentrations of natural wetlands (Moore *et al.,* 2012).

3.1.4 Divergence in Mineral and Organic NO_3-N Removal Curves

The mineral wetland reduced NO_3-N significantly faster than the organic treatment in 10 of the 18 batch run studies (α=0.05). Mineral and organic NO_3-N removal curves began to diverge around day 3 of batch runs particularly during both the growing season and larger N load evaluations (Figure 7). The divergence of NO_3-N removal curves was a recurring phenomenon, and led to the significant differences observed between organic and mineral wetland NO_3-N removal rates during the growing seasons (Table 6).

Of course water temperature significantly interacted with season ($p < 0.0001$), but it was not found to be significantly different between mesocosms during each batch run study (α=0.05). Therefore, physical and biogeochemical processes that occurred within the wetland systems during various seasons were determined to have the overarching impact on observed differences in NO_3-N removal performances between wetland treatments. Reduction of NO_3-N concentrations observed between the mineral and organic wetland systems during the spring was significantly different within 7-10 days following NO_3-N loading. Significant differences between the organic and mineral wetland mesocosm NO_3-N removal curves were also observed in many of the summer and fall batch studies.

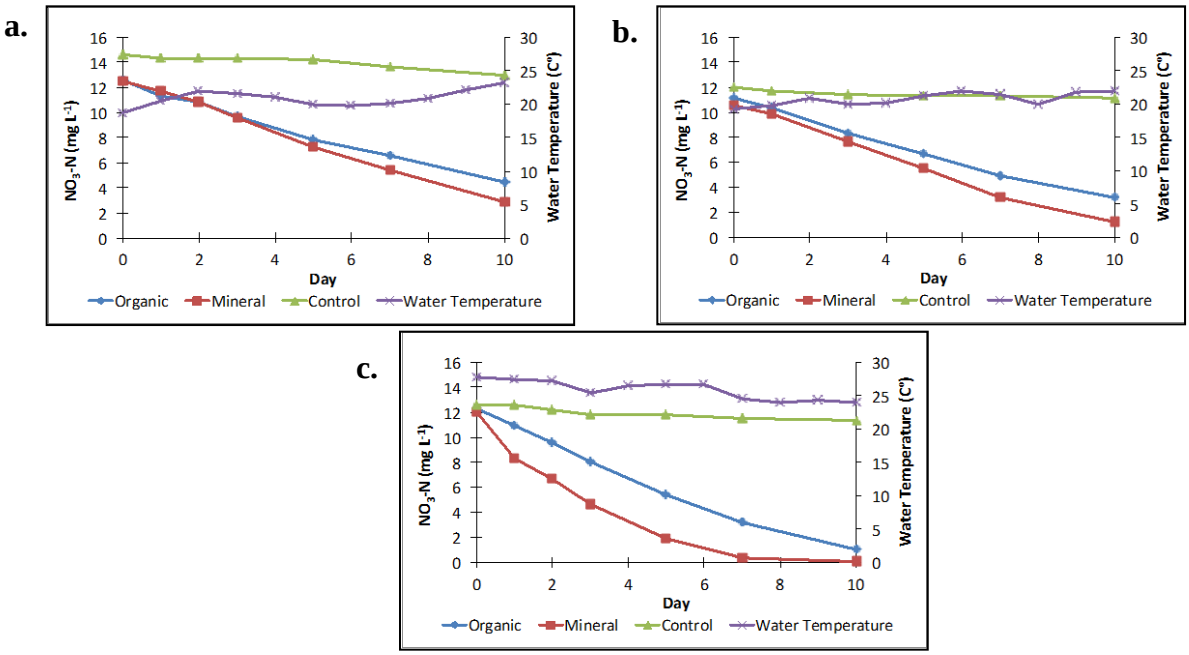

Figure 7: 3.6 g NO_3-N m^{-2} load for a. Fall, b. Spring, and c. Summer.

Table 6: Statistics for batch run studies that had significant differences in NO_3-N removal between the organic and mineral wetland mesocosm systems. The day specified is the day the significant differences began to occur between the mineral and organic wetland mesocosms. Significant differences were determined for α=0.05.

Differences Between Mineral and Organic Mesocosms	Day	p-value
Spring (0.6 g m^{-2})	10	0.0381
Spring (0.9 g m^{-2})	7	0.0355
Spring (3.6 g m^{-2})	10	<0.001
Summer (0.9 g m^{-2})	7	<0.0001
Summer (2.2 g m^{-2})	10	0.0116
Summer (3.6 g m^{-2})	10	0.0251
Fall (0.6 g m^{-2})	10	0.0061
Fall (0.9 g m^{-2})	10	0.0144
Fall (3.6 g m^{-2})	10	0.0002

Potential causes for the observed differences in NO_3-N removal curves between the mineral and organic wetland treatments were further investigated. Plant uptake and denitrification were the two removal mechanisms considered most important in this study. Walbridge and Lockaby (1992) completed a review on N removal mechanisms of forested wetlands and reported denitrification could account for up to 95.9 mg N m^{-2} d^{-1}, while plant uptake could account for up to 14.2 mg N m^{-2} d^{-1}. Therefore, plant uptake and denitrification were further assessed.

3.1.5 Biomass Establishment and N Plant Uptake

The *S. tabernaemontani* was allowed 16 months to establish prior to the initial batch run. Above ground biomass remained nearly unchanged from 2011 to 2014 in the mineral wetland systems with average plant heights that ranged from 120 to 130 cm. Above ground

biomass increased in the organic wetland systems in terms of mass, height (64 to 121 cm during the experiment period), and diameter (Figure 8). Below ground biomass increased dramatically from 2011 to 2013 in both wetland systems. Prior to the addition of nitrogen rich drainage water in 2013, the mineral treatment had over 2X more below ground biomass compared to the organic wetland treatment. Following the initiation of the batch run experiments below ground biomass became more similar between the two wetland treatments. However, the effect of nitrogen addition or soil type causing these changes required further investigation. Biomass weight per unit area was in the range of other mesocosm studies that have evaluated *S. tabernaemontani* over two years of establishment, which has ranged from 0.1 to 5.5 kg m^{-2} in the aboveground and 0.1 to 1.5 kg m^{-2} in the belowground (Burchell *et al.*, 2007; Svengsouk and Mitsch, 2001). However, the above ground biomass was at the lower end and the below ground biomass was at the higher end of reported values from past studies. *S. tabernaemontani* growth can be negatively impacted by water-level drawdown, which may have contributed to the lower above ground plant growth in this study (Hunter *et al.*, 2000), since water-level often resided at the soil/water interface in between batch run studies.

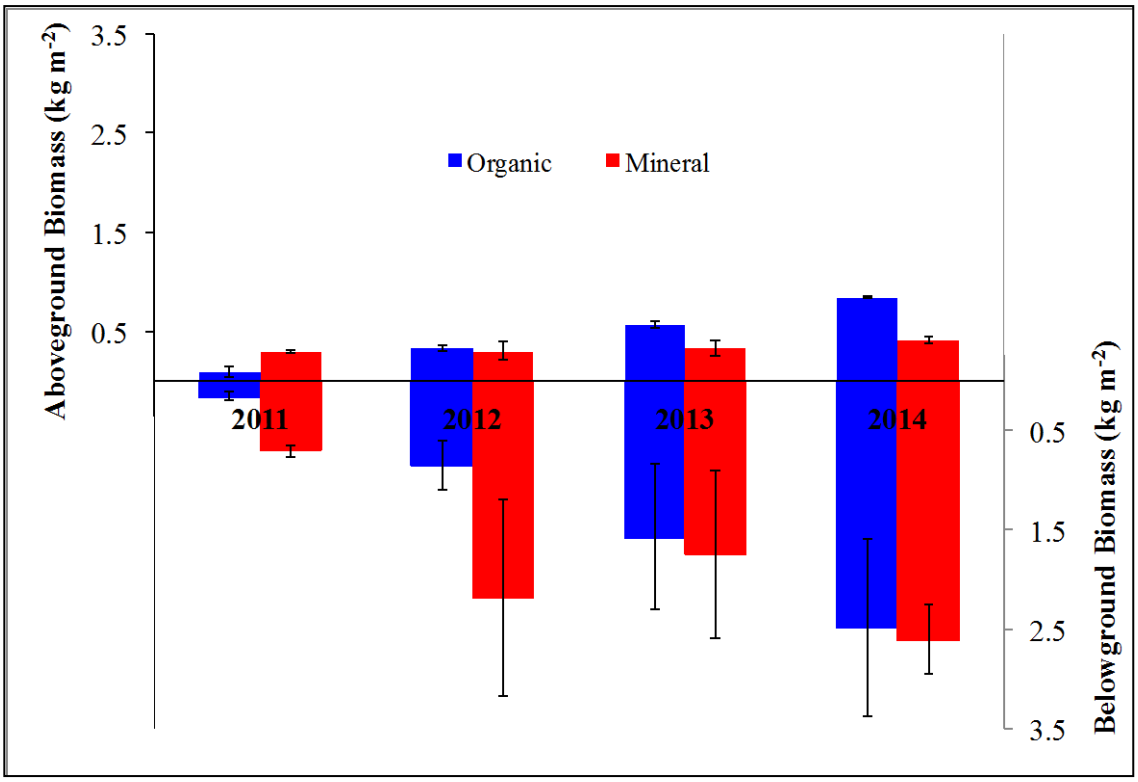

Figure 8: Yearly average above and below ground biomass of S. tabernaemontani. Error bars represent ± 1 standard deviation.

Total nitrogen incorporated into the biomass between the mineral and organic treatments was also measured. The results of TN in the biomass pools can be found Figure 9. Recall the organic systems had more soil nitrogen compared to the mineral systems. TN values in the below and above ground biomass were significantly different between the mineral and organic treatments prior to adding NO_3-N rich drainage water into the mesocosms (2011-2012) (α=0.05). However, after NO_3-N removal experiments began, significant differences were no

longer observed between the TN biomass pools in the above and below ground biomass (2013-2014) (α=0.05). Higher plant TN content in the below and above ground biomass of the organic systems compared to the mineral system suggests plants were assimilating more soil nitrogen for growth in 2011 and 2012 prior to the addition of simulated NO_3-N rich drainage water.

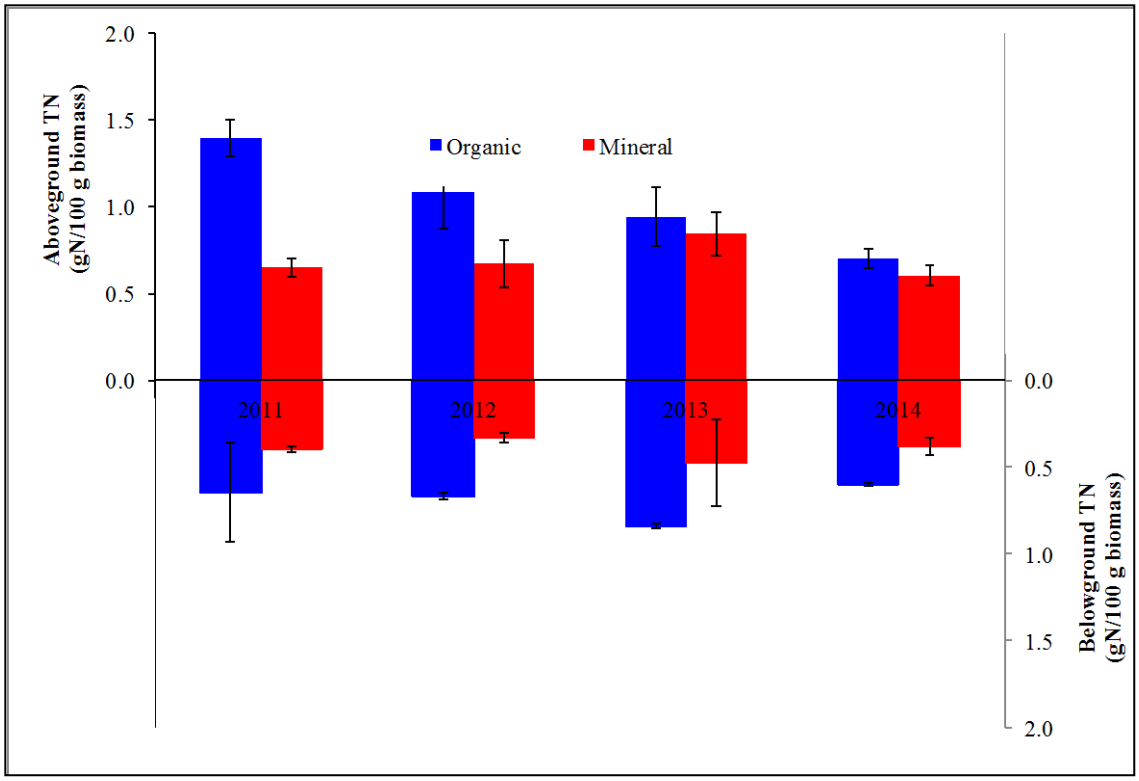

Figure 9: Mean above and below ground biomass total nitrogen content of *S. tabernaemontani* near the end of the growing season in each treatment.

3.1.6 Assessment of the Impact of Denitrification Limiting Parameters

Environmental factors that have been found to influence NO_3-N reduction efficiencies in wetlands were compared between the control, mineral, and organic wetland systems. The most significant impact on NO_3-N reduction over time in both the mineral and organic systems was seasonal variations ($p < 0.001$). However, denitrification has been found to also be highly variable and dependent on DO concentrations, N load, soil redox, water pH, temperature, and DOC concentrations (Puckett, 2004). Therefore, each parameter was evaluated throughout the batch run experiments to determine if conditions suitable for denitrification existed in the wetland mesocosms and evaluate if denitrification could have impacted observed differences between treatment NO_3-N removal rates. P-values for differences between water temperatures, DO concentrations, DOC concentrations, water pH, and redox values between mesocosms for each season are displayed in Table 7 and Figures 10-12. Significant differences observed between mesocosms during the growing season were primarily water pH and DOC concentrations.

Table 7: P-values observed for comparisons of denitrification limiting parameters between the mineral and organic treatments. Significant differences are highlighted in red ($p < 0.05$).

Parameter	Seasonal Differences Between Mesocosms

	Fall	Spring	Summer	Winter
Temperature	0.9316	0.9959	0.9666	-
Dissolved Oxygen (5 cm from soil/water interface)	0.5056	0.0641	0.0049	0.4992
Dissolved Oxygen (5 cm from air/water interface)	0.007	0.0979	<0.001	0.6318
Dissolved Organic Carbon	<0.001	<0.001	<0.001	<0.001
Water pH	<0.001	<0.001	<0.001	<0.001
Redox (5 cm)	0.2048	0.1409	0.0295	0.008
Redox (15 cm)	0.6897	0.1542	0.0026	0.7553

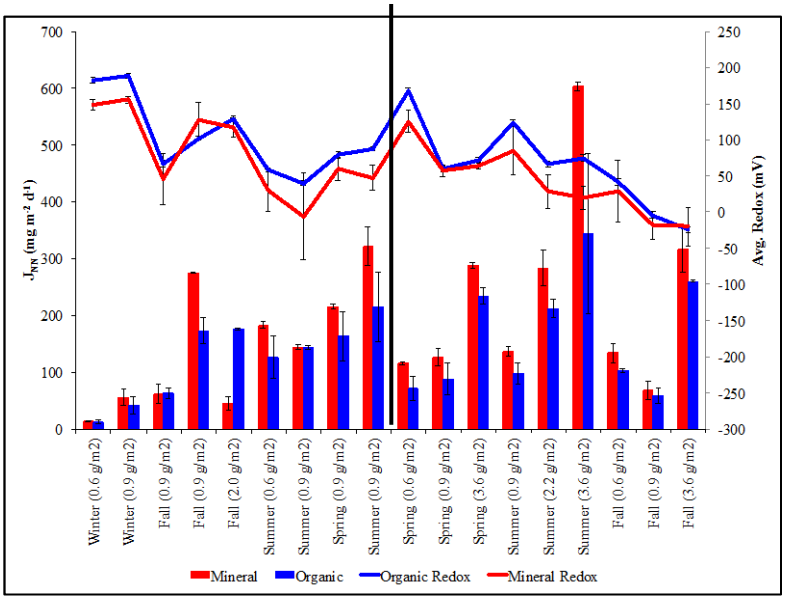

Figure 10: Average NO_3-N removal rates with standard deviations for the mineral and organic mesocosms compared to the average redox values at 5 cm soil depths for the two mesocosm wetland treatments. *The black separator line distinguishes batch runs without significant differences in NO_3-N removal rates (J_{NN}) (to the left) and those with significant differences (to the right) between the two mesocosm treatments.

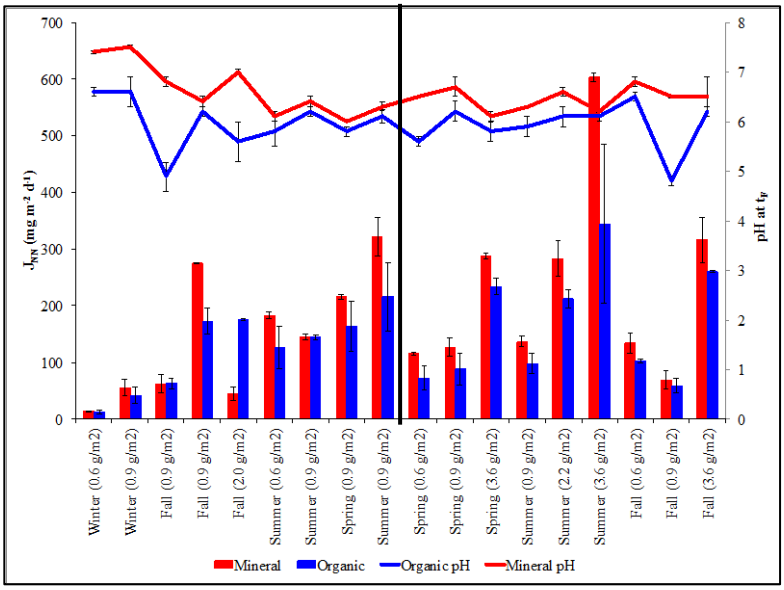

Figure 11: Average NO_3-N removal rates with standard deviations for the mineral and organic mesocosms compared to the water column pH values at the final sampling time (t_F) for the two mesocosm wetland treatments. *The black separator line distinguishes batch runs without significant differences in NO_3-N removal rates (J_{NN}) (to the left) and those with significant differences (to the right) between the two mesocosm treatments.

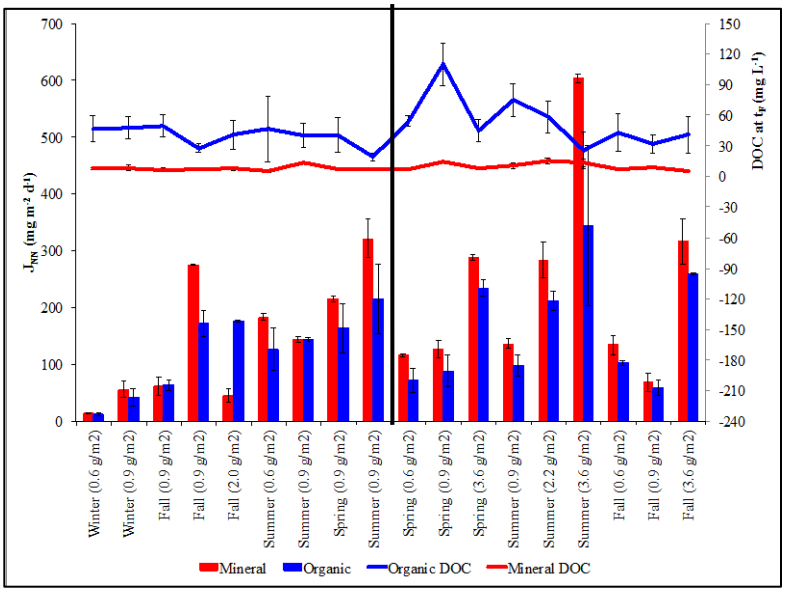

Figure 12: Average NO_3-N removal rates with standard deviations for the mineral and organic mesocosms compared to the water column dissolved organic carbon (DOC) concentrations at the final sampling time (t_F) for the two mesocosm wetland treatments. The black separator line distinguishes batch runs without significant differences in NO_3-N removal rates (J_{NN}) (to the left) and those with significant differences (to the right) between the two mesocosm treatments.

All denitrification enzymes are inhibited by oxygen (Ishida *et al.*, 2006; Sylvia *et al.*, 1998). Trevors (1985) did not observe denitrification during periods where the O_2

concentrations exceeded 4.5 mg L^{-1} in the water column of an agricultural soil study, which were similar to water O_2 values observed in this study. However, Crumpton and Phipps (1992) reported wetland systems with water column DO concentrations between 6-10 mg L^{-1} simultaneously having DO concentrations <0.01 mg L^{-1} within 2 mm from the soil-water interface. Dissolved oxygen was monitored at the top and bottom of the water column throughout each batch run study in this experiment. Initial concentrations ranged from 6.9 to 13.2 mg L^{-1} in the organic systems and 7.4 to 12.4 mg L^{-1} in the mineral wetland system at the air/water interface during the growing season. Observed DO concentrations at the completion of batch studies at the air/water interface ranged from 0.5 to 10.0 mg L^{-1} and 1.3 to 9.9 mg L^{-1} in the organic and mineral wetland systems, respectively during the growing season. Smaller ranges in DO concentrations at the completion of the batch studies were observed in both wetland systems at the soil/water interface, with concentrations ranging between 0.7 and 5.8 in the organic systems and 1.5 to 7.2 in the mineral systems during the growing season. Average DO concentrations decreased over time during each experiment in both wetland systems. Higher average DO concentrations were observed at the completion of each batch study when average water temperatures were below 11 °C (> 5 mg L^{-1}) compared to warmer average water temperatures (< 5 mg L^{-1}), since water retains more oxygen as temperatures and microbial activity decrease. Additional, although DO concentrations were significantly affected by season (α=0.0001) and were significantly lower in the organic wetland systems during the summer and fall compared to the mineral systems (α=0.01), the mineral system was observed to provide higher NO_3-N removal rates than the organic wetland system. This was surprising since facultative anaerobes that complete denitrification prefer O_2 over NO_3^-, leading to the expectation of more NO_3-N removal in the organic system compared to the mineral system, which was not observed. Therefore, water column DO concentrations likely did not contribute to significant differences in NO_3-N removal between mesocosms.

Soil redox was utilized in this study to assess the oxidation state in the soil column at 15 and 30 cm depths. Mean soil redox was below 250 mV at the beginning of all 18 batch run studies at both depths and remained relatively constant throughout the course of each experiment Figure 10). Patrick (1960) found denitrification rates became limited at redox potentials higher than 250 mV, with decreasing NO_3^--N concentrations associated with decreasing redox potential. Cey *et al.* (1999) also used redox potentials to provide supporting evidence of denitrification occurring within a riparian zone in southern Ontario. A sharp decline in NO_3^--N concentrations was observed in that study as redox readings dropped below 200 mV. In our study, average soil redox values conducive for denitrification were observed throughout the experiments (-61 to 237 mV), which indicated low dissolved oxygen concentrations below the soil/water interface in both wetland systems. Additionally, since the redox values were low in both the mesocosm treatment wetlands and were not significantly different between treatments during most seasons (α=0.05), it was not able to explain removal rate differences between the two wetland systems.

pH is also critical to denitrification rates because denitrifying bacteria have been found to function best near neutrality. Denitrifiers have been found to prefer pH ranges between 5.5 and 8.0 (Rust *et al.*, 2000). Lower soil pH (<4) has been found to inhibit enzyme activity that controls denitrification rates (Sylvia *et al.*, 1998), but denitrification has been observed to remain an important NO_3-N removal mechanism even at low pH values (Cleemput *et al.*, 1975). Acidic soils, like the ones used in this experiment, can limit the functionality of denitrification enzymes used by microorganisms by hindering the process or prematurely

stopping denitrification after the formation of nitrite and/or N_2O and allow for nitrite build to levels toxic to plants further reducing NO_3-N removal rates (Tari and Casiszár, 2003; Sylvia *et al.,* 1998; Rivett *et al.,* 2008). pH was significantly different between the two soils and within the water column of the two treatments during the growing season (α=0.0001), with the organic wetland being more acidic. Water pHs ranged between 4.8-6.6 and 6.0-7.5 in the organic and mineral wetlands, respectively, during the 7 to 10 days of inundation periods (Figure 11). The difference in the pH values may have contributed to removal rate differences associated with denitrification between the organic and mineral wetland systems by inhibiting denitrification in the organic soils during the growing season.

The presence and quality of organic carbon, often the primary limiting agent for denitrification in restored and constructed wetland systems, serves as a critical electron donor and source of carbon for microbial biomass production (Warneke *et al.,* 2011; Burchell *et al.,* 2007). Significant differences were observed between the organic and mineral wetland mesocosms DOC concentrations throughout the year (α=0.0001). DOC concentrations ranged between 7 to 133 mg L^{-1} with an average of 39 mg L^{-1} in the organic wetland system, while concentrations ranged from 3 to 26 mg L^{-1} with an average of 9 mg L^{-1} in the mineral wetland systems. Carbon source availability can vary depending on past land use, vegetative structure and type, litter, soil type, age of wetland, and season (Liu *et al.,* 2010; Hefting *et. al,* 2005). Burchell *et al.* (2007) found that NO_3-N reductions were faster after the addition of organic matter to wetland mesocosm soils that were carbon-limited, supporting the importance of available carbon in these environments. DOC concentrations had an inverse relationship to NO_3-N removal rates in this study. However, both the organic and mineral mesocosms in this study had high DOC concentrations, much higher than 4-8 mg L^{-1} particularly in the organic system (Figure 12), which is sufficient to support denitrification (Knies, 2009; Spruill *et.* al, 1997). Therefore carbon limitations did not appear to be a major factor in observed differences in NO_3-N removal rates through potential denitrification between treatments.

Finally, although DO concentrations were not measured in the porewater of this study, redox measurements were indicative of low concentrations at 5 and 15 cm deep. Water quality measurements from dialysis porewater samplers indicated that NO_3-N concentrations were below 0.05 mg L^{-1} within 1 cm of the soil-water interface of the mineral and wetland mesocosms 72 hours following the addition of NO_3-N. This may indicate low DO concentrations even closer to the soil/water interface, and any NO_3-N present in the water column that diffused into the anaerobic soil layer likely quickly underwent denitrification (Reddy and DeLaune, 2008). Therefore, the likelihood of denitrifying conditions being satisfied and denitrification occurring was high in both the mineral and organic wetland systems. Concentrations profiles from the evaluation are displayed in Figures 13 and 14.

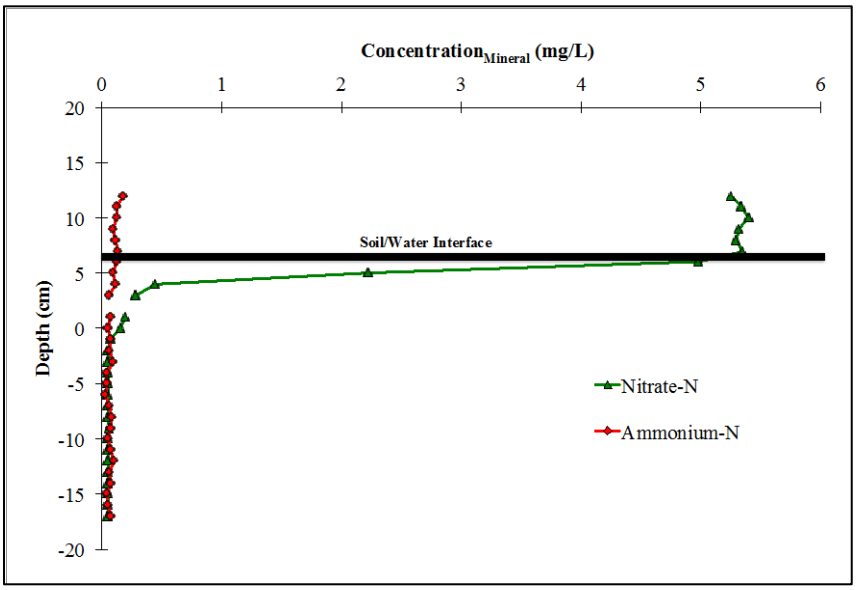

Figure 13: NO_3-N and NH_4-N concentration profiles in the mineral wetland mesocosms. The black line represents the soil/water interface with the water column above and the soil column below.

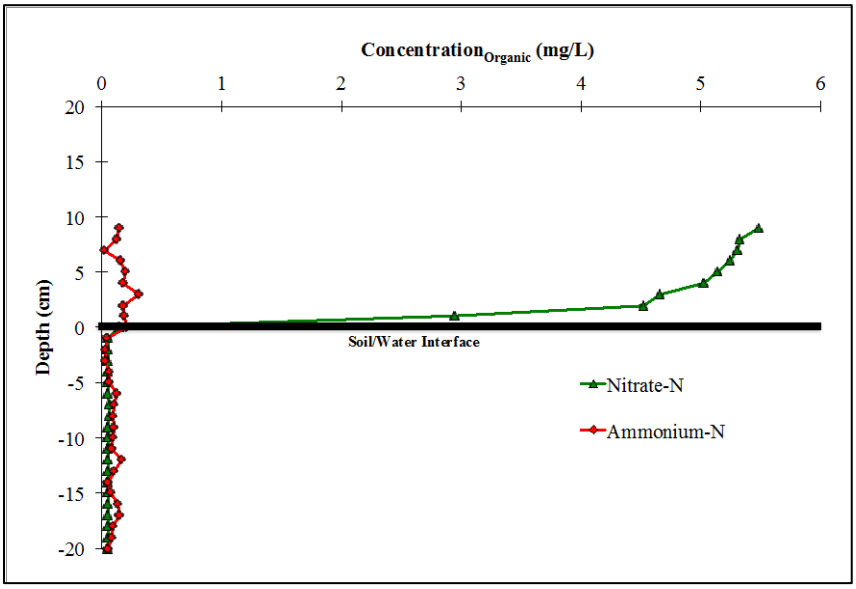

Figure 14: NO_3-N and NH_4-N concentration profiles in the organic wetland mesocosms. The black line represents the soil/water interface with the water column above and the soil column below.

3.1.7 Contribution of Plant Uptake and Denitrification

Plant uptake is generally assumed to be a secondary contributor to NO_3-N reduction in wetlands. However, total uptake of N from nutrient enriched water by wetland plants is difficult to measure, but has been estimated to vary between 16 to 75% (Burchell *et al.*, 2007; DeBusk and Reddy, 1987). During the first year of establishment, significant differences in TN per unit area of the above ground *S. tabernaemontani* were not observed between the two

treatments (α=0.05). Significantly higher TN per unit area of *S. tabernaemontani* was observed in the organic wetland systems compared to the mineral systems from 2012 to 2014 (α=0.05) (Figure 15). Min *et al.* (2011) observed higher mineralization, which would produce NH_4^+-N and NO_3-N for plant uptake, in lower pH wetland soils (5.2 to 6.4) at the microcosm scale compared to higher pH soils (7.0 to 7.4). Additionally, they observed mineralization to decrease as NH_4^+-N and NO_3-N were added to the systems in lower pH soils, but have little effect on the higher pH soils. Therefore, the mineral wetland plants may have had more limited opportunities to obtain N from the their higher pH soils through mineralization than the organic wetland plants, essentially resulting in more NO_3-N removal from the water N pool in the mineral systems comparison with the organic systems.

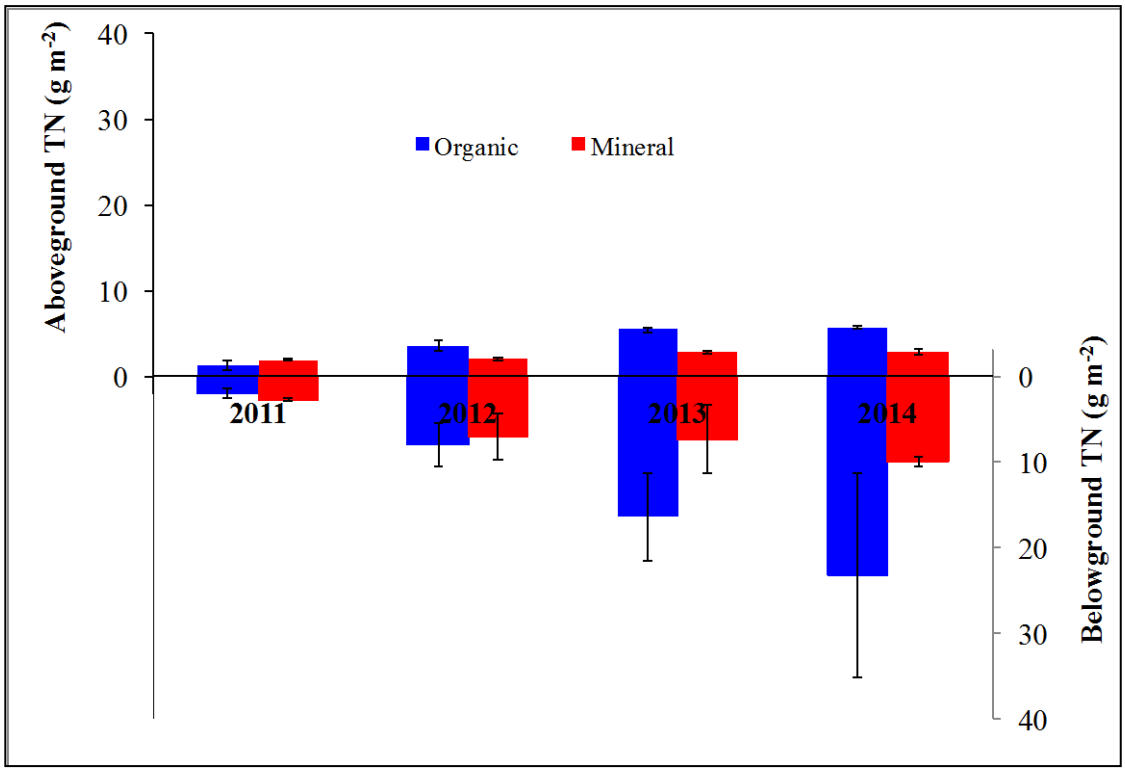

Figure 15: Total nitrogen per unit area in biomass from fall 2011-2012 (before N loading) and fall 2013-2014 (after N loading).

In this study, distinct visual coloration differences between the *S. tabernaemontani* in the organic and mineral treatments were also observed (Figure 16). Nitrogen deficiencies have been found to cause plant stems to become light green or yellow in color (Evans, 2003). The organic wetlands had dark green stem colors both before and after N loading. However, the mineral wetland plants had dark green stems in 2011 immediately following planting, light green stems in 2012, dark green stems in 2013 and 2014, and light green stems in 2015. Recall simulated NO_3^-N rich drainage water was not added until 2013 and batch run studies were completed at the end of the growing season of 2014. The color differences alone suggest the plants in the mineral wetland systems utilized more of the nitrogen in the simulated drainage water to overcome nitrogen limitations in the soil. The obvious exception was in 2011, but since the bulrush were planted as plugs that included plant nutrients, this likely masked nitrogen deficiencies early on. Additionally, the higher availability of N in the organic soils

likely resulted in the organic treatments having more N available for luxury uptake from the soil N pool, particularly based on TN results of the below ground biomass. Svengsouk and Mitsch (2001) suggested similar hypotheses in a mesocosm study with *S. tabernaemontani*, where following fertilization, the plants had an increase in tissue nutrients believed to be from the plants' high absorption capacity and nutrient storage in the roots. However, the contributions of N in the biomass from applied drainage water and the soils remains unclear using the methods discussed in this paper.

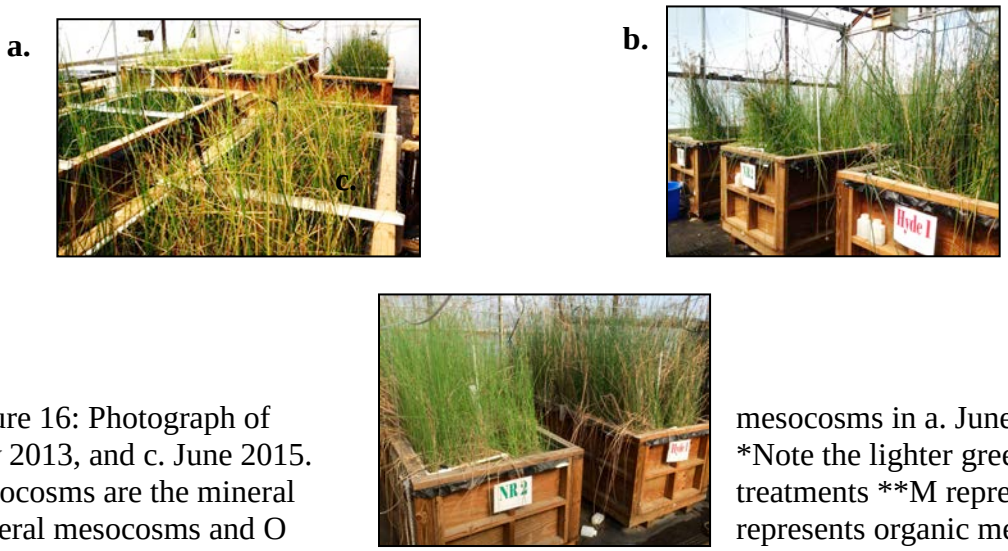

Figure 16: Photograph of mesocosms in a. June 2012, b. July 2013, and c. June 2015. *Note the lighter green mesocosms are the mineral treatments **M represents mineral mesocosms and O represents organic mesocosms.

A simplified mass balance analysis was attempted in this study for the wetland mesocosms during the growing seasons of 2012 thru 2104 to estimate the maximum potential plant uptake had on NO_3-N removal from the water column. Estimates were based on the assumption that plant uptake of N was linear through time and all N taken up by plants was obtained from the water column. Based on TN in above and below ground biomass and the growing season (210 days) plants were estimated to have an average daily N uptake rate of 58 and 93 mg m^{-2} day^{-1} in the mineral and organic wetland mesocosms, respectively, in 2013, while average daily N uptake rates were estimated to be 59 and 136 mg m^{-2} day^{-1} in the mineral and organic wetland mesocosms, respectively, in 2014.

All remaining NO_3-N reduction not accounted for by plant uptake was assumed to be due to denitrification, since conditions appeared favorable for this process to proceed. The minimum removal of applied yearly NO_3-N from the water column through denitrification was estimated to be 45% and 70% in the organic and mineral systems, respectively. These results were similar to those observed in Burchell *et al.* (2007), which estimated denitrification to account for 65 to 78% of NO_3-N removal in a wetland mesocosm study using a similar method and assumptions. However, the assumption that plant N uptake only came from the NO_3-N rich drainage is undoubtedly inaccurate, but results are a potentially conservative estimate of loss through denitrification. Therefore, to better define the roles of plant uptake and denitrification on observed NO_3-N reductions in drainage water a ^{15}N tracer enrichment study was completed and is further discussed in Section 4.

3.1.8 Mass Spectrometer Hourly Results

Readings from the UV-Vis spectrometer provided more insight into NO_3-N and DOC concentrations in the water column that occurred on an hourly basis, rather than daily. Changes at this frequency have rarely been available in the past. Spectrometer readings were calibrated with NO_3^--N and DOC concentrations from grab samples and evaluated in R Studio (RStudio, Inc., Boston) using PLSR code developed by Etheridge *et al.* (2014).

The mineral, organic, and control wetland treatments had high correlations between spectrometer readings and laboratory-measured NO_3-N concentrations (Appendix 4). NO_3-N was calibrated with water quality grab samples collected in the batch studies and were evaluated individually for each mesocosm and batch runs. Only three DOC grab samples were collected during each batch study from individual mesocosms for spectrometer calibrations. Therefore, DOC readings from the spectrometer were calibrated using all batch study DOC grab sample concentrations in one calibration simulation for each treatment (organic, mineral, and control) instead completing numerous calibrations for individual mesocosms and batch runs as completed in the NO_3-N assessment. Photosynthetic radiation rates were collected from a State Climate Office weather site approximately 1 mile from the study location (REED). Prominent diurnal cycles were observed in both NO_3-N and DOC readings from the UV-Vis spectrometer in most runs completed during the growing season. Two processes likely had the largest impact on these observations: photochemical mineralization and nitrification.

NO_3-N concentrations were observed to decrease daily after noon, or approximately 7 hours after sunrise, and continued into the early evening hours of this study (Figures 17 and 18). These UV-Vis spectrometer measurement trends were confirmed with 6 hour grab samples during one of the batch studies. Penton *et al.* (2013) observed a 7 hour lag time in both O_2 flux and N_2 production after the initiation of light in a flooded agroecosystem in Hawaii. NO_3-N concentrations occasionally increased during the 6 hour lag period after sunrise of this study. NO_3-N concentrations in the organic systems increased by as much as 0.08 mg L^{-1} hr^{-1} and 0.04 mg L^{-1} hr^{-1} in batch studies during the growing season with N loads of 0.9 g m^{-2} and 3.6 g m^{-2}, respectively; however, smaller increases were observed in the mineral systems (0.05 mg L^{-1} hr^{-1} and 0.02 mg L^{-1} hr^{-1} N loads of 0.9 g m^{-2} and 3.6 g m^{-2}, respectively). These increases may have been due to NH_4^+-N, produced from direct photochemical mineralization, that was nitrified to NO_3-N as O_2 was released at the root tips during photosynthesis and diffused into the water column (Rysgaard *et al.*, 1995). Direct photochemical mineralization is a process where sunlight is absorbed into dissolved organic matter (DOM) reducing the molecular weight of the material and forming photoproducts (Zepp *et al.*, 1995). NH_4^+-N has been observed as a photoproduct of direct photochemical mineralization of humic substances and bulk DOM in wetland, estuary, river, and pond studies (Bushaw *et al.*, 1996).

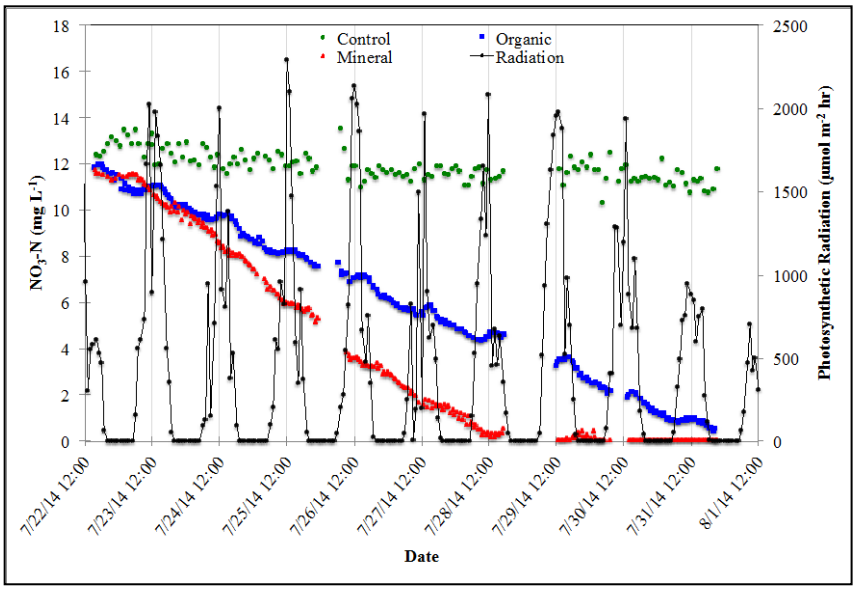

Figure 17: Hourly NO_3-N concentrations from the Spectro:Lyzer and photosynthetic radiation rates for 3.6 g m^{-2} N load batch run experiment completed in Summer 2014. R^2= 94.61 (organic), 99.72 (mineral), and 99.98 (control) between observed and UV-spectrometer NO_3-N values.

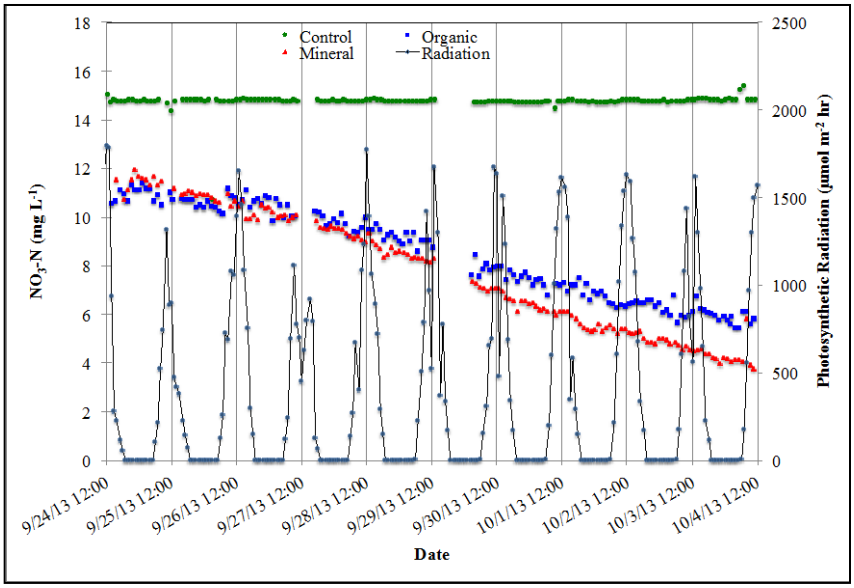

Figure 18*:* Hourly NO_3-N concentrations from the Spectro:Lyzer and photosynthetic radiation rates for 3.6 g m^{-2} N load batch run experiment completed in Fall 2013. R^2= 97.21 (organic), 98.66 (mineral), and 59.11 (control) between observed and UV-spectrometer NO_3-N values.

Nitrification has been observed to preferentially occur during the daytime due to production of oxygen from photosynthesis, while NO_3-N removal rates increase in the water column often at night due to the high oxygen demand of microbial mineralization and low oxygen concentrations (Rysgaard *et al.*, 1995), which supports the diurnal NO_3-N observations observed in this study. The larger observed daily increases in NO_3-N concentrations in the

organic systems compared to the mineral system may have contributed to the differences in removal rates between the two systems, since the organic system may have had a larger internal source of NO_3-N. Vähätalo and Wetzel (2013) evaluated the long-term photochemical and microbial decomposition of DOM of wetland derived humic DOM at the microcosm scale using a C^{13} isotope enrichment study. Photochemical mineralization was found to reduce decomposition time of common rush (*Juncus effusus*) by approximately 50% (459 days) compared to biological decomposition in darkness (898 days). NH_4^+-N produced from photochemical mineralization of organic matter in estuarine surface water has been observed to range between 0.005 to 0.027 mg NH_4^+-N L^{-1} hr^{-1} during the day, with NH_4^+-N production increasing as pH decreased from 6.0 to 3.5 (Wang *et al.*, 2000). Therefore, photochemical mineralization may have additionally impacted the observed differences in removal rates between the wetland systems observed in our study because even more NH_4^+-N may have been produced in the more acidic organic soil system compared to the mineral soil system.

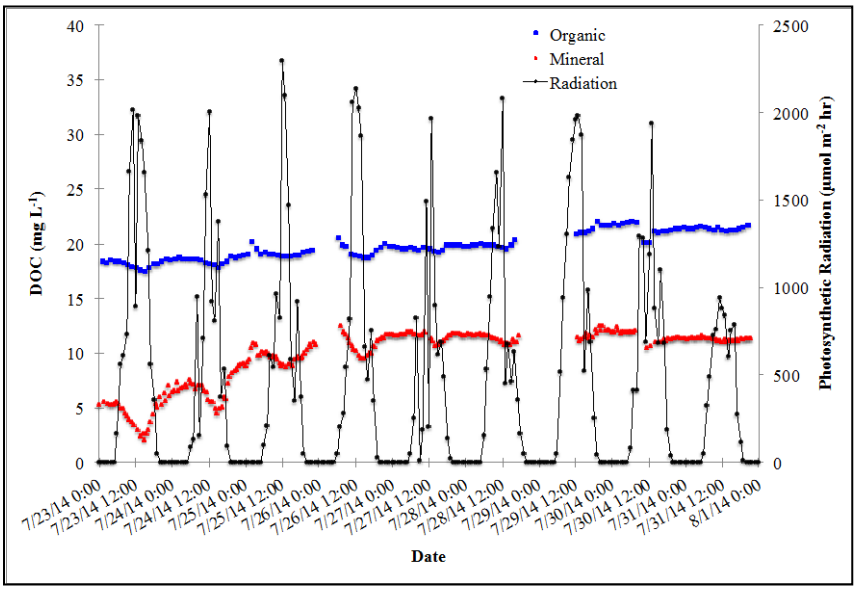

Figure 19: Hourly DOC concentrations from the Spectro:Lyzer and photosynthetic radiation rates for 3.6 g m^{-2} N load batch run experiment completed in Summer 2014. * Control values were unable to be calibrated for this experiment. R^2= 97.32 (organic) and 98.99 (mineral) between observed and UV-spectrometer NO_3-N values.

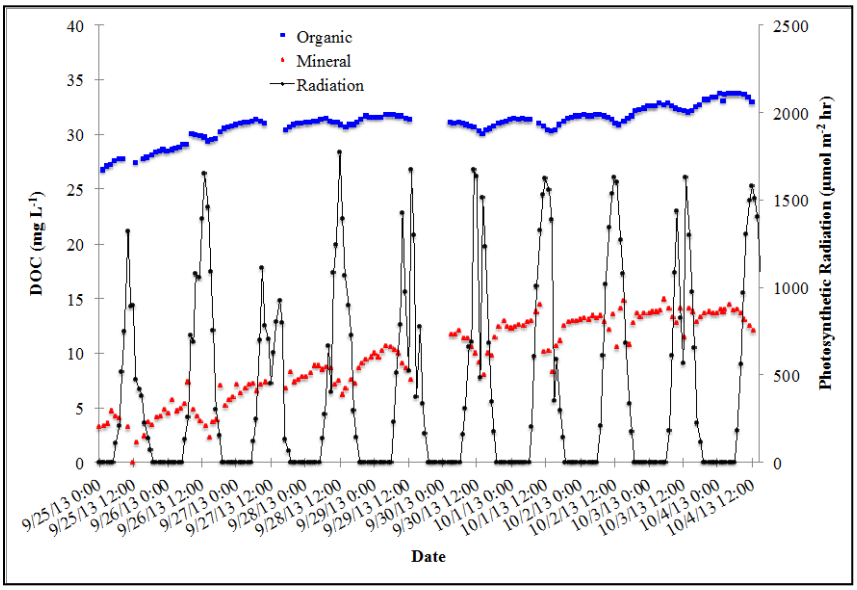

Figure 20*:* Hourly DOC concentrations from the Spectro:Lyzer and photosynthetic radiation rates for 3.6 g m^{-2} N load batch run experiment completed in Fall 2013. * Control values were unable to be calibrated for this experiment. R^2= 97.32 (organic) and 98.99 (mineral) between observed and UV-spectrometer NO_3-N values.

DOC appeared to increase overnight during our study and likely allowed the gradient between the soil/water interface begin to equilibrate while photochemical mineralization was not occurring. As dissolved organic matter (DOM) mineralizes a gradient is created between the surface water and soil pore water (Reddy and DeLaune, 2008). The concentration gradient between the sediment-water interface enables diffusion between the lower DOM concentrations and higher DOM concentrations until equilibrium is formed between the pore water and water column. Therefore, the DOC observations also support our theory that photochemical mineralization likely occurred within these systems and provided an internal NO_3-N source, particularly in the organic wetlands.

The mineral wetland systems had larger observed water column DOC *fluctuations* (3 to 5 mg L^{-1}) compared to the organic system (1 to 3 mg L^{-1}). Recall DOC concentrations had an inverse relationship to NO_3-N removal rates in this study. The mineral soil in this study was used for agricultural production for decades, while the organic soil was only used for silviculture and had been out of production for over 20 years. Liu *et al.* (2010) evaluated land use effects on labile carbon fractions for a natural wetland, uncultivated and degraded wetland, and cultivated wetland comprised of the same soil types. Labile carbon contents were significantly higher in cultivated soils compared to uncultivated and natural wetland soils. Therefore, the mineral soils in this study may have had more labile carbon available for denitrification compared to the organic soils resulting in higher NO_3-N removal rates.

3.2 NO_3-N Kinetic Models

3.2.1 Kinetic Model Fit to Individual Batch Run Observations

Observed daily NO_3-N concentrations were plotted over time for the batch runs to evaluate if the dataset's fit the zero order and first order models. Zero order values were

evaluated by fitting a linear line to NO_3-N concentration at time t versus time, while the first order model fit was evaluated by plotting the initial NO_3-N concentration divided by the NO_3-N concentration at time t versus time. The zero order kinetic model had a R^2 that ranged between 0.78 and 0.99 with an average of 0.97 in the mineral system, while the organic wetland systems had a R^2 that ranged from 0.81 to 0.99 with an average of 0.97. Mineral wetland treatments had an R^2 that ranged between 0.70 and 0.99 with an average of 0.95 in the first order model, while the organic wetland systems had an R^2 that ranged from 0.73 to 0.99 with an average of 0.94 for individual batch runs. The lower R^2 values were observed during the winter months when average water temperature was below 12 °C. All evaluations during the growing season had R^2 values above 0.90 for both the zero and first order fits to observed datasets.

The fit for the TIS model over time was evaluated by plotting $\left(\left(\frac{C_t}{C_o}\right)^{-\frac{1}{N}} - 1\right)N$ against time, where N was the number of tanks, which was assumed to be number of times water was circulated in the mesocosms or the hydraulic retention time since the turnover rate was once per day. The TIS model displayed strong fits for all of the evaluated runs with a R^2 that ranged between 0.98 and 1 with an average of 0.99 for both the mineral and the organic wetland systems, which was likely because of the impact of the N overriding the effect of concentration changes over time. The removal rate coefficients were then determined at 20 °C using the Arrhenius relationship for each of the three models since all exhibited strong fits.

The efficiency loss model was evaluated in R Studio to empirically solve for ρ_{EL} and α for individual mesocosms during batch run using NO_3-N concentration observations at each sampling point. The two unknown values (α and ρ_{EL}) were able to be determined for 80% of the total collected datasets and had good fits ($p>0.01$ for ρ_{EL} and $p>0.2$ for α). The mineral wetland treatments had an R^2 that ranged between 0.93 and 0.99 with an average of 0.98, while the organic wetland systems had an R^2 that ranged from 0.95 and 0.99 with an average of 0.98. ρ_{EL} was then determined for 20 °C using the Arrhenius relationship. R studio was unable to solve for α values in several runs due to limited datasets from quick NO_3-N removal periods or the NO_3-N change over time resembling a zero or first order decay relationship resulting in an α of 0 or 1, respectively. A α value that represented the individual wetland systems was difficult to determine since empirically determined α values often varied between 0-1 within the same treatment and batch run. Interactions between the α values and season, NO_3-N load, temperature and DO were not observed. However, differences between the α values and water depth were observed particularly in the mineral wetland systems. Therefore, α values empirically determined in R Studio were separated into treatment and initial water depths (18 and 30 cm). Average α values were then calculated based on initial water depth for each treatment and used as the initial input of α for the efficiency loss model to fit observed NO_3-N removal rates in the 9 of 18 batch run studies. The α values were then adjusted until the best fit was found between observed and predicted values.

The first nine of the 18 batch runs were used to determine K_s and J_{max} values for the two distinct wetland systems (Figure 21). K_s was the concentration at which point the NO_3-N removal rate was at half of the maximum NO_3-N removal rate (J_{max}) for the mineral and organic systems. The relationship between J_{NN} and C_f was evaluated using a Lineweaver-Burke plot to empirically determine the maximum areal removal rate (J_{max}) and the half-saturation constants (K_s) for the Monod model for each mesocosm and replicate. J_{max} and K_s were then averaged for replicates of each treatment. The organic wetland system had an

average maximum removal rate (J_{max}) of 0.38 ± 0.10 g m^{-2} d^{-1}, while the mineral systems had an average maximum removal rate of 0.50 ± 0.08 g m^{-2} d^{-1}. The average half-saturation constants (K_s) were 5.96 ± 2.84 and 5.63 ± 2.45 mg L^{-1} for the mineral and organic systems, respectively. The first-order mass transfer coefficient (ρ_M) is often estimated assuming $C_o << K_s$. However, this was not always true for our batch studies and may have led to inaccurate removal rate predictions by this model.

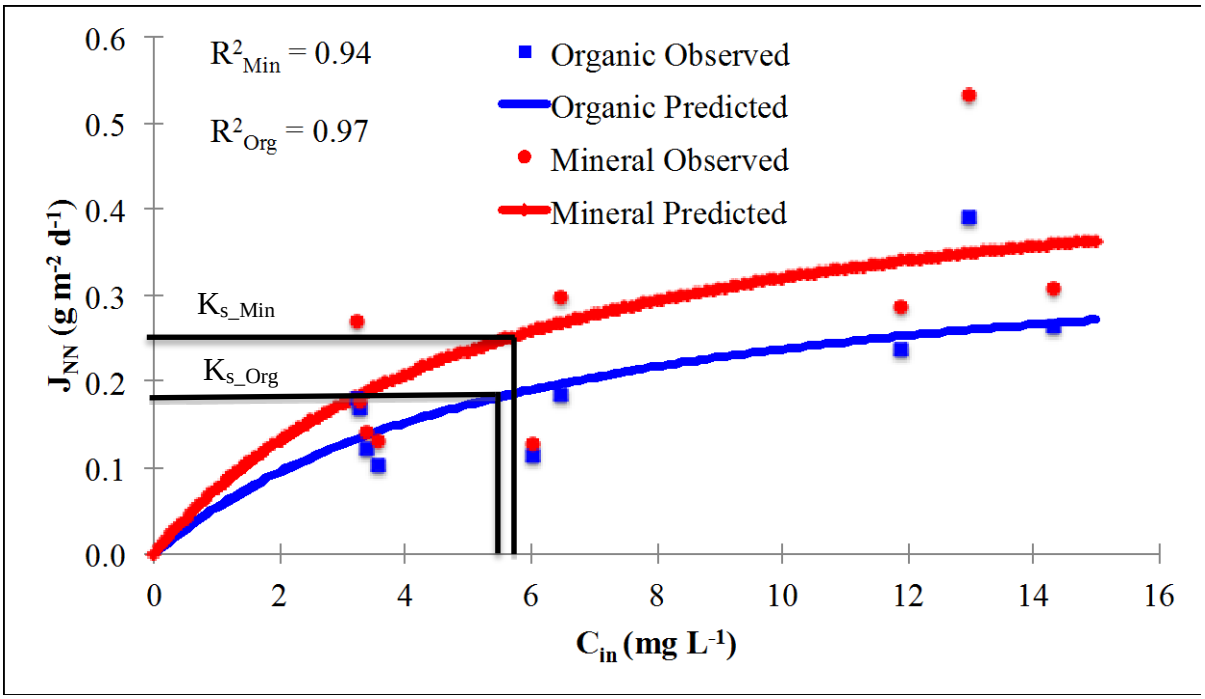

Figure 21: Areal removal rate (J_{NN}) versus initial NO_3-N concentration (C_0) to determine K_s and J_{max}. Nine of the 18 batch run datasets were used to estimate half-saturation constant (K_s) and maximum removal rate (J_{max}).

3.2.2 Development of Removal Rate Coefficients

Removal rate coefficients were calculated for each model using the first 9 of 18 batch runs. Computed values can be found along with published values from past mesocosm and full-scale wetland studies for comparison in Table 8. To our knowledge, no studies have reported using the efficiency loss and zero order models at the mesocosm scale, therefore, comparisons were made with full-scale systems. In general, our results were consistent with observed values from past published wetland studies.

Table 8: List of areal nitrate-N removal rate coefficients and efficiency loss constants (α) for average water temperature of 20 °C.

Wetland System	Initial Target Concentration ($mg\ L^{-1}$)	NO_3—N Removal Rate Coefficients for T_{20}					EL Constant (α) (unitless)	Reference
		J_{ZO} ($mg\ m^{-2}\ d^{-1}$) [θ: R^2]	ρ_{FO} ($cm\ d^{-1}$) [θ: R^2]	ρ_{EL} ($cm\ d^{-1}$) [θ: R^2]	ρ_M ($cm\ d^{-1}$) [θ: R^2]	ρ_{TIS} ($cm\ d^{-1}$) [θ: R^2]		
Mineral Mesocosm	2.5 – 15	94 ± 11 [1.03 ± 0.10: 0.58 to 0.66]	4.92 ± 0.8 [1.15 ± 0.02: 0.89 to 0.98]	10.2 [1.10: 0.72]	9.96 ± 2.26 [No Correlation]	5.78 ± 1.08 [1.16± 0.02: 0.89 to 0.97]	0.6 (15 cm depth) 0.7 (30 cm depth)	This study
Organic Mesocosm	2.5 – 15	92 ± 8 [1.04 ± 0.01: 0.06 to 0.15]	4.1 ± 1.0 [1.09 ± 0.06: 0.82 to 0.93]	8.0 [1.18: 0.67]	6.79 ± 1.48 [No Correlation]	4.79 ± 1.17 [1.15± 0.03: 0.83 to 0.90]	0.7 (15 cm depth) 0.7 (30 cm depth)	This study
Constructed Treatment Mesocosm	19		2.1 -2.9					Gebremariam and Beutel (2008)
Restored Riparian Microcosm	8.9				9.39			Karpuzcu and Stringfellow, 2012
Surface-Flow Constructed Mesocosm	32 - 117		5.7 – 16.5					Burchell *et al.*, 2007
Fluvial Wetlands	0.1 – 3.7			3 – 9.3			Not Reported	Wollheim *et al.*, 2014
Free Surface Constructed Wetlands	10 - 26	200 – 5,000						Horne, 1995
Event Driven Constructed Wetlands	0.05 – 2					34.5		Kadlec, 2010
Continuous Flow Constructed Wetlands Mesocosms						9.9		Kadlec, 2010

**[θ: r^2] represents the calculated theta and R^2 to determine the NO_3-N coefficients at average water temperature T=20°C.*

3.2.3 Comparison of Kinetic Model Fits

Observed NO_3-N removal rates from the remaining 9 batch run datasets (not used for calculating removal rate coefficients) were used to compare the predicted values produced by each of the kinetic models developed and evaluate the goodness of fit for each model. Initial and final concentrations along with estimated removal rate coefficients adjusted for average water temperature and the efficiency loss constant (α) developed (Table 9) were used to make predictions and compared to the observed removal rates to evaluate the goodness of fit of each of the kinetic models. A regression of the average $J_{Predicted}$ vs. $J_{Observed}$ for each of the five models are displayed in Figure 23. The first order, efficiency loss, and TIS models had the strongest fits between the predicted and measured values with $R^2 \geq 0.95$, but the efficiency loss model had a slightly better fit than the first order and TIS models (Table 9).

The fit of the zero order and Monod models was weak between the predicted and observed J_{NN} for all statistical parameters (Table 9). The zero order model consistently under predicted the J_{NN} for all NO_3-N loads, while the Monod model over predicted rates at low concentrations and under predicted NO_3-N removal rates at higher concentrations. Therefore, it was determined that the zero order and Monod models were not adequate predictors for NO_3-N removal in these wetland systems and were excluded from further analysis.

Figure 22: Regression of the a.) zero order, b.) first order decay, c.) efficiency loss, d.) tanks in series, and e.) Monod kinetic models for correlating predicted and observed average NO_3-N removal rates for the two restored wetland systems adjusted for average water temperature.

a.)

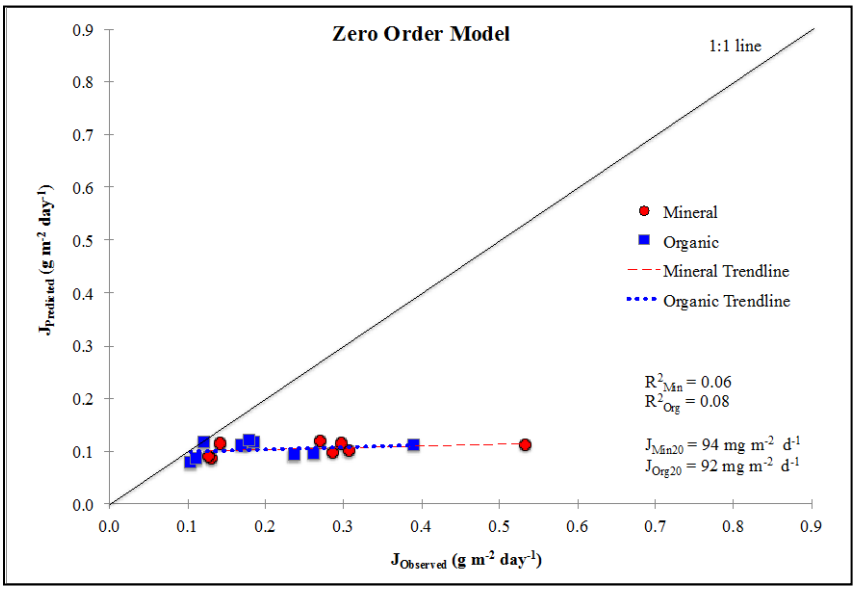

b.)

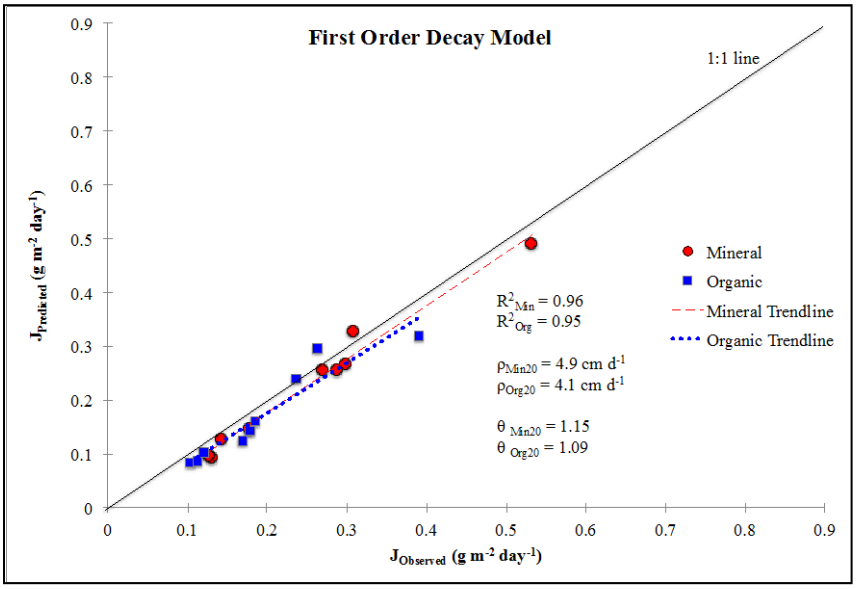

c.)

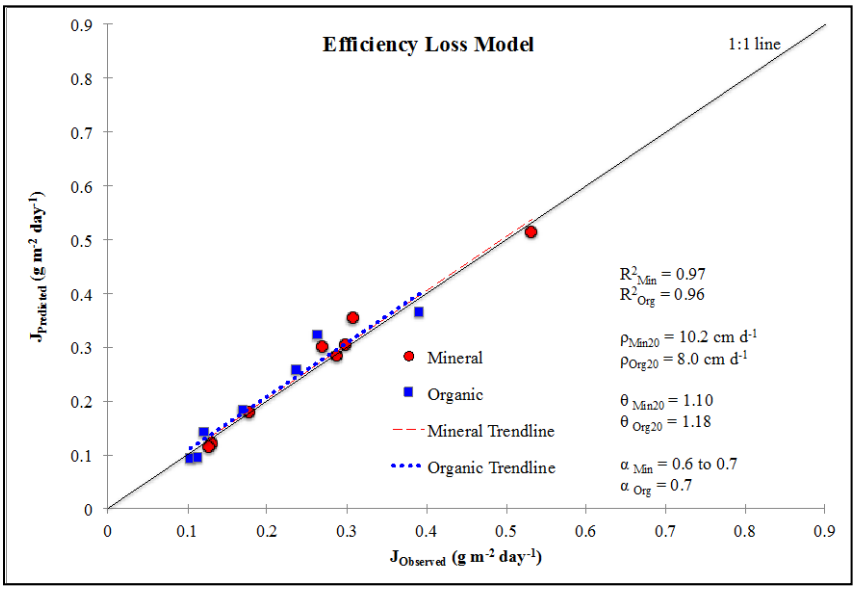
Efficiency Loss Model
1:1 line
$J_{Predicted}$ (g m^{-2} day^{-1})
$J_{Observed}$ (g m^{-2} day^{-1})
R^2_{Min} = 0.97
R^2_{Org} = 0.96
ρ_{Min20} = 10.2 cm d^{-1}
ρ_{Org20} = 8.0 cm d^{-1}
θ_{Min20} = 1.10
θ_{Org20} = 1.18
α_{Min} = 0.6 to 0.7
α_{Org} = 0.7
Mineral
Organic
Mineral Trendline
Organic Trendline

d.)

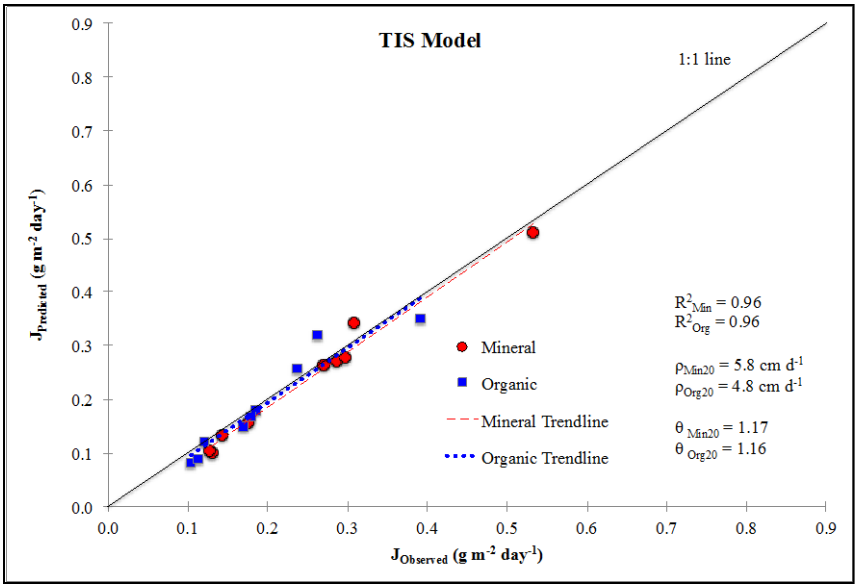
TIS Model
1:1 line
$J_{Predicted}$ (g m^{-2} day^{-1})
$J_{Observed}$ (g m^{-2} day^{-1})
R^2_{Min} = 0.96
R^2_{Org} = 0.96
ρ_{Min20} = 5.8 cm d^{-1}
ρ_{Org20} = 4.8 cm d^{-1}
θ_{Min20} = 1.17
θ_{Org20} = 1.16
Mineral
Organic
Mineral Trendline
Organic Trendline

e.)

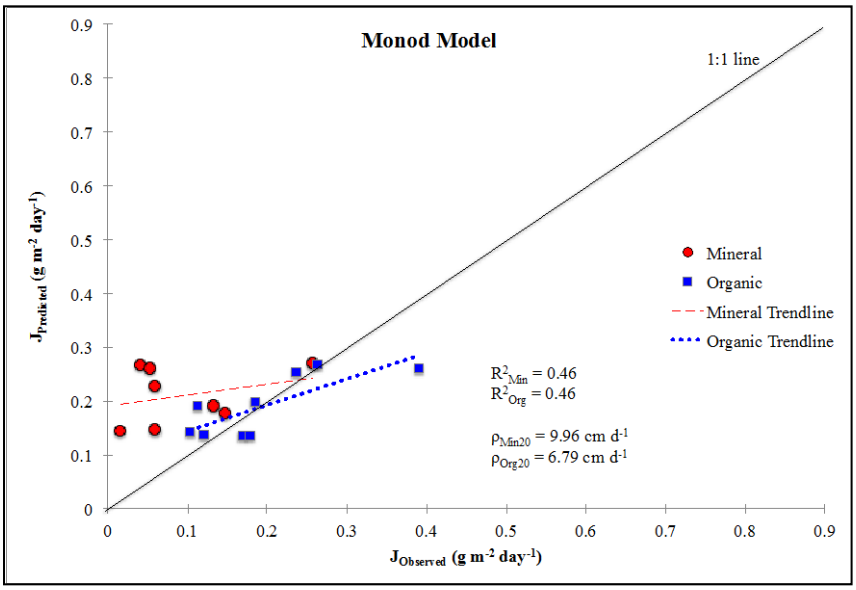

Table 9: Statistical parameters used to evaluate goodness of fit of predicted versus observed NO_3-N removal rate for each kinetic model.

Wetland System	Mineral					Organic				
	ZO	FO	EL	TIS	M	ZO	FO	EL	TIS	M
R^2	0.06	0.96	0.97	0.96	0.46	0.08	0.95	0.96	0.96	0.46
RRMSE	0.61	0.12	0.10	0.10	3.68	0.61	0.20	0.10	0.11	0.82
MEF	-1.59	0.90	0.94	0.93	-0.22	-0.81	0.81	0.96	0.94	0.42
ME (g m^{-2} d^{-1})	0.10	0.02	-0.01	0.01	-0.17	0.08	0.03	0.00	0.01	-0.06
MAE (g m^{-2} d^{-1})	0.10	0.02	0.07	0.02	0.17	0.08	0.03	0.10	0.02	0.68
NPE (%)	-49.86	-9.07	4.10	-5.23	36.85	-42.79	-16.46	1.10	-7.23	58.79

*Statistical acronyms represent: Coefficient of determination (R^2), Relative root mean square error (RRMSE), Model efficiency (MEF), mean error (ME), mean absolute error (MAE), and normalized percent error (NPE). **Kinetic acronyms represent: Zero order (ZO), first order (FO), efficiency loss (EL), tanks in series (TIS), and Monod (M) models.

The weak fits between the predicted and observed J_{NN} were not surprising for the zero order and Monod models. Based on assumptions for the zero order model, J_{NN} is not affected by increased loads of NO_3-N. During every season, as NO_3-N loads increased the observed removal rates also increased. Therefore, the assumptions required to use the zero order model were not met for these systems. K_s values, empirically calculated as 5.96 mg L^{-1} for the mineral system and 5.63 mg L^{-1} for the organic system, were not significantly larger than C_o (initial concentrations) in batch runs where target C_o were 2.5 mg L^{-1}. K_s values were assumed to be significantly greater than C_0 to estimate ρ_M, which likely resulted in inaccurate estimates. Zero and Monod kinetic models are often used in wastewater treatment wetland systems where high initial NO_3-N concentrations allow for the systems to become saturated resulting in a maximum removal rate (J_{zo}), which in this case would be equivalent to the J_{max} of the Monod kinetic model. However, based on observed removal rates, the wetland mesocosm systems never reached a saturation point likely resulting in inaccurate estimates for the removal coefficients for the zero order and Monod kinetic models. Therefore, these models are not

recommended to be used for lightly loaded wetlands receiving low NO_3-N concentrations, similar to the systems evaluated in this study.

Stronger statistical results were observed for the first order, efficiency loss, and TIS models. Each of the models predicted NO_3-N removal rates based on initial NO_3-N loads and did not require the determination of saturation coefficients such as K_s. The first order model and TIS model had similar fits. The efficiency loss model had the best fit between predicted and observed NO_3-N removal rates. Therefore, since the first order model is the most common model used for these systems, a more thorough investigation was conducted between the first order and efficiency loss models to determine the best method of modeling the full scale wetland systems. The TIS model was not included since it had similar fits to the first order model and required an extra parameter (N) that may be difficult to determine at the field scale.

Hydraulic retention time of surface water must stay within the range of 1 to 10 days in the full-scale wetland environments to preserve established and recently planted trees (Petru *et al.*, 2014; Teskey and Hinckley, 1977). Therefore, NO_3-N concentrations predicted to leave the wetland systems after a hydraulic retention time of 7 days were compared between the first order and efficiency loss models along with observed concentrations for each batch run study (Figures 23 and 24).

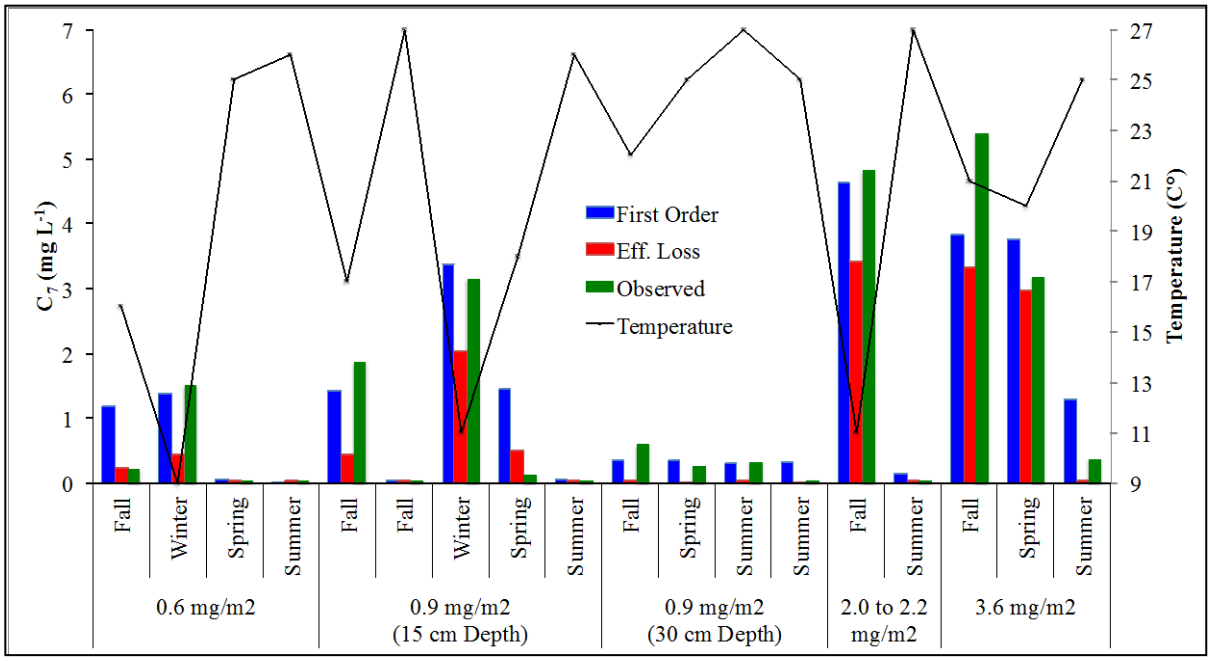

Figure 23: Predicted NO_3-N concentrations after 7 days of residence time (C_7) in the mineral wetland system for the efficiency loss and first order kinetic models compared to observed values.

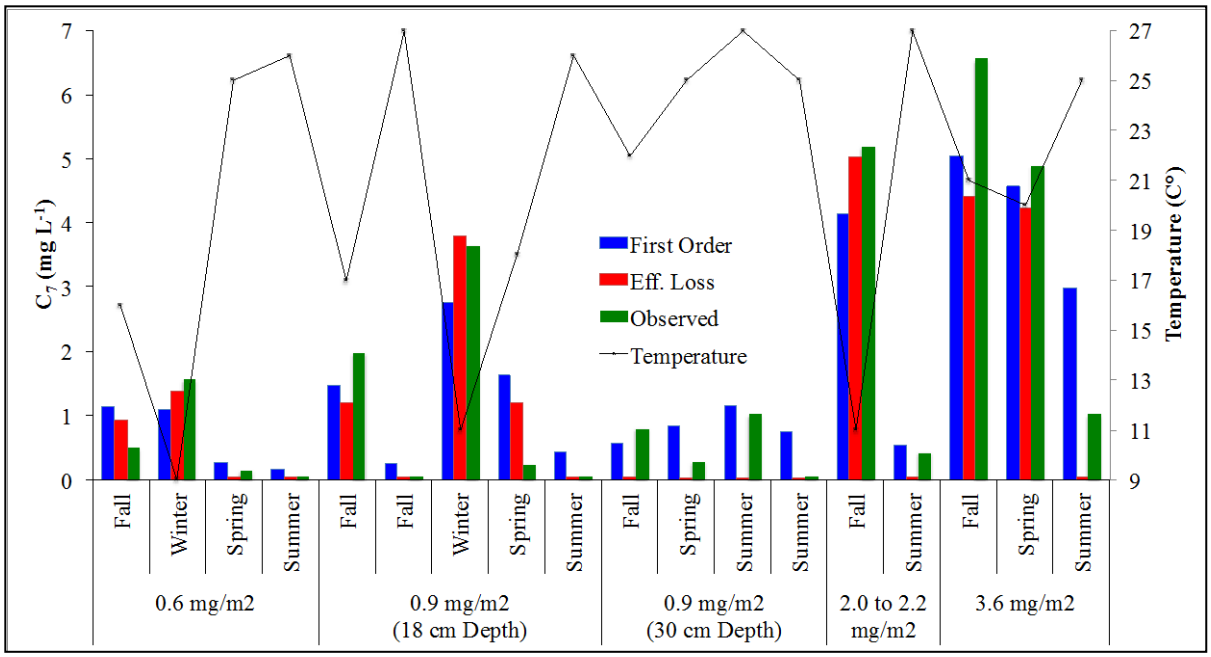

Figure 24: Predicted NO_3-N concentrations after 7 days of residence time (C_7) in the organic wetland system for the efficiency loss and first order kinetic models compared to observed values.

Predicted C_7 (NO_3-N concentrations after 7 days within the wetland mesocosm) values from the first order model over predicted NO_3-N concentrations on average 0.09 mg L^{-1} more than observed NO_3-N concentrations, with a maximum over prediction of 1.97 mg L^{-1} and under prediction of 1.59 mg L^{-1} compared to observed C_7 values. The efficiency loss model predicted C_7 values to under predict NO_3-N concentrations after 7 days on average by 0.4 mg L^{-1}, with maximum over predictions of only 0.98 mg L^{-1} and under prediction by as much as 2.1 mg L^{-1}. Differences between the two fitted models' predictions of NO_3-N concentrations can be explained with the assumption criteria for each kinetic model. In the efficiency loss model, as NO_3-N becomes more limited the model accounts for additional demand by plants and microbes. The first order model instead assumes the demand for NO_3-N will remain constant throughout the evaluated time period (O'Brien *et al.*, 2007). Both fitted models had a tendency to predict lower final NO_3-N concentrations during the end or outside the growing season than was observed, when average water temperatures were often below 11 °C. However, during the growing season the first order model tended to predict higher NO_3-N concentrations during the growing season, while the efficiency loss model often predicted lower NO_3-N concentrations when compared with observations. Therefore, the first order model should provide slightly more conservative predictions than the efficiency loss model particularly during the growing season. Hydraulic retention time was most limited during the growing season due to constraints to preserve established and newly planted tree health at restoration sites. However, less conservative predictions were expected outside the growing season and longer retention times are recommended since inundation periods will not have as great of an impact on tree health during these times.

The first order decay model was further evaluated by accounting for predicted and measured removal rates between each sampling point (Day 1 to 2, 2 to 3, 3 to 5, 5 to 7, and 7 to 10). Although the removal rates varied throughout each batch run (based on residence time,

NO_3-N concentrations in the water column, season, etc.), the first order model remained a reasonable fit for all sampling intervals evaluated (R^2_{Org}=0.70 and R^2_{Min}=0.73). Average ρ_{FO} values at 20 °C increased as retention time increased ranging from 4.52 cm d^{-1} with 1 day retention and peaking at 10.0 cm d^{-1} after 5 days of residence time in the organic systems. The mineral systems had similar trends with average ρ_{FO} values at 20 °C increasing from an average 4.8 cm d^{-1} with 1 day retention and peaking at 10.7 cm d^{-1} after 7 days of residence time in the wetland mesocosms. The ρ_{FO} values that were not adjusted for temperature were observed to be as high as 35.0 cm d^{-1} and 36.0 cm d^{-1} in the organic and mineral wetland mesocosms, respectively, during the temperatures above 25 °C in the growing season.

Although the efficiency loss model had a slighter stronger ability to predict final NO_3-N concentration than the first order decay model, the α constant must be empirically calculated for several batch runs to be accurately determined, which is often not practical for wetland designers. Therefore, the first order decay model was recommended to predict maximum NO_3-N removal rates for the full-scale wetland restorations.

3.2.4 Theoretical Wetland Predictions

A theoretical wetland with a size of 210 ha, similar to the Phase 1 of the wetland restoration in Hyde County, was used to provide an initial estimate of the maximum hydrologic loading capacity for the two wetland soils (mineral and organic), based on the first order NO_3-N removal model developed. The sites were expected to receive agricultural drainage with NO_3-N concentrations of 2.5 mg L^{-1}. The maximum hydrologic loading capacities for the wetlands with NO_3-N concentrations leaving the wetland with 0.1 mg L^{-1} (96% reduction), 0.5 mg L^{-1} (80% reduction), 1.0 mg L^{-1} (60% reduction), and 1.75 mg L^{-1} (30% reduction) were evaluated at various average water temperatures.

Based on the estimated removal rates, the maximum loading rates of agricultural drainage water that could be applied were estimated to meet the range of target outflow concentrations at the end of wetland areas (C_{eff}) utilizing the following equation (Burchell *et al.,* 2007; Reed *et al.,* 1995):

$$L = \frac{n * \rho_{20}}{\ln \frac{C_{eff}}{C_{in}}} \theta^{(T-20)} \qquad \textbf{Eq. 13}$$

where L is the maximum loading rate into the wetland (m d^{-1}), C_{eff} is the effluent NO_3-N concentration (mg L^{-1}), C_{in} is the influent NO_3-N concentration (mg L^{-1}), T is the temperature (C°), ρ_{20} is the NO_3-N mass transfer coefficient (0.049 m d^{-1} and 0.041 m d^{-1} for the mineral and organic systems, respectively) at 20 °C, n is the porosity (approximately 0.95 in surface flow wetlands), and θ (1.15 and 1.09 for the mineral and organic systems, respectively). The ρ_{20} and θ were values determined by fitting observed data from the mesocosm batch studies to first order decay model (Table 10).

Maximum hydrologic loading capacities for the two wetland systems for varying NO_3-N removal goals and average water temperatures can be found in Table 10. Based on 96% removal goals, the mineral and organic wetland systems have the predicted capacity to receive 1.5 and 1.2 cm day^{-1}, respectively, assuming average water temperature are 20 °C. However, if the goal was only to comply with the Tar Pamlico River Basin Rule (30% removal), the mineral and organic wetland systems have the predicted capacity to receive up to 13.1 and 10.8

cm day^{-1}, respectively, and meet the target removal threshold. This table provides an example of how powerful these decay constants can be in determining how wetlands like these can be managed.

Table 10: Predicted maximum hydrologic loading capacities for the future restored wetlands assuming n of 0.95, and C_{in} of 2.5 mg L^{-1} using the first order decay kinetic model assuming steady flow conditions 365 day yr^{-1}.

NO_3-N % Reduction	**96%**		**80%**		**60%**		**30%**	
Target C_{eff} (mg L^{-1})	**0.1**		**0.5**		**1.0**		**1.75**	
Avg. Water Temperature (C°)	**Mineral (cm day^{-1})**	**Organic (cm day^{-1})**	**Mineral (cm day^{-1})**	**Organic (cm day^{-1})**	**Mineral (cm day^{-1})**	**Organic (cm day^{-1})**	**Mineral (cm day^{-1})**	**Organic (cm day^{-1})**
10	0.4	0.5	0.7	1.0	1.3	1.8	3.2	4.6
15	0.7	0.8	1.4	1.6	2.5	2.7	6.5	7.0
20	1.5	1.2	2.9	2.4	5.1	4.2	13.1	10.8
25	2.9	1.8	5.8	3.7	10.3	6.5	26.4	16.6
30	5.9	2.8	11.7	5.7	20.6	10.0	53.0	25.6

3.3 ^{15}N Enrichment Studies

3.3.1 Observed overall NO_3-N removal

Water temperatures during the ^{15}N enrichment studies ranged from 20 to 30 °C. All studies were initiated around 12 PM and weather during the day was predominately sunny throughout the experiments. Water movement through the wetland mesocosms was approximately 1000 L day^{-1}. $^{14+15}NO_3^-N$ concentrations were reduced by 92% and 91% within 7 days in the organic and mineral wetland mesocosms, respectively, in the 0.9 g m^{-2} ^{15}N isotope enrichment study (Figure 25; Table 11). Similarly, $^{14+15}NO_3^-N$ concentrations were reduced by 90% and 99% within 10 days in the organic and mineral wetland mesocosms, respectively, in the 3.6 g m^{-2} ^{15}N isotope enrichment study (Figure 26). The removal of NO_3-N was significantly faster in the mineral wetland systems compared to the organic systems during the 3.6 g m^{-2} loading experiments ($p < 0.05$), while significant differences in NO_3-N removal between treatments were not observed in the 0.9 g m^{-2} load experiment.

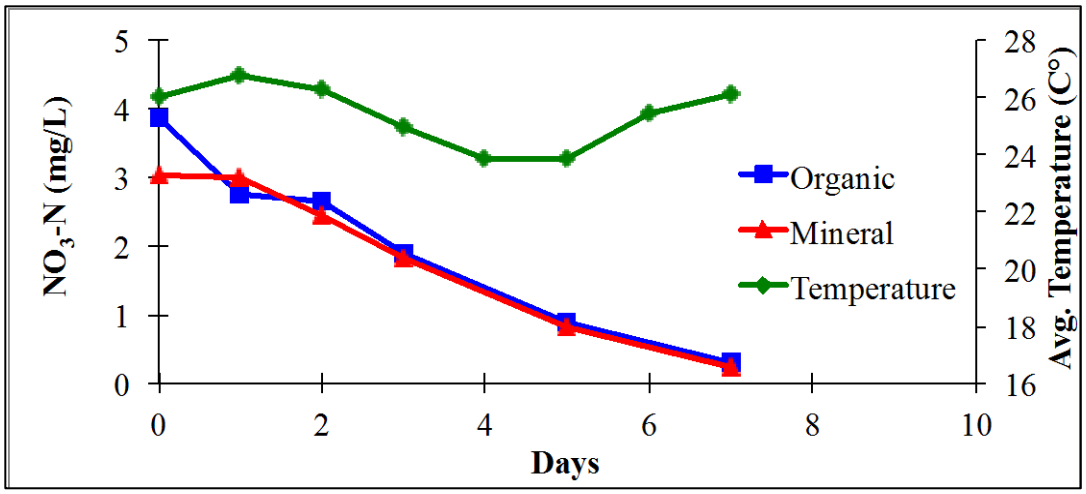

Figure 25: $^{14+15}$NO-N reductions in the 0.9 g $^{14+15}NO_3$-N m^{-2} load ^{15}N enrichment study with average daily water temperature.

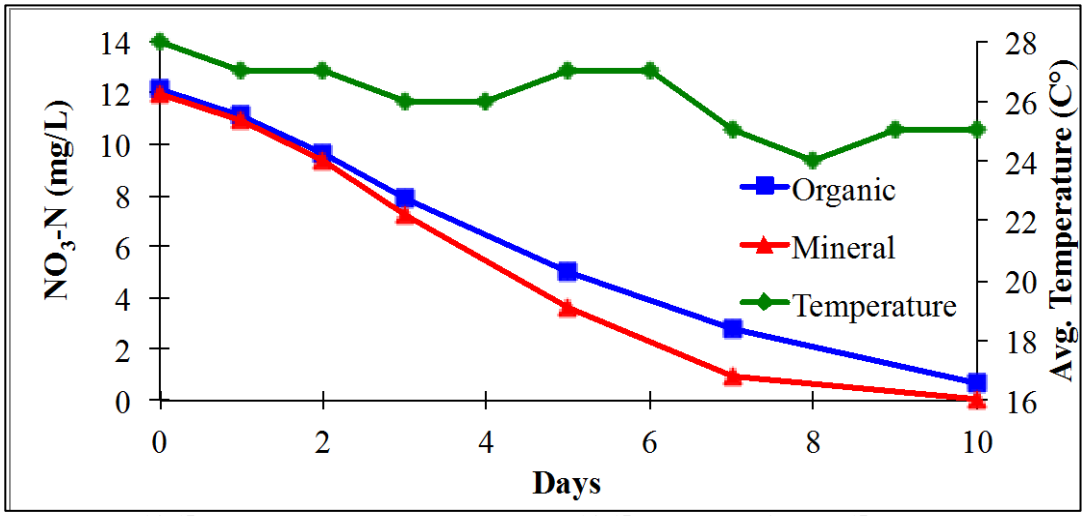

Figure 26: $^{14+15}$NO-N reductions in the 3.6 g $^{14+15}NO_3$-N m^{-2} load ^{15}N enrichment study with average daily water temperature.

Table 11: Summary of ^{15}N isotope enrichment experiments.

Study	Mean Water Temperature	Water Depth	Load	Mean NO_3^-N % Reduction		J_{NN} ± SD	
				$Wetland_{Min}$	$Wetland_{Org}$	$Wetland_{Min}$	$Wetland_{Org}$
	°C	cm	g m^{-2}	----------%		--------mg m^{-2}--------	
Exp. 1	22 – 28	30	0.9	92	91	150	150
Exp. 2	23 – 28	30	3.6	98	90	544	394

Conditions favorable for denitrification were observed in both experiments (Rivett *et al.*, 2008; Puckett, 2004). Dissolved oxygen in the water column decreased to <5 mg L^{-1} during both studies. Wetland systems with dissolved oxygen concentrations as high as 6 - 10 mg L^{-1} in surface water have been found to reduce dissolved oxygen concentrations to <0.01 mg L^{-1} within 2 mm from the soil-water interface (Crumpton and Phipps, 1992). Low soil redox values were measured during this study (-93 - 125 mV) further supporting the likelihood of low dissolved oxygen concentrations in the soil column and high denitrification potential, since

readings below 250 mV have been found to provide conditions favorable for NO_3^--N reduction through denitrification (Cey *et al.*,1999; Patrick, 1960). The wetland mesocosms had DOC concentrations that ranged from 7 to 16.4 mg L^{-1} in the mineral system and 11 to 60 mg L^{-1} in the organic system, much higher concentrations than those that have been observed to support denitrification (4-8 mg/L) particularly in the organic systems (Sloan et al, 1999; Spruill *et.* al, 1997; Obenhuber and Lowrance, 1991; Lowrance and Smittle, 1988). Water pH ranged from 5.9 to 6.4 in the organic systems and 6.0 to 6. 5 in the mineral systems. Denitrifying bacteria have been found to function best near neutrality, because low pH inhibits enzyme activity and thus denitrification rates, which may have impacted differences in observed removal rates between treatments (Sylvia *et al.*, 1998; Broome, 1990). NH_4^+-N concentrations in the water column decreased from 0.59 to 0.48 mg $L^{-1}$and 0.68 to 0.63 mg L^{-1} in the organic and mineral wetland systems, respectively, to below detectable values (<0.05 mg L^{-1}) within 48 hours of enrichment supporting NO_3-N as the primary form of N in the water column.

Addition of the $^{15}NO_3$-N and Br^- solution increased $^{15}NO_3$-N and Br^- concentrations in the water column of the mesocosms in both ^{15}N enrichment tracer studies. Br^- concentrations stabilized within 24 hours, which indicated the system was well mixed and the enrichment solution was mixed into the system adequately (Figures 27 and 28). Concentrations remained relative consistent following 2 days of water recirculating through the mesocosm in the organic systems, while concentrations increased slightly in the mineral systems. Br^- concentrations were then used to adjust water quality measurements (NO_3-N, NH_4^+-N, DOC, $^{15}N_2$-N, and $^{15}NO_3$-N) to account for evapotranspiration within the systems. NO_3^-/Br^- ratios decreased throughout the experiment indicating biological removal of NO_3-N occurring within the wetland mesocosms, while Br^- remained in the water column.

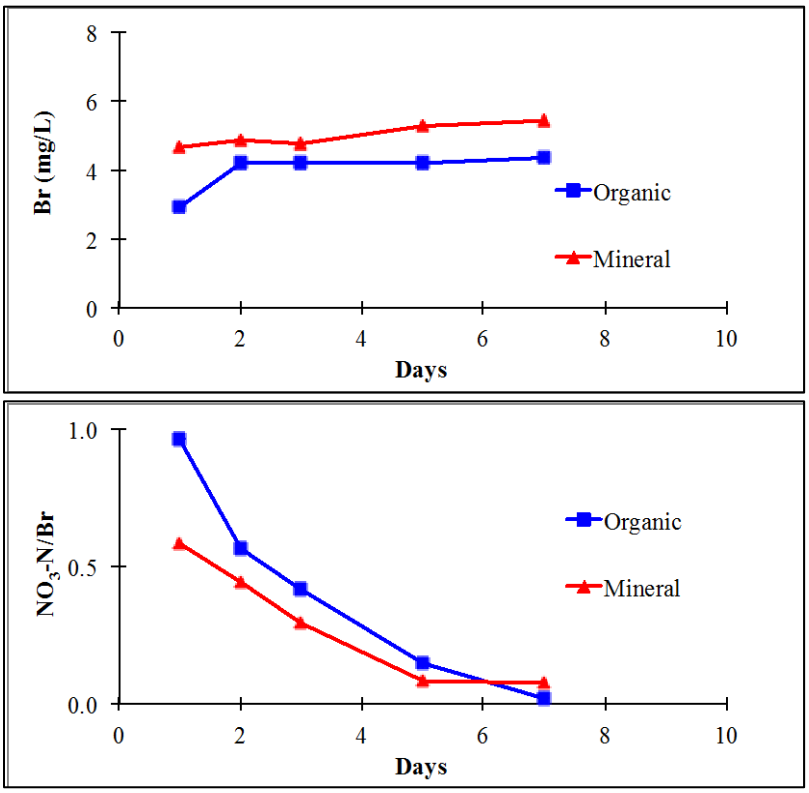

Figure 27: Surface water chemical concentrations in the wetland mesocosms through time for the first ^{15}N enrichment study with target NO_3-N load of 0.9 g m^{-2}.

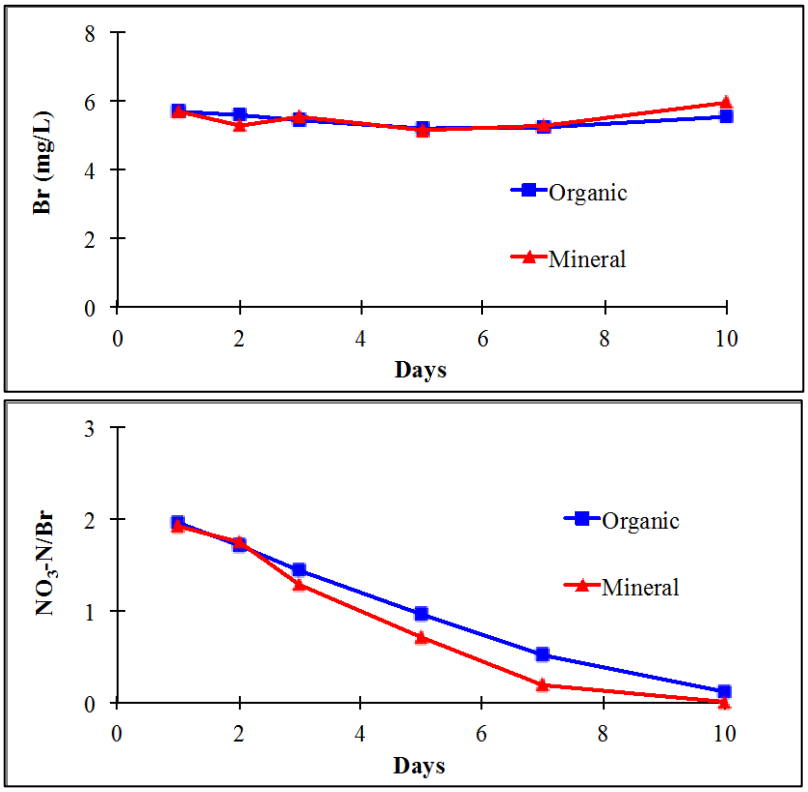

Figure 28: Surface water chemical concentrations in the wetland mesocosms through time for the second ^{15}N enrichment study with target NO_3-N load of 3.6 g m^{-21}.

3.3.2 ^{15}N Enrichment of the Mesocosms

Following the ^{15}N enrichments, there was a significant increase from the initial $\delta^{15}N$ natural abundance signatures in each N pool (Table 12 and 13). The natural occurring ^{15}N in the system (often assumed 0.364 At% or 0.364% of all natural occurring $^{14+15}N$) was important to identify to accurately calculate the percent ^{15}N recovery and reduce error (Harrison *et al.*, 2012). Non-enriched values were found to be within the expected range. All changes in $\delta^{15}N$ from pre to post enrichment were found to be significant in the biomass, soil, gas, and water pools (α=0.05). These differences meant % enrichment at the onset of the experiments was enough to use the tracer to distinguish $^{15}NO_3$-N transformation routes.

Table 12: Summary of biomass and soil enrichment measurements for the 0.9 g NO_3-N m^{-2} load ^{15}N enrichment study. N=3 for each category of soil and biomass non-enriched and enriched samples.

2013		Non-Enriched Average			Enriched Average		
		%N	$\delta^{15}N$ (permil)	At% (100*Atom Fraction)	%N	$\delta^{15}N$ (permil)	At% (100*Atom Fraction)
Mineral	Dead Biomass$^{\tau}$	0.83 ± 0.18	23.20 ± 3.71	0.3748 ± 0.0014	0.83 ± 0.18	338.17 ± 262.50	0.4895 ± 0.0955
	Live Biomass$^{\tau}$	0.80 ± 0.12	19.87 ± 4.86	0.3735 ± 0.0018	0.80 ± 0.12	3,628.66 ± 1547.28	1.6712 ± 0.5487
	Other Biomass$^{\Psi}$	1.19 ± 0.63	32.46 ± 2.70	0.3781 ± 0.0010	1.19 ± 0.63	3,727.72 ± 2134.13	1.7045 ± 0.7611
	Root Biomass$^{\tau}$	0.44 ± 0.11	12.39 ± 3.73	0.3708 ± 0.0014	0.44 ± 0.11	731.94 ± 132.61	0.6327 ± 0.0481
	Seed Biomass$^{\tau}$	0.91 ± 0.04	24.00 ± 6.30	0.3751 ± 0.0023	0.91 ± 0.04	99.68 ± 57.88	0.4027 ± 0.0211
	0-1 cm Soil	0.14 ± 0.05	4.05 ± 1.05	0.3678 ± 0.0004	0.14 ± 0.05	42.91 ± 24.41	0.3819 ± 0.0089
	1 -5 cm Soil	0.13 ± 0.01	3.77 ± 0.59	0.3677 ± 0.0002	0.13 ± 0.01	67.42 ± 40.65	0.3909 ± 0.0148
	6-15 cm soil	0.12 ± 0.02	3.30 ± 0.31	0.3675 ± 0.0001	0.12 ± 0.02	29.20 ± 16.02	0.3769 ± 0.0058
Organic	Dead Biomass$^{\tau}$	0.86 ± 0.13	10.29 ± 1.36	0.3700 ± 0.0005	0.86 ± 0.13	789.25 ± 203.17	0.6535 ± 0.0737
	Live Biomass$^{\tau}$	0.99 ± 0.29	17.47 ± 7.31	0.3727 ± 0.0027	0.99 ± 0.29	5,607.60 ± 85.08	1.6830 ± 0.0302
	Other Biomass$^{\Psi}$	-	-	-	-	-	-
	Root Biomass$^{\tau}$	0.95 ± 0.13	8.26 ± 4.05	0.3693 ± 0.0015	0.95 ± 0.13	1,581.48 ± 1118.00	0.9390 ± 0.4028
	Seed Biomass$^{\tau}$	0.99 ± 0.13	14.31 ± 2.26	0.3715 ± 0.0008	0.99 ± 0.13	1,094.51 ± 1405.58	0.7624 ± 0.5075
	0-1 cm Soil	0.99 ± 0.10	2.31 ± 0.22	0.3671 ± 0.0001	0.99 ± 0.10	96.73 ± 50.47	0.4016 ± 0.0184
	1 -5 cm Soil	0.85 ± 0.19	1.88 ± 0.33	0.3668 ± 0.0004	0.85 ± 0.19	74.34 ± 39.13	0.3934 ± 0.0143
	6-15 cm soil	0.80 ± 0.20	1.62 ± 0.59	0.3667 ± 0.0004	0.80 ± 0.20	28.89 ± 5.14	0.3768 ± 0.0019

$^{\tau}$ Biomass was *S. tabernaemontani*. $^{\Psi}$Biomass was species other than *S. tabernaemontani.*

Table 13: Summary of biomass and soil enrichment measurements for the 3.6 g NO_3-N m^{-2} load ^{15}N enrichment study. N=5 for each category of soil and biomass non-enriched and enriched samples.

2014		Non-Enriched Average			Enriched Average		
		%N	$\delta^{15}N$ (permil)	At% (100*Atom Fraction)	%N	$\delta^{15}N$ (permil)	At% (100*Atom Fraction)
Mineral	Dead Biomass$^{\tau}$	0.70 ± 0.12	18.38 ± 2.23	0.3730 ± 0.0008	0.70 ± 0.12	3,980.70 ± 1315.17	1.7964 ± 0.4666
	Live Biomass$^{\tau}$	0.62 ± 0.06	12.02 ± 1.18	0.3707 ± 0.0004	0.62 ± 0.06	4,250.41 ± 849.92	1.8930 ± 0.3007
	Other Biomass$^{\Psi}$	1.44 ± 0.18	15.93 ± 1.86	0.3721 ± 0.0007	1.44 ± 0.18	9,297.70 ± 2979.59	3.6406 ± 1.0134
	Root Biomass$^{\tau}$	0.36 ± 0.23	14.12 ± 1.32	0.3714 ± 0.0005	0.36 ± 0.23	2,804.20 ± 831.28	1.4868 ± 0.2970
	Seed Biomass$^{\tau}$	1.32 ± 0.15	19.49 ± 19.49	0.3734 ± 0.0023	1.32 ± 0.15	1,882.97 ± 728.58	1.0482 ± 0.2625
	0-1 cm Soil	0.27 ± 0.14	12.59 ± 4.37	0.3709 ± 0.0016	0.27 ± 0.14	1,359.35 ± 1112.96	0.8586 ± 0.4014
	1-5 cm Soil	0.15 ± 0.02	5.30 ± 0.49	0.3682 ± 0.0002	0.15 ± 0.02	243.29 ± 230.89	0.4549 ± 0.0841
	6-15 cm soil	0.17 ± 0.02	6.13 ± 1.45	0.3685 ± 0.0005	0.17 ± 0.02	38.01 ± 16.87	0.3802 ± 0.0062
	NH_4^+-N 0-2 cm Soil	-	13.03 ± 0.99	0.3710 ± 0.0004	-	8,889.00 ± 1919.36	3.5051 ± 0.6551
	NH_4^+-N 2-5 cm Soil	-	15.29 ± 4.84	0.3719 ± 0.0018	-	1,076.57 ± 332.00	0.7576 ± 0.1203
	Algae in Water Column	0.31 ± 0.21	23.36 ± 9.19	0.3748 ± 0.0034	0.31 ± 0.21	4,133.87 ± 2538.30	1.8469 ± 0.9030
	Algae on Tank	0.18 ± 0.05	13.96 ± 5.54	0.3714 ± 0.0020	0.18 ± 0.05	5,039.34 ± 855.10	2.1715 ± 0.3013
Organic	Dead Biomass$^{\tau}$	1.02 ± 0.32	14.52 ± 0.63	0.3716 ± 0.0002	1.02 ± 0.32	2,333.17 ± 435.11	1.2103 ± 0.1559
	Live Biomass$^{\tau}$	0.89 ± 0.09	10.75 ± 1.68	0.3702 ± 0.0006	0.89 ± 0.09	1,355.79 ± 495.73	0.8582 ± 0.1795
	Other Biomass$^{\Psi}$	-	-	-	-	-	-
	Root Biomass$^{\tau}$	1.21 ± 0.22	12.54 ± 1.85	0.3709 ± 0.0007	1.21 ± 0.22	1,333.00 ± 517.94	0.8501 ± 0.1872
	Seed Biomass$^{\tau}$	1.41 ± 0.21	18.82 ± 9.01	0.3732 ± 0.0033	1.41 ± 0.21	488.24 ± 131.50	0.5441 ± 0.0478
	0-1 cm Soil	1.05 ± 0.14	6.26 ± 1.60	0.3686 ± 0.0006	1.05 ± 0.14	144.45 ± 210.12	0.4499 ± 0.0377
	1-5 cm Soil	0.83 ± 0.16	3.50 ± 0.74	0.3676 ± 0.0003	0.83 ± 0.16	73.64 ± 60.30	0.3932 ± 0.0220
	6-15 cm soil	0.78 ± 0.23	2.60 ± 0.46	0.3672 ± 0.0002	0.78 ± 0.23	38.13 ± 50.14	0.3802 ± 0.0183
	NH_4^+-N 0-2 cm Soil	-	13.08 ± 3.54	0.3711 ± 0.0013	-	12,234.70 ± 6253.37	4.2793 ± 2.0742
	NH_4^+-N 2-5 cm Soil	-	5.02 ± 0.82	0.3681 ± 0.0003	-	1,288.53 ± 603.54	0.8340 ± 0.2179
	Algae in Water Column	0.72 ± 0.67	18.23 ± 2.66	0.3729 ± 0.0010	0.72 ± 0.67	5,464.23 ± 3066.75	2.3164 ± 1.0784
	Algae on Tank	0.15 ± 0.07	22.01 ± 4.78	0.3743 ± 0.0017	0.15 ± 0.07	4,828.11 ± 1760.42	2.0956 ± 0.6191

$^{\tau}$ Biomass was *S. tabernaemontani*. $^{\Psi}$Biomass was species other than *S. tabernaemontani.*

3.3.3 ^{15}N Mass Balance Method

A mass balance was completed to evaluate N transformations occurring within each wetland mesocosm during the two ^{15}N enrichment studies. 279 and 127 mg $^{15}NO_3$-N m^{-2} was added into the organic and mineral wetland mesocosms, respectively, at the beginning of the 0.9 g m^{-2} ^{15}N enrichment experiment. Following 7 days of enrichment only 22 and 11 mg $^{15}NO_3$-N m^{-2} or 8 and 9% of the added ^{15}N remained in the water of the organic and mineral wetland systems, respectively. 784 and 587 mg $^{15}NO_3$-N m^{-2} was added to the organic and mineral wetland mesocosms, respectively, at the beginning of the 3.6 g m^{-2} ^{15}N enrichment experiments. Following 10 days of enrichment 97 and 6 mg $^{15}NO_3$-N m^{-2} or 12 and 1% of the added ^{15}N remained in the water of the organic and mineral wetland systems, respectively. Other pools (plant biomass, soil, and gas) were then investigated to determine the fate of the $^{15}NO_3$-N within the wetland systems. The percent of ^{15}N recovered in each pool was assumed to be equivalent for the distribution of $^{14+15}N$ added to the each pool.

3.3.3.1 Biomass and Soil Pools

Plant uptake accounted for 25-48% of the ^{15}N recovered in the two wetland mesocosm studies. Following 7 days of enrichment in the 0.9 g m^{-2} study 134 and 43 mg $^{15}NO_3$-N m^{-2} or 48 and 34% of the removed ^{15}N was accounted for in the plant biomass in the organic and mineral systems, respectively. After 10 days of enrichment in the 3.6 g m^{-2} study, 195 and 151 mg $^{15}NO_3$-N m^{-2} or 25 and 26% was recovered in the organic and mineral plant biomass, respectively. Similar results were reported in a study of ^{15}N enrichment study of two oxbow wetlands, where plants accounted for 0-39% of ^{15}N removal (Harrison *et al.*, 2012). Samples in this study were broken into various portions of the *S. tabernaemontani* (Figures 29 and 30): live, dead, seed, and roots. The dominant quantity of ^{15}N incorporated into the *S. tabernaemontani* in the organic systems was in the roots for the two enrichment experiments. However, significant amounts of ^{15}N was incorporated in the both the roots and aboveground live biomass during the 0.9 g m^{-2} NO_3-N load experiment, while the majority of the ^{15}N was incorporated into the roots of the *S. tabernaemontani* in the 3.6 g m^{-2} NO_3-N load experiment in the mineral treatment. Assuming that ^{14}N was taken up at the same rate of ^{15}N the $^{14+15}NO_3$-N removal incorporated into the biomass ranged from 285 to 464 mg m^{-2} in the 0.9 g m^{-2} experiment and 994 to 1,006 mg m^{-2} in the 3.6 g m^{-2} experiment.

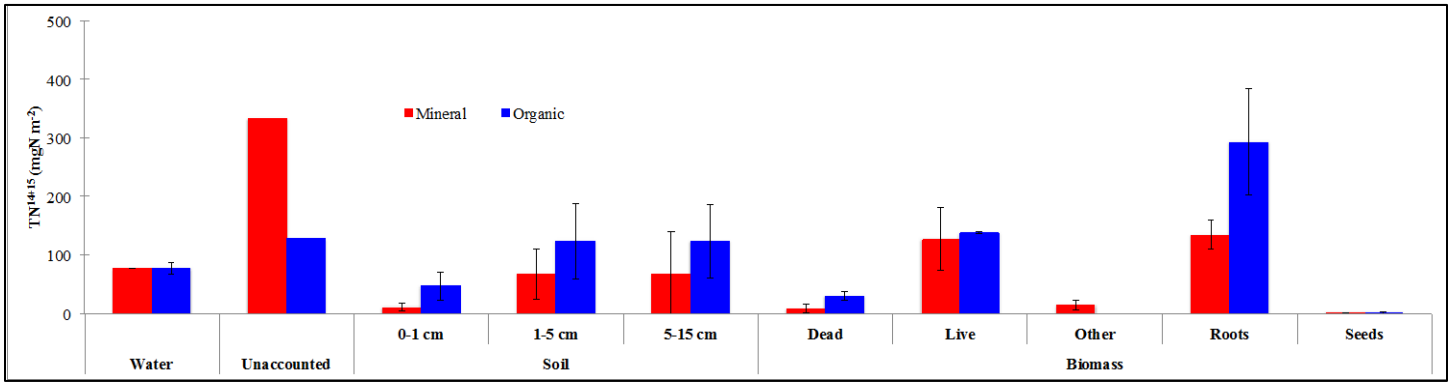

Figure 28: Estimated $^{14+15}N$ distribution in N pools within the wetland biomass and soil pools for the 0.9 g m^{-2} NO_3-N load wetland mesocosm experiment 7 days following isotope enrichment. N=3 for each category of soil and biomass non-enriched and enriched samples.

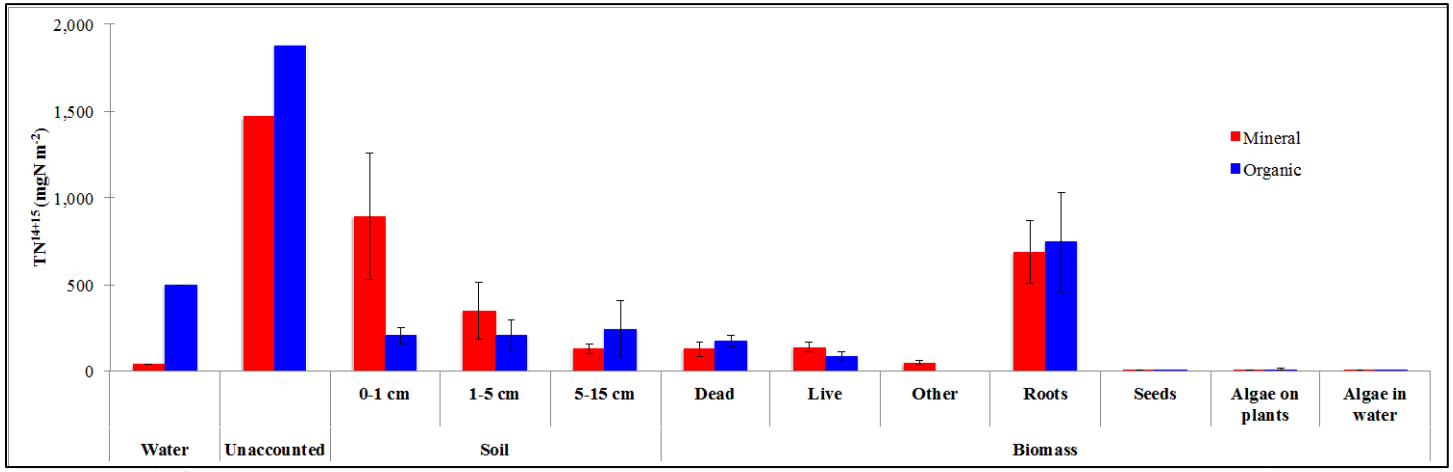

Figure 29: Estimated $^{14+15}N$ distribution in N pools within the wetland biomass and soil pools for the 3.6 g m^{-2} NO_3-N load wetland mesocosm experiment 10 days following isotope enrichment. N=5 for each category of soil and biomass non-enriched and enriched samples.

A substantial amount of ^{15}N was recovered in the soil pool (Figures 29 and 30). ^{15}N accounted for in the sediment ranged from 16-35% in the two wetland ^{15}N enrichment studies. Following 7 days of enrichment in the 0.9 g m^{-2} study 86 and 22 mg $^{15}NO_3$-N m^{-2} or 31 and 17% was accounted for in the top 15 cm of sediment in the organic and mineral systems, respectively. After 10 days of enrichment in the 3.6 g m^{-2} study 126 and 207 mg $^{15}NO_3$-N m^{-2} or 16 and 35% was accounted for in the organic and mineral sediment, respectively. $^{14+15}NO_3$-N removal incorporated into the soil, assuming ^{14}N was taken up at the same rate of ^{15}N, ranged from 146 to 296 mg m^{-2} in the 0.9 g m^{-2} experiment and 646 to 1,363 mg m^{-2} in the 3.6 g m^{-2} experiment.

The majority of the ^{15}N in the soil was observed in the top 0-1 cm particularly in the 3.6 g m^{-2} study. The soil pool also had the largest error associated with it due to its variable %N within the 3 (0.9 $^{14+15}N$ g m^{-2} enrichment experiment) to 5 replicates (3.6 $^{14+15}N$ g m^{-2} enrichment experiment) for each evaluated soil depth and variable ^{15}N sample concentrations, which may have been due to difficulties avoiding ^{15}N contamination from fine plant roots and overlying ^{15}N enriched water during sampling on Day 7 or 10. The mineral soil had higher error than the organic system potentially due to its lower permeability, which may have allowed water to infiltrate less uniformly, compared to the organic wetland systems. Sample sizes of at least 10 for each soil depth evaluated would be recommended for future ^{15}N enrichment experiments to reduce error.

3.3.3.2 ^{15}N Gas Pool

A large amount of the ^{15}N was not recovered in the water, sediment, and plant biomass pools (Figures 29 and 30). Often unrecovered ^{15}N is assumed to be denitrification (Harrison *et al.*, 2012). In this study, the release of $^{15}N_2$ was evaluated to estimate directly denitrification rates within the two wetland mesocosm systems. Water temperature and water velocity significantly affect the rate of gas exchange across the air-water interface in wetland systems, and are therefore critical parameters needed to quantify gas losses (Young and Huryn, 1999; Bennett and Rathbun, 1972). Therefore, aeration coefficients were determined in individual mesocosms prior to each of the ^{15}N enrichment studies.

The aeration coefficients for N_2 (k_{N2}) were determined using an exponentially fit model of the Ar reduction over time (Koop-Jakobson and Giblin, 2009). Argon aeration coefficients and Schmidt ratios were used to estimate the N_2 aeration coefficients in each wetland mesocosm system prior to the ^{15}N enrichment studies. N_2 aeration coefficients were estimated to be 0.074 and 0.037 hr^{-1} in the mineral and organic wetland mesocosm systems during the first ^{15}N enrichment study and 0.11 hr^{-1} and 0.094 hr^{-1} in the mineral and organic wetland mesocosm systems, respectively, during the second ^{15}N second enrichment study. Aeration coefficient results can be found in Appendix 5.

Aeration coefficients are extremely sensitive to wind, temperature, biomass thickness, and flow velocity, emphasizing the importance to evaluating these values prior to or during ^{15}N enrichment tracer studies. One possibility for the differences between the two enrichment studies may have been due to the low sensitivity for adjusting the pump velocity or thicker macrophyte roots accelerating the transfer of dissolved gases (Chanton *et al.*, 1989) between the first and second ^{15}N enrichment studies. Regardless, differences between aeration coefficients between the first and second experiments further support the importance of evaluating these values close to or during experiments when assessing gas losses.

A first order removal model developed by Tobias (2014) was then calibrated using observed NO_3-N, N_2-N, $^{15}NO_3$-N, and $^{15}N_2$-N values from water samples taken throughout

the experiments and the N_2 aeration coefficients determined from the Ar enrichment experiment. Like the assessments that determined NO_3-N removal fit a first order model, the first order removal models developed by Tobias (2014) also produced a reasonable fit for NO_3-N, $^{15}NO_3$-N, and $^{15}N_2$-N in both systems during the two ^{15}N enrichment studies (Figure 31). The mole fraction (MF) is the ratio of ^{15}N moles:$^{14+15}N$ moles and $\delta^{15}N$ (permil) is the differences between sample readings and one or another of the widely used natural abundance .

N_2 production through microbial denitrification increased as NO_3-N loading increased. Based on the results of the model developed to estimate gas losses, ^{15}N accounted for in the gas pool ranged from 9-32% depending on wetland systems and NO_3-N load. Following 7 days of enrichment in the 0.9 g m^{-2} study, 25 mg $^{15}NO_3$-N m^{-2} or 9 and 20% was accounted for in the gas pool of the organic and mineral systems, respectively. After 10 days of enrichment in the 3.6 g m^{-2} study 251 and 123 mg $^{15}NO_3$-N m^{-2} or 25-26% was accounted for in the organic and mineral gas pool, respectively. Assuming that ^{14}N was taken up at the same rate of ^{15}N the $^{14+15}NO_3$-N removal attributed to denitrification ranged from 82 to 166 mg m^{-2} in the 0.9 g m^{-2} experiment and 811 to 1,288 mg m^{-2} in the 3.6 g m^{-2} experiment.

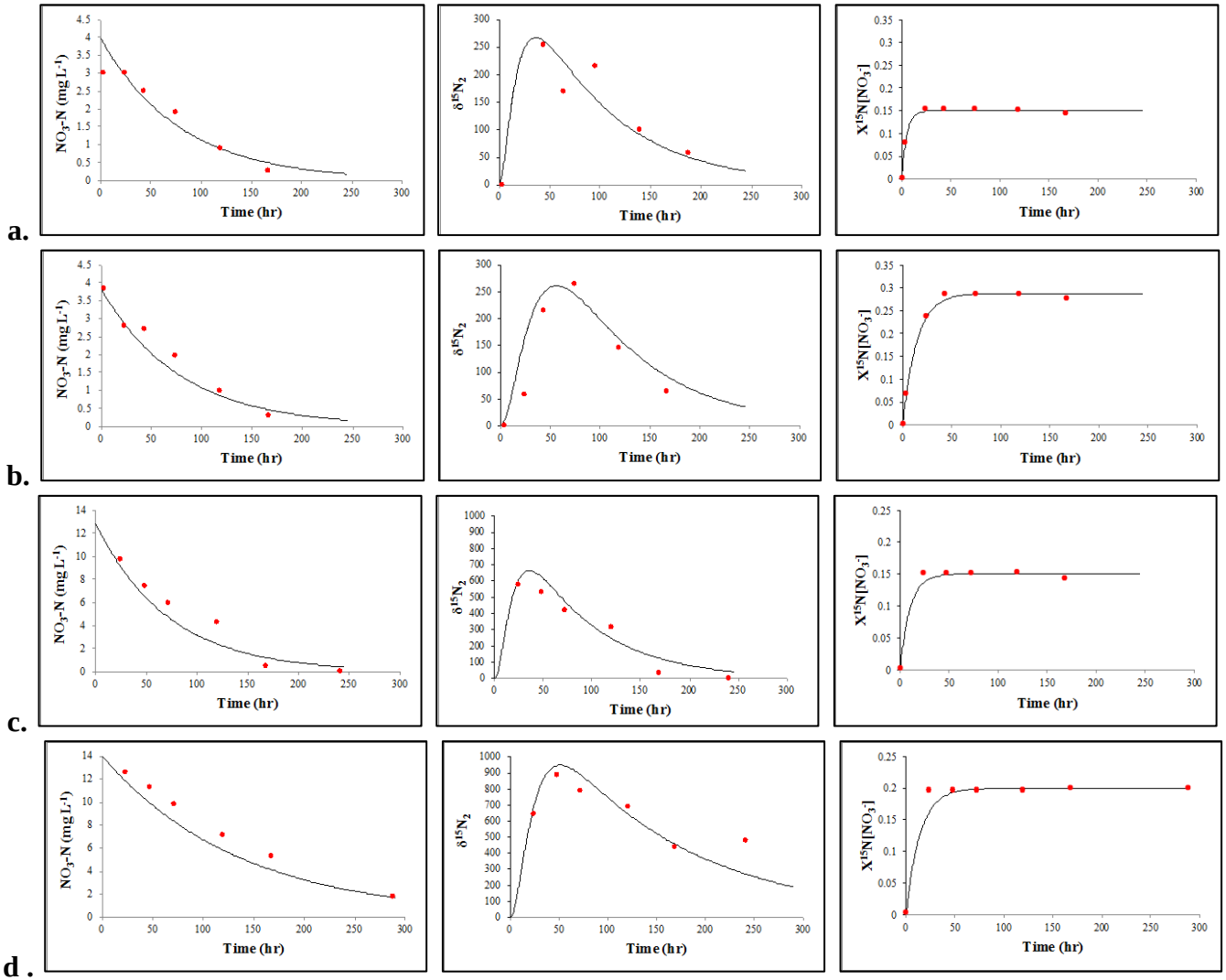

Figure 30: First order model for the a. mineral systems in the 0.9 g m^{-2} ^{15}N enrichment study, b. organic systems in the 0.9 g m^{-2} ^{15}N enrichment study, c. mineral systems in the 3.6 g m^{-2} ^{15}N enrichment study, and d. organic systems in the 3.6 g m^{-2} ^{15}N enrichment study. The points were collected data points during the experiment and the line represents the model's fit to the measured data points.

3.3.4 Mass Balance Summary and Implications of the Fate NO_3-N

A summary of the overall mass balance assessment can be found in Figure 33, Table 14, and 15. During the 0.9 g m^{-2} experiment ^{15}N was heavily distributed in the biomass pools in both the organic and mineral wetland systems. Alternatively, during the 3.6 g m^{-2} experiment recovered ^{15}N was more evenly distributed between pools in organic and mineral wetland treatments. Unaccounted for ^{15}N ranged between 4 to 20% depending on treatment and experiment and likely could be reduced in future experiments with more rigorous plant and soil sampling, since these were the pools with the largest variability in ^{15}N values.

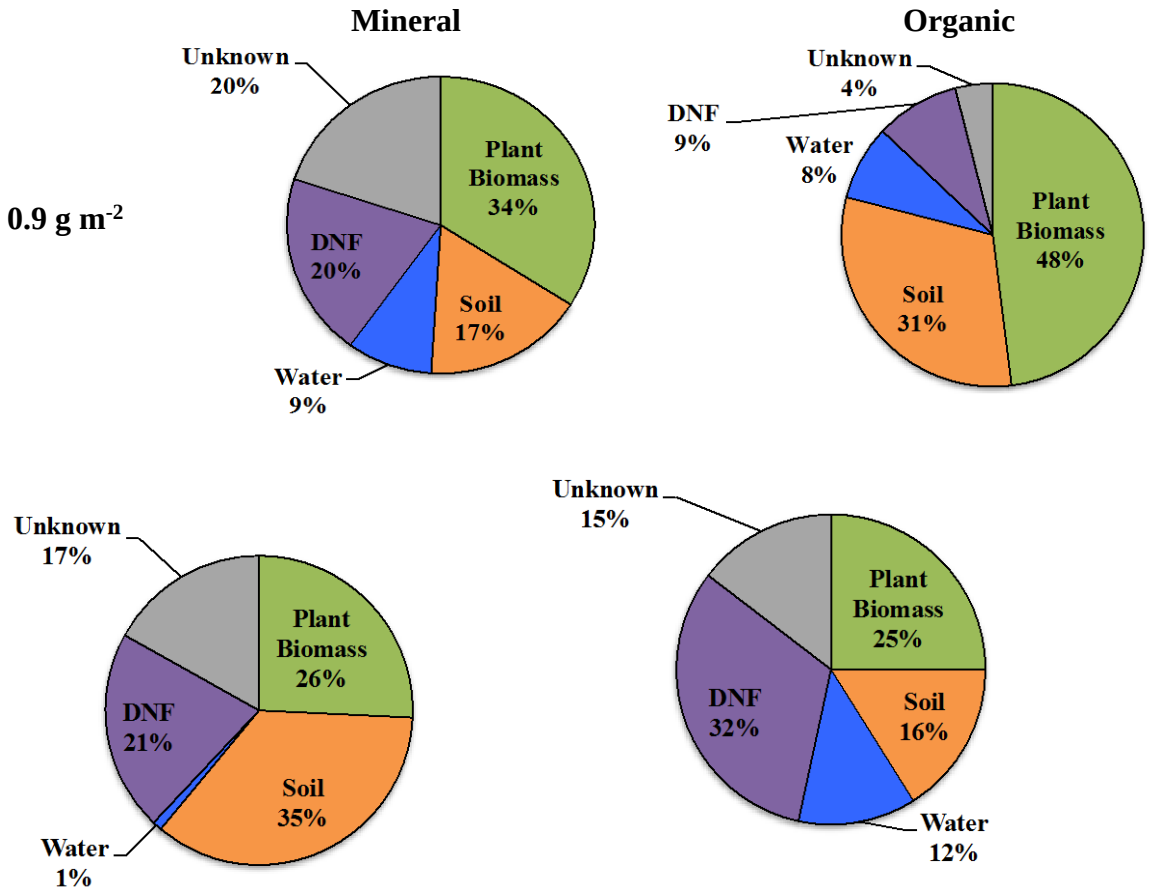

Figure 31: ^{15}N distribution in N pools within the wetland mesocosm for the 0.9 g m^{-2} loading 7 days following isotope enrichment (top) and the 3.6 g m^{-2} loading 10 days following isotope enrichment (bottom). Note DNF represents denitrification.

Table 14: Summary N pools at the completion of 0.9 g m^2 NO_3-N enrichment study (7 days). * Estimated $^{14+15}N$ assumes that ^{14}N is transformed at the same rate as ^{15}N by all N pools. To determine mg m^{-2} d^{-1} values divide $^{14+15}N$ values by 7 days. Note DNF represents denitrification.

Treatment	Pool	^{15}N Recovered (% of ^{15}N Total Added)	^{15}N Recovered (mg m^{-2})	*Estimated $^{14+15}N$ Overall Recovered (mg m^{-2})	*Estimated Mean Daily $^{14+15}N$ Removal/ Assimilation (mg m^{-2} d^{-1})
Organic	**Water**	8.0 ± 1.0	22.4 ± 2.8	77.4 ± 9.8	11.1 ± 1.4
	Plant Biomass	48.1 ± 10.6	134.4 ± 29.5	464.2 ± 102.0	66.3 ± 14.6
	Dead	*3.2 ± 0.8*	*8.9 ± 2.3*	*30.7 ± 7.9*	*4.4 ± 1.1*
	Live	*14.3 ± 0.2*	*40.0 ± 0.6*	*138.2 ± 1.9*	*19.7 ± 0.3*
	Other	-	-	-	-
	Roots	*30.5 ± 9.4*	*85.1 ± 26.2*	*293.8 ± 90.5*	*42.0 ± 12.9*
	Seeds	*0.2 ± 0.2*	*0.4 ± 0.5*	*1.5 ± 1.7*	*0.2 ± 0.2*
	Soil	30.7 ± 15.9	85.6 ± 44.5	295.8 ± 153.5	42.3 ± 21.9
	0-1 cm	*4.9 ± 2.6*	*13.6 ± 7.3*	*47.1 ± 25.1*	*6.7 ± 3.6*
	1-5 cm	*12.9 ± 6.7*	*36.1 ± 18.8*	*124.6 ± 64.8*	*17.8 ± 9.3*
	5-15 cm	*12.9 ± 6.6*	*35.9 ± 18.4*	*124.1 ± 63.7*	*17.7 ± 9.1*
	DNF	9.0 ± 0.7	25.1 ± 0.2	81.8 ± 0.6	11.7 ± 0.1
	Total Added	**100%**	**279**	**965**	
	Total Recovered	**96%**	**268**	**919**	
Mineral	**Water**	9.1 ± 0.01	11.6 ± 0.02	76.9 ± 0.1	11.0 ± 0.02
	Plant Biomass	33.9 ± 11.1	43.1 ± 14.1	285.8 ± 93.4	40.8 ± 13.4
	Dead	*1.0 ± 0.9*	*1.3 ± 1.1*	*8.7 ± 7.2*	*1.3 ± 1.0*
	Live	*15.1 ± 6.4*	*19.2 ± 8.1*	*127.4 ± 53.7*	*18.2 ± 7.7*
	Other	*1.7 ± 1.0*	*2.2 ± 1.3*	*14.6 ± 8.4*	*2.1 ± 1.2*
	Roots	*16.0 ± 2.9*	*20.3 ± 3.6*	*134.9 ± 24.1*	*19.4 ± 3.4*
	Seeds	*0.02 ± 0.02*	*0.03 ± 0.02*	*0.2 ± 0.1*	*0.03 ± 0.02*
	Soil	17.4 ± 14.5	22.0 ± 18.5	146.1 ± 122.5	20.9 ± 17.5
	0-1 cm	*1.4 ± 0.8*	*1.7 ± 1.0*	*11.4 ± 6.8*	*1.6 ± 1.0*
	1-5 cm	*8.1 ± 5.1*	*10.3 ± 6.5*	*68.0 ± 42.8*	*9.7 ± 6.1*
	5-15 cm	*7.9 ± 8.7*	*10.1 ± 11.0*	*66.7 ± 72.8*	*9.5 ± 10.4*
	DNF	20.0 ± 2.0	25.4 ± 0.5	166.0 ± 3.3	23.7 ± 0.5
	Total Added	**100%**	**127**	**842**	
	Total Recovered	**80%**	**102**	**675**	

Table 15: Summary N pools at the completion of 3.6 g m^2 NO_3-N enrichment study (10 days). * Estimated $^{14+15}N$ assumes that ^{14}N is transformed at the same rate as ^{15}N by all N pools. To determine mg m^{-2} d^{-1} values divide $^{14+15}N$ values by 10 days.

Treatment	Pool	^{15}N Recovered (% of Total ^{15}N Added)	^{15}N Recovered (mg m^{-2})	Estimated $^{14+15}N$ Overall Recovered (mg m^{-2})	Estimated Mean Daily $^{14+15}N$ Removal/ Assimilation (mg m^{-2} d^{-1})
Organic	**Water**	**12.3 ± 0.03**	**96.8 ± 0.2**	**496.9 ± 1.2**	**49.7 ± 0.1**
	Plant Biomass	**25.0 ± 8.9**	**195.9 ± 69.4**	**1,005.9 ± 356.1**	**100.6 ± 35.6**
	Dead	*4.2 ± 0.8*	*33.0 ± 6.1*	*169.5 ± 31.5*	*17.0 ± 3.2*
	Live	*2.0 ± 0.7*	*15.8 ± 5.8*	*81.1 ± 29.7*	*8.1 ± 3.0*
	Other	-	-	-	-
	Roots	*18.5 ± 7.2*	*144.8 ± 56.4*	*743.5 ± 289.4*	*74.4 ± 28.9*
	Seeds	*0.06 ± 0.02*	*0.46 ± 0.12*	*2.4 ± 0.6*	*0.2 ± 0.06*
	Algae on plants	*0.2 ± 0.1*	*1.55 ± 0.86*	*8.0 ± 4.4*	*0.80 ± 0.44*
	Algae in water	*0.04 ± 0.01*	*0.28 ± 0.10*	*1.5 ± 0.5*	*0.15 ± 0.05*
	Soil	**16.1 ± 7.5**	**126.0 ± 58.6**	**646.6 ± 300.6**	**64.7 ± 30.1**
	0-1 cm	*5.1 ± 1.2*	*39.6 ± 9.0*	*203.1 ± 46.3*	*20.3 ± 4.6*
	1-5 cm	*5.1 ± 2.1*	*39.6 ± 16.8*	*203.1 ± 86.2*	*20.3 ± 8.6*
	5-15 cm	*6.0 ± 4.2*	*46.8 ± 32.7*	*240.3 ± 168.0*	*24.0 ± 16.8*
	DNF	**32.0 ± 2.9**	**251.0 ± 7.3**	**1288.4 ± 37.4**	**128.8 ± 3.74**
	Total Added	**100%**	**784**	**4,026**	
	Total Recovered	**85%**	**670**	**3,164**	
Mineral	**Water**	**1.0 ± 0.03**	**5.8 ± 0.2**	**37.8 ± 1.0**	**3.8 ± 0.1**
	Plant Biomass	**25.6 ± 6.9**	**151.2 ± 40.5**	**994.0 ± 265.9**	**99.4 ± 26.6**
	Dead	*3.2 ± 1.1*	*18.9 ± 6.2*	*123.9 ± 40.6*	*12.4 ± 4.1*
	Live	*3.5 ± 0.7*	*20.6 ± 4.1*	*135.2 ± 26.7*	*13.5 ± 2.7*
	Other	*1.1 ± 0.4*	*6.6 ± 2.0*	*43.1 ± 13.4*	*4.3 ± 1.3*
	Roots	*17.7 ± 4.7*	*103.7 ± 27.6*	*681.5 ± 181.2*	*68.2 ± 18.1*
	Seeds	*0.1 ± 0.05*	*0.69 ± 0.3*	*4.6 ± 1.8*	*0.46 ± 0.18*
	Algae on plants	*0.09 ± 0.05*	*0.50 ± 0.3*	*3.3 ± 2.0*	*0.33 ± 0.20*
	Algae in water	*0.06 ± 0.01*	*0.36 ± 0.1*	*2.4 ± 0.4*	*0.24 ± 0.04*
	Soil	**35.3 ± 14.6**	**207.5 ± 85.6**	**1363.8 ± 562.7**	**136.4 ± 56.3**
	0-1 cm	*23.1 ± 9.5*	*135.5 ± 55.5*	*890.3 ± 364.9*	*89.0 ± 36.5*
	1-5 cm	*8.9 ± 4.3*	*52.4 ± 25.4*	*344.5 ± 166.7*	*34.5 ± 16.7*
	5-15 cm	*3.3 ± 0.8*	*19.6 ± 4.7*	*129.0 ± 31.2*	*12.9 ± 3.1*
	DNF	**21.0 ± 6.7**	**123.3 ± 8.3**	**810.7 ± 54.3**	**81.1 ± 5.4**
	Total Added	**100%**	**587**	**3,860**	
	Total Recovered	**83%**	**488**	**3,368**	

3.3.5 Discussion – ^{15}N tracer study

Differences in recovered ^{15}N were observed between treatments and loading rates in all evaluated N pools (water, biomass, soil, and gas). The mineral wetland reduced NO_3-N in the water column significantly faster than the organic treatment in higher loading ^{15}N

experiment (α=0.05), which was also observed in 10 of the 18 batch non-tracer studies (discussed earlier). Removal curves often diverged particularly during the larger N load evaluations, which were observed in this study.

During the 0.9 g m^{-2} NO_3-N load experiment ^{15}N was evenly distributed in the aboveground and belowground biomass in the mineral wetland systems, while during the 3.6 g m^{-2} NO_3-N load experiment more recovered ^{15}N was accounted for in the belowground biomass. The organic system had more recovered ^{15}N accounted for in the belowground biomass and had similar daily uptake rates in both ^{15}N enrichment experiments. Similar observations have been made in other wetland studies. Petrucio and Esteves (2000) observed increased plant uptake rates as N loading rates increased, likely due to luxury uptake to store N in the roots for sustaining plants during N limited periods. Svengsouk and Mitsch (2001) also suggested similar findings in a mesocosm study with *S. tabernaemontani*, where following fertilization, the plants had an increase in tissue nutrients suggested to be from the plants' high absorption capacity and nutrient storage in the roots.

Plants are often considered inferior to soil microbes in regard to N assimilation during shorter incubation periods particularly for NH_4^+-N and ON (Harrison et al., 2007, 2008; Bardgett et al., 2003; Hodge et al., 2000; Jackson et al., 1989). Microbes have a higher ratio of surface area to volume, wider spatial distribution, and increased assimilation affinities compared to plant roots (Lipson and Näsholm, 2001). However, microbes have a shorter turnover period of N compared to plant roots, which allows N to be released back into the soil quicker (Kaštovská and Šantrůčková, 2011; Hodge et al., 2000; Bardgett et al., 2003). Therefore, during longer incubation periods plants often outcompete microbes and accumulate a higher amount of ^{15}N (Harrison et al., 2008; Hodge et al., 2000). However, recovered ^{15}N in the soil pool of the wetland mesocosms evaluated in this study contributed a significant portion to the overall ^{15}N mass balance.

Organic and inorganic forms of N were assessed in this project to determine the likely form of recovered ^{15}N in the soil pool. Based on two dialysis porewater samplers installed during the mesocosms following a 0.9 g m^{-2} loading, NO_3-N and NH_4-N concentrations were below 0.05 mg L^{-1} within 1 cm of the soil-water interface of the mineral and wetland mesocosms 72 hours following the addition of NO_3-N. Additionally, $^{15}NH_4$-N absorbed to the sediment was analyzed and found to not contribute significantly to the ^{15}N recovered in the soil pool (2% of the total recovered ^{15}N in the soil pool). Therefore, the high ^{15}N in the soil was believed to be related to soil microbial assimilation.

Vitousek and Matson (1984) observed 83% of recovered ^{15}N to be in the microbial soil pool in a forested ecosystem in North Carolina. High ^{15}N retentions were attributed to carbon availability in the systems. Additionally, a meta-analysis of ^{15}N enrichment tracer studies of forested and grassland systems recovered 20-25% of applied ^{15}N in organic soils, while 15-40% of ^{15}N was recovered in the mineral soils after less than 1 week of enrichment (Templer *et al.*, 2012). High ^{15}N retention were positively correlated with C:N ratios in the mineral soils, while ^{15}N recovered was negatively correlated with TN concentrations in the organic soils, likely from the soils being already saturated with N.

Therefore, N availability likely resulted in the differences between the mineral and organic microbial assimilation rates. During the 0.9 g m^{-2} experiment the estimated soil assimilation $^{14+15}N$ rates were 2X higher in the organic (42 mg m^{-2} d^{-1}) compared to the mineral systems (21 mg m^{-2} d^{-1}). However, during the 3.6 g m^{-2} experiment soil assimilation

rates in the organic systems were 2X smaller (65 mg m^{-2} d^{-1}) compared to the mineral system (136 mg m^{-2} d^{-1}). Recall in the 3.6 g m^{-2} experiment that more ^{15}N was recovered in the water column in the organic system (12%) compared to the mineral system (1%). Likely the microbial and biomass pools had become saturated with N at the higher loading rates, while the N limited mineral system was able to continue assimilating N, which was similar to observations made by Templer *et al.* (2012) comparing N limited to N rich wetland systems utilizing ^{15}N enrichment tracers.

Although the organic system was hypothesized to provide a greater potential for denitrification to occur based on carbon values compared to the mineral system, observed ^{15}N denitrification rates were higher in the mineral system at the lower loading rates (0.9 g m^{-2}), while they were similar at the higher loading rates (3.6 g m^{-2}). The differences at the lower loading rates in the organic systems compared to the mineral system in the first ^{15}N experiment was likely caused by the affinity for NO_3-N assimilation being higher at lower pH values and the microbial and biomass pools not being N saturated at the lower loading rates compared to the higher loading rates (Brix *et al.*, 2002; Templer *et al.*, 2012). The higher load ^{15}N experiment likely saturated the biomass and microbial N pools and resulting in more NO_3-N being available for denitrification. Therefore, estimated denitrification rates were similar in both the organic and mineral treatments in the higher load ^{15}N experiment.

^{15}N remaining in the wetland soil pools 5 to 10 days following the study may have resulted in higher actual denitrification rates in both systems than estimated. Recall that the soils were sampled only 7-10 days after loading and there was evidence of significant complete denitrification that was occurring at the end of the period. It is also possible that ^{15}N assimilated into the mesocosms microbial soil pools could have been transformed through microbial denitrification or re-assimilated by microbes and plants in the days following the final sampling event as microbes died and mineralization, ammonification, and nitrification occurred. However, additional samples could have been collected perhaps 7-14 days after the experiment to test this hypothesis.

4. Summary of Overall Conclusions

Utilizing restored wetlands to treat agricultural drainage water is a promising method to reduce N exports to downstream sensitive ecosystems. The work presented in this report was centered on developing a model to predict the volume of drainage water that could be pumped into a currently degraded forested wetland ecosystem without harming the downstream ecosystems and the structure of the existing forested wetland ecosystem. The studies that supported this overall goal revealed quite a few conclusions that can be applied not only to the target restoration in Hyde County NC, but to other treatment wetlands as well.

This first part of this study, potential removal rates of NO_3-N for two distinct wetland environments slated to receive agricultural drainage water in future wetland restoration projects were evaluated. Five kinetic models that are often utilized to determine NO_3-N removal rates within wetland systems were assessed. Based on the results of this study, the following conclusions were drawn:

1) Significant differences were observed between the mineral and organic wetland mesocosms in experiments during the growing season (α=0.05). Higher removal rates were observed in the mineral wetland systems (Deloss soil) compared to the organic systems (Scuppernong soil). NO_3-N removal rates ranged from 14 to 603 mg m^{-2} d^{-1} in the mineral wetland mesocosms and 13 to 344 mg m^{-2} d^{-1} in the organic wetlands systems, with the highest rates of removal observed during the growing season.
2) Significant NO_3-N removal was also observed during the winter months when average water temperatures were as low as 9° C.
3) The first order decay model was determined the most practical model due to its conservative predictions compared to the efficiency loss model, simplicity, and reasonable fit. NO_3-N removal rates developed at the mesocosm scale have also been reported to be conservative estimates for full-scale wetlands. Therefore, the first order decay model was a relatively accurate model that generally did not overpredict removal rates, particularly during the growing season when the hydraulic retention times may be more limited.
4) Estimated ρ_{20} values for the first order model for NO_3-N removal predictions in the mineral and organic restored wetlands were 4.9 cm d^{-1} and 4.1 cm d^{-1}, respectively. θ values for temperature adjustment were estimated to be 1.15 and 1.09 for the mineral and organic systems, respectively.

Although not discussed in the details of this report, Messer (2015) http://www.lib.ncsu.edu/resolver/1840.16/10634 used these results coupled with hydrologic data collected from the site to begin the process of developing a pumping strategy for the restoration site in Hyde County. The volume of drainage water rerouted into the wetland will be equivalent to the amount of water no longer pumped into the nearby Pamlico Sound, so maximizing this amount is crucial to the success of the overall fill-scale project. It was determined that hydraulic retention time associated with NO_3-N treatment will control the pumping volumes applied to the site over 80% of the time. Initial estimates showed the restoration had the potential to remove an average of 4,950 kg NO_3-N per year

based on the assumption that influent NO_3-N concentrations were 2.5 mg L^{-1} and effluent target NO_3-N concentrations were 0.1 mg L^{-1}.

The second part of the study provided insight to nitrogen and carbon cycling occurring within these systems throughout the year using the advance scientific techniques of UV-spectrophotometry and ^{15}N tracer studies. Findings advanced the understanding of the nitrogen dynamics within these systems, which could improve wetland design methods for increasing permanent nitrogen removal based on incoming NO_3-N loads (denitrification rates increased and were more similar at higher NO_3-N loading rates for these two wetland systems) and soil type (higher pH soils may provide higher denitrification potential at lower loading rates).

1) Prominent diurnal cycles were observed in both NO_3-N and DOC readings from the UV-Vis spectrometer in most runs completed during the growing season. Two processes likely had the largest impact on these observations: photochemical mineralization and nitrification.
2) Significant reductions of $^{14+15}NO$-N were observed in both ^{15}N enrichment studies in the mineral (91-99%) and organic (90-91%) wetland mesocosms.
3) Of the ^{15}N recovered, 25 – 48 % was assimilated into the biomass and 16-35%, into the soil. Denitrification accounted for 9-32% of the recovered ^{15}N, showing that both wetland treatment systems provided suitable conditions to allow denitrification to occur, but remained lower than often assumed for these systems. Biomass assimilation accounted for 41 to 101 mg m^{-2} day^{-1} of the NO_3-N removal and denitrification accounted for 12 to 129 mg m^{-2} day^{-1} of NO_3-N removal.
5) Observed differences between the mineral and organic wetland systems suggest that N limited soils in the mineral systems and lower pH values in the organic systems may have impacted the fate of recovered ^{15}N.

5. Future Work

This water management model and plan will continue to be developed to guide stakeholders on pumping agricultural drainage water to the wetland restoration area in Hyde County. Additionally results from this work will result in at least 3 peer-reviewed scientific journal articles. The NO_3-N removal models developed at the mesocosm scale will be tested for accuracy at nearby existing full scale wetland cells in Hyde County prior to completion of the restoration project in 2016-2017 though an additional WRRI grant.

Appendix 1 – Nitrate removal models

A1.1 NO_3-N Removal Kinetic Model Overview

The most simplistic quantitative model, the zero order model (ZO), assumes contaminant reduction is independent of NO_3-N concentration. Zero order NO_3-N models have been used to model NO_3-N removal in wetlands (Mitsch *et al.*, 2005; Horne, 1995) assuming a constant consumption rate of NO_3-N. Therefore, the J_{NN} would be constant equaling J_{ZO}, the area based NO_3-N removal rate (g m^{-2} d^{-1}). These systems can be characterized by a linear NO_3-N concentration profile, which is often unrealistic in systems with larger residence times that allow NO_3-N to become limited. However, zero order NO_3-N kinetics have also been observed in systems with substrate concentrations significantly larger than the half-saturation constant (K_s) and assumes the system is closed, anoxic, completely or partially mixed, independent of hydraulic loading rates, and insignificantly influenced by other kinetic reactions occurring within the system (Bekins *et al.*, 1998). The model can be expressed as (Bollag and Stotzky, 2000):

$$J_{ZO} = \frac{(C_1 - C_t) * D}{t} \quad \textbf{Eq. A1}$$

Where, C_1 was the NO_3-N concentration in the wetland mesocosm 24 hours after simulated drainage was added to allow the system to be well mixed (mg L^{-1}), C_t was the NO_3-N concentration at end of the analysis (mg L^{-1}), t was the residence time from 24 hours after simulated drainage water was added to the system (Day 1) to the final sampling day (Day 10 or the last sampling day where C_t>0.05), and D was water depth (m). Once a J_{ZO} was estimated using observed NO_3-N removal datasets from the first 9 of the 18 mesocosm studies, C_t was predicted using the following equation to estimate NO_3-N removal rates in the wetland restorations systems for the remaining 9 batch studies:

$$C_t = C_0 - \frac{J_{ZO} * t}{D} \quad \textbf{Eq. A2}$$

Where, C_0 was the initial NO_3-N concentration added to the mesocosms from the mixing tank (mg L^{-1}) during each of the batch runs, t was the hydraulic retention time from Day 0 to the final sampling day (Day 10 or the last sampling day where C_t>0.05), J_{ZO} area based NO_3-N removal rate (g m^{-2} d^{-1}) estimated with Eq. 5a and D was water depth (m).

The second model, the first order decay response model (FO), assumes NO_3-N reduction rates are directly proportional to NO_3-N concentration (O'Brien, 2007). Therefore, removal rates (J_{NN}) increase linearly with NO_3-N concentration assuming removal efficiency does to not change in relation to NO_3-N load (Aumen, 1990). The model also assumes that the substrate concentration is significantly smaller than the half-saturation constant (K_s), the system is well mixed, has no significant influences from water losses or gains, and is dependent on only one reactant (Böhlke *et al.*, 2009; Bekins *et al.*, 1998; Chescheir *et al.*, 1991; Reddy, 1978). The ρ_{FO}, the mass transfer coefficient (cm d^{-1}), is independent of the depth of the water column above the sediment and accounts for the intrinsic ability for the soil to retain NO_3-N, which is often ignored by using the removal rate constants (k) in first order decay response models evaluations. The model can be expressed mathematically as (Turlan *et al.*, 2007):

$$\rho_{FO} = -\left(\frac{D * ln\frac{C_t}{C_1}}{t}\right) \quad \textbf{Eq. A3}$$

Where, C_1 was the NO_3-N concentration in the wetland mesocosm 24 hours after simulated drainage was added to allow the system to be well mixed (mg L^{-1}), C_t was the NO_3-N concentration at end of the analysis (mg L^{-1}), t was the hydraulic retention time from 24 hours after simulated drainage water was added to the system (Day 1) to the final sampling day (Day 10 or the last sampling day where C_t>0.05), D was water depth (m), and ρ_{FO} was the mass transfer coefficient (cm d^{-1}). C_t was predicted using the following equation to determine maximum NO_3-N loading capacities of the wetland restorations after ρ_{FO} was estimated using observed NO_3-N removal datasets from the mesocosm studies:

$$C_t = C_0 e^{-\left(\frac{\rho_{FO} * t}{D}\right)} \quad \textbf{Eq. A4}$$

Where, C_0 was the initial NO_3-N concentration added to the mesocosms from the mixing tank (mg L^{-1}) during each of the batch runs, t was the hydraulic retention time from Day 0 to the final sampling day (Day 10 or the last sampling day where C_t>0.05), ρ_{FO} was the mass transfer coefficient (cm d^{-1}) estimated with Eq. 6a, and D was water depth (m).

The third model, the efficiency loss model (EL), is similar to the first order removal model, but it accounts for the efficiency of the process rate relative to NO_3-N concentration decline over time (O'Brien *et al.*, 2007). Similar to the first order rate model, the model assumes that the substrate concentration is significantly smaller than K_s, the system is well mixed, and has no significant influences from water losses or gains. However, the model assumes a power relationship represented by the coefficient α, in which the order is less than 1. The model can be expressed as:

$$\rho_{EL} = \left(\frac{(C_t)^{1-\alpha} - C_1^{1-\alpha}}{t}\right)^{\left(\frac{1}{\alpha-1}\right)} D \quad \textbf{Eq. A5}$$

Where ρ_{EL} was the mass transfer coefficient (cm d^{-1}), α was a unitless constant that varies between 0 and 1, D was water depth (cm), C_1 was the NO_3-N concentration in the wetland mesocosm 24 hours after simulated drainage was added to allow the system to be well mixed (mg L^{-1}), C_t was the NO_3-N concentration at end of the analysis (mg L^{-1}), and t was the hydraulic retention time from 24 hours after simulated drainage water was added to the system (Day 1) to the final sampling day (Day 10 or the last sampling day where C_t>0.05),. The model was evaluated empirically in R Studio (2014) to solve for α and ρ_{EL} for individual mesocosms using 9 of the 18 batch run datasets. C_t was then predicted using the ρ_{EL} and averaged α values for the remaining 9 batch studies not used to determine removal coefficients. Predicted C_t NO_3-N concentrations were then compared to observed NO_3-N concentration datasets from the mesocosm studies using the following equation:

$$C_t = \left(\frac{\rho_{EL}{}^{(\alpha-1)}}{D} t + C_0^{1-\alpha}\right)^{\frac{1}{1-\alpha}} \quad \textbf{Eq. A6}$$

Where, C_0 was the initial NO_3-N concentration added to the mesocosms from the mixing tank (mg L^{-1}) during each of the batch runs, t was the hydraulic retention time from Day 0 to the final sampling day (Day 10 or the last sampling day where C_t>0.05), ρ_{EL} was the mass transfer coefficient (cm d^{-1}) estimated empirically with Eq. 7a, α was a unitless constant estimated empirically with Eq. 7a, and D was water depth (m).

The simulated drainage turned over in the wetland mesocosm systems once a day during each of the experiments. Therefore, the tanks in series (TIS) model, the fourth evaluated model, took into account the effects of the period of mixing occurring within the mesocosm and was used to represent the number of times the water turned over during an experiment. The model was used to investigate the effects in event driven systems, which wetlands receiving agricultural drainage water commonly are, and determine if the model

could account for the recirculation through wetland mesocosms (Kadlec, 2010). The TIS model assumes that NO_3-N rich water passes through multiple wetlands in series and looses contaminants in each tank, there is no water loss or gains, the system is steady flow, and the mass transfer coefficient (ρ_{TIS}) does not vary with time of exposure to the wetland system (Kadlec and Wallace, 2009). The TIS model can be expressed as:

$$\rho_{TIS} = \frac{\left(\left(\frac{C_t}{C_1}\right)^{-\frac{1}{N}} - 1\right) ND}{t} \quad \textbf{Eq. A7}$$

Where, ρ_{TIS} was the mass transfer coefficient (cm d^{-1}), C_1 was the NO_3-N concentration in the wetland mesocosm 24 hours after simulated drainage was added to allow the system to be well mixed (mg L^{-1}), C_t was the NO_3-N concentration at end of the analysis (mg L^{-1}), t was the hydraulic retention time from 24 hours after simulated drainage water was added to the system (Day 1) to the final sampling day (Day 10 or the last sampling day where C_t>0.05), N was the number of tanks, and D (cm) is the water depth. N was assumed to be equal to the number of days for each batch run experiment since drainage water was turned over within each mesocosm once a day. Additionally, past mesocosm studies using the TIS model at the mesocosm scale have used the hydraulic retention time for their N value as well (Kadlec and Wallace, 2009). Once ρ_{TIS} was estimated using the first 9 of the 18 observed NO_3-N removal datasets in the mesocosm studies, C_t was predicted using the following equation for comparison to observations in the remaining 9 batch run studies:

$$C_t = C_o \left(1 + \frac{\rho_{TIS} t}{ND}\right)^{-N} \quad \textbf{Eq. A8}$$

Where, C_0 was the initial NO_3-N concentration added to the mesocosms from the mixing tank (mg L^{-1}) during each of the batch runs, t was the hydraulic retention time from Day 0 to the final sampling day (Day 10 or the last sampling day where C_t>0.05), ρ_{TIS} was the mass transfer coefficient (cm d^{-1}) estimated empirically with Eq. 8a, N was the hydraulic retention time, and D was water depth (m).

The fifth model evaluated was the Monod model (M), also referred to as the Michaelis-Menten model for theoretical considerations, which often represents biologically mediated reactions that display first order decay kinetics at low concentrations and zero order kinetics at higher concentrations, resulting in a hyperbolic relationship between J_{NN} and NO_3-N concentrations. Zero order kinetics has been observed when NO_3-N concentrations exceeded biological demand of the system, while first order decay kinetics have been observed when NO_3-N concentrations are below the biological demand of the system (Messer and Brezonik, 1984). Therefore, the model ultimately interpolates between a zero order and first order model. The model assumes there are no intermediate or product inhibitions and the system is at steady state (Stringfellow, *et al.*, 2013). The model can be expressed as:

$$J_M = \frac{J_{max} * C_o}{K_s + C_o} \quad \textbf{Eq. A9}$$

Where, J_M was the area based NO_3-N loss rate (mg m^{-2} d^{-1}), J_{max} was the maximum removal rate achieved by the system (mg m^{-2} d^{-1}), C_o (mg L^{-1}) was the initial NO_3-N concentration, and K_s (mg L^{-1}) was the half saturation constant. K_s and J_{max} were determined graphically using a Lineweaver-Burke plot (Lineweaver and Burk, 1934) with observed J_{NN} and C_F (concentration at the last sampling time) values. The first-order mass

transfer coefficient (ρ_M), was then estimated assuming $C_o << K_s$ using the following equation (Karpuzcu *et al.,* 2012; Messer and Brezonik, 1984):

$$\rho_M = \frac{D * J_{max}}{K_s} \quad \textbf{Eq. A10}$$

Where, D was the water depth, J_{max} was the maximum removal rate achieved by the system estimated empirically with Eq. 4.6a ($m\,d^{-1}$), and K_s ($mg\,L^{-1}$) was the half saturation constant estimated empirically with Eq. 9a.

Appendix 2 –Ar and ^{15}N Experimental Protocol

Argon GTV Study Protocol

Slug Mixing and Introduction

1.) Four 66 L buckets will be filled with 50 L of tap water.
2.) Argon gas will be sparged into the four buckets utilizing a four way manifold with 1 m gas tight tubing connected to 13 cm air stone. The buckets will each have a piece of plywood placed overtop to decrease gas loss. Argon gas will be sparged into the buckets for 2 hours controlled with a gas regulator.
3.) At approximately 1 hr 30 min following the initiation of the argon bubbling, 3.5 g NaBr per bucket will be added to the mixing solution to achieve concentrations of 50 mgL^{-1} Br^- for each slug.
4.) After Argon gas has been sparged for 2 hours and NaBr mixed into the slug for 15 minutes, 100 L of the slug will be pumped into the NR2 (Mineral) and Hyde 2 (Organic) mesocosms using a 12- volt, low flow submersible pump (Waterra, WSP-12V-5).

Argon Tracer Sampling

1.) Argon samples will be taken from each mixing tank prior to pumping the slug into the mesocosms.
2.) Duplicate argon samples will then be taken at the following time intervals following the Ar slug being introduced into the mesocosms: 0 min, 30 min, 1 hr, 2 hr, 4 hr, 8 hr, 12 hr, 16 hr, 20 hr, 24 hr, 36 hr, and 48 hr.
3.) Two samples will be taken in the center of the mesocosms at 3 ft and 9 ft down the length of the mesocosms during each sampling event along with salinity and temperature readings with a YSI.
4.) Samples will be taken utilizing a lab grade peristaltic pump (Cole Palmer, 57160) attached to the tubing.
5.) Samples will be pumped from the sampling locations at approximately 15 cm down into the water column and into an exetainer (provided by the University of Connecticut Marine Sciences Analytical Instruments Lab). Bottles will be slowly filled until a bead of water is present on the top of the bottle.
6.) Bottles will then be capped.
7.) Samples will be shipped upside down in 1 L Nalgene bottles that are filled with tap water to the following address:

    Department of Marine Sciences
    University of Connecticut
    1080 Shennecossett Road
    Groton, CT 06340

Bromide Tracer Sampling

1.) Duplicate Bromide samples will be taken from each mixing tank prior to pumping the slug into the mesocosms.
2.) Bromide samples will then be taken at the following time intervals following the Ar slug being introduced into the mesocosms: 0 min, 30 min, 1 hr, 2 hr, 4 hr, 8 hr, 12 hr, 16 hr, 20 hr, and 24 hr.

3.) Two samples will be taken in the center of the mesocosms at 3 ft and 9 ft down the length of the mesocosms during each sampling event.
4.) Samples will be taken utilizing a lab grade peristaltic pump (Cole Palmer, 57160) from the sampling locations at approximately 15 cm down into the water column and into 500 mL Nalgene bottles and placed on ice.
5.) Samples will be analyzed at the NCSU Soil Science EATS Lab.

^{15}N Enrichment Study Protocol

Application of ^{15}N into Mesocosms

1.) A mesocosm tracer study will be start on Tuesday July 22nd.
2.) The Organic 2 and Mineral 2 mesocosms will be filled with simulated drainage water from the tank to the depth of 9.25 in (190 gallons) and 10.75 in (224 gallons) respectively.
3.) A solution of 36 g of KNO_3-^{15}N will be added to the Organic 2 mesocosm and 16 g of KNO_3-^{15}N will be add to the Mineral 2 mesocosm as water is being added into the system with two separate 1 gallon pitchers.
4.) Each pitcher will also have 6.5 g of NaBr added to them to assess dilution and enrich the water to have approximately 5 mg/L of Br^-.
5.) The mesocosms will then be filled to 12 in with faucet water to get the correct concentration of NO_3^-N in the mesocosms.

Plant and Soil Samples

1.) Prior to initiation of the study live bulrush, dead bulrush, seeds, roots, and other plant material in five 5 cm diameter areas in the Organic 2 and Mineral 2 mesocosms will be sampled along with soils at the 0-1 cm, 1-5 cm, and 5-15 cm depths at 5 sampling locations.
2.) 10 days after the application of ^{15}N in the system live bulrush, dead bulrush, seeds, roots, and other plant material in five 5 cm diameter areas in the Organic 2 and Mineral 2 mesocosms will be sampled along with soils at the 0-1, 1-5 cm and 5-15 cm depths at 5 sampling locations.
3.) Plant and soil material will be dried and finely milled.
4.) Tin capsules will be tared on a micro-scale.
5.) Using a clean spatula, the sample will be weighed and transferred into the sample capsule until 3-5 μmol of N is achieved.
6.) The top of the capsule will be crimped with a pair of straight foreceps and folded over snugly.
7.) The final weight of the capsule will be recorded after it is sealed
8.) The lid of the culture tray will be secured with laboratory label tape.
9.) Samples will be shipped to UC Davis for analysis.

NO_3-^{15}N Samples

1.) 90 ozs of water will be sampled on days 0,1,2,3,5,7, and 10 of the study and water will be filtered with a 60 mL syringe with a 0.45 μM filter in the greenhouse at the time of sampling for the NO_3-^{15}N samples. NO_3-^{15}N samples will be taken at the 3 m and 9 m locations along the length of the two mesocosms. There will be a total of 28 samples.
2.) Filtered water will be put into amber polyethylene bottles.

3.) One pellet of NaOH will be added to the NO_3-^{15}N to get the pH to 11-11.5.
4.) The bottle will then be screwed shut and the caps will be secured with electrical tape.
5.) Bottles will be placed in the laboratory refrigerator until shipped.
6.) The bottles will be shipped to the following address in a cooler with 2 L of frozen water placed inside for analysis:

USGS--Isotope Laboratory
431 National Center
12201 Sunrise Valley Dr.
Reston, VA 20192
(703) 648-5859

N_2-^{15}N Samples

1.) 125 ozs of water will be sampled on days 1,2,3,5,7, and 10 of the study in 125 mL serum sample bottles provide by USGS.
2.) Samples will be taken in duplicates at the 3 m and 9 m locations along the length of the two mesocosms. Additional 2 samples will be taken along the vertical profile at depths above the soil surface and at 5 cm from the soil surface to access differences in the profile on sampling day 3 and 7. There will be a total of 36 samples.
3.) The water discharge tube will be placed in the bottom of the sample bottle and filled with at least 500 mL until all bubbles are removed and a meniscus is formed along the top of the bottle.
4.) One pellet of KOH will be added.
5.) A stopper with a needle inserted in the top will be used to release air and cap the bottle once the needle is removed.
6.) The sample name and water temperature will be recorded on the sample label.
7.) Bottles will be placed in laboratory refrigerator until shipped
8.) The bottles will be shipped to the following address in a small cooler with 2 L of frozen water placed inside for analysis:

USGS--Isotope Laboratory
431 National Center
12201 Sunrise Valley Dr
Reston, VA 20192
(703) 648-5859

NH_4^+-N Sampling

1.) Soil samples will be taken from 0-10 cm at 3 sampling locations in the Organic 2 and Mineral 2 mesocosms prior to the ^{15}N enrichment and 10 days after the ^{15}N enrichment.
2.) Samples will be frozen in the laboratory refrigerator in labeled plastic bags until shipment.
3.) The bottles will be shipped to the following address in a small cooler with 2 L of frozen water placed inside for analysis:

Department of Marine Sciences
University of Connecticut

1080 Shennecossett Road
Groton, CT 06340

^{15}N Microbial Sampling Along the Mesocosm Walls and Plant Stems

1.) Microbial and algal biomass will be sampled at 3 locations in the Organic 2 and Mineral 2 mesocosms prior to the ^{15}N enrichment and 10 days after the ^{15}N enrichment including around the plant stems, the water, and along the walls of the mesocosm.
2.) Samples will be taken around the plant stems and along the mesocosm wall using 25 mm ashed GFF filters that allow a minimum passage of 0.7 microns. The filters will be rubbed against the wall and around the stems of plants to collect the cultures.
3.) Samples will be frozen in the laboratory refrigerator in labeled plastic bags until shipment.
4.) The bottles will be shipped to the following address in a small cooler with 2 L of frozen water placed inside for analysis:

Department of Marine Sciences
University of Connecticut
1080 Shennecossett Road
Groton, CT 06340

Microbial ^{15}N Enrichment Biofilm Water Sampling

1.) Microbial and algal biomass will be sampled on days 1 and 10 in the Organic 2 and Mineral 2 mesocosms.
2.) Populations in the water will be collected by filtering water through using 25 mm ashed GFF filters that allow a minimum passage of 0.7 microns until the filters become too difficult to continue filtering. Duplicate samples will be taken.
3.) Samples will be frozen in the laboratory refrigerator in labeled plastic bags until shipment.
4.) The bottles will be shipped to the following address in a small cooler with 2 L of frozen water placed inside for analysis:

Department of Marine Sciences
University of Connecticut
1080 Shennecossett Road
Groton, CT 06340

N_2O Sampling

1.) N_2O samples are planned to be taken during the batch study proposed for late July, 2013 to evaluate the size of the N_2O pool within the mesocosms systems.
2.) The batch run is planned to have 30 cm of simulated drainage water with NO_3-N concentrations of 10 mgL^{-1}.
3.) N_2O samples will be taken days 0, 1, 2, 3, 5, 7, and 10 of the batch run.
4.) Two samples will be taken in the center of the mesocosms at 3 ft and 9 ft down the length of the mesocosms during each sampling event.
5.) Samples will be taken utilizing a lab grade peristaltic pump (Cole Palmer, 57160) with a 60 cc luer lok syringe attached to the tubing. Water will be pumped slowly into the luer lock system to get a gas tight sample.

6.) Water from the mesocosms will be pumped from the sampling locations into a 60 cc syringe.
7.) The syringe will be tapped until all air bubbles are released.
8.) 10 mL of the sample in the syringe will be put into 30 mL serum bottles that have been flushed with helium and contain 200 μL of KOH (provided by the University of Connecticut Marine Sciences Analytical Instruments Lab).

Bromide Tracer Sampling

1.) Duplicate Bromide samples will be taken from each mixing tank prior to pumping the slug into the mesocosms.
2.) Bromide samples will then be taken at the following time intervals following the Ar slug being introduced into the mesocosms: 0 min, 30 min, 1 hr, 2 hr, 4 hr, 8 hr, 12 hr, 16 hr, 20 hr, and 24 hr.
3.) Two samples will be taken in the center of the mesocosms at 3 ft and 9 ft down the length of the mesocosms during each sampling event.
4.) Samples will be taken utilizing a lab grade peristaltic pump (Cole Palmer, 57160) from the sampling locations at approximately 15 cm down into the water column and into 500 mL nalgene bottles and placed on ice.
5.) Samples will be analyzed at the NCSU Soil Science EATS Lab.

Appendix 3 – All batch studies

Batch Run 1

Run:	1
Date:	9/25/2012 - 10/4/2012
Depth of Water:	12 in
Target NO_3-N (mg L^{-1}) Concentration:	2.5
Water Recirculation:	1 turnover per day
Antecedent Conditions:	1.5 in

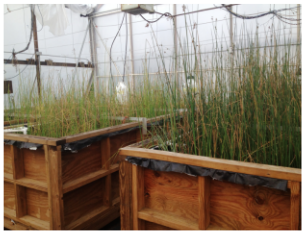

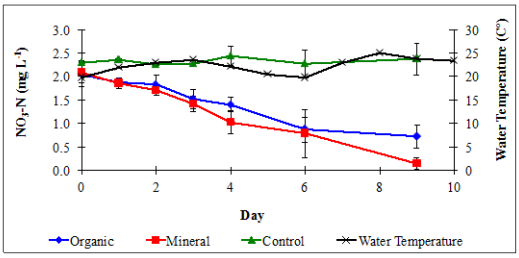

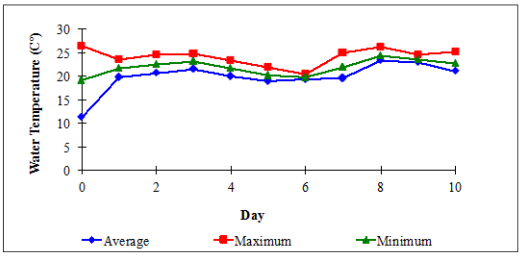

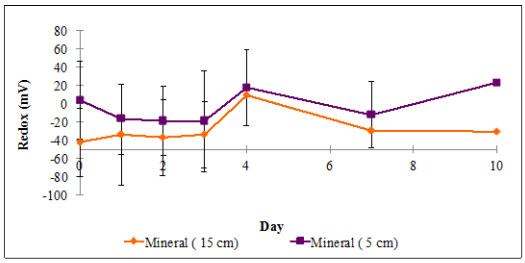

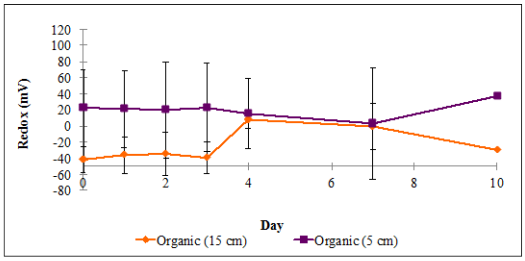

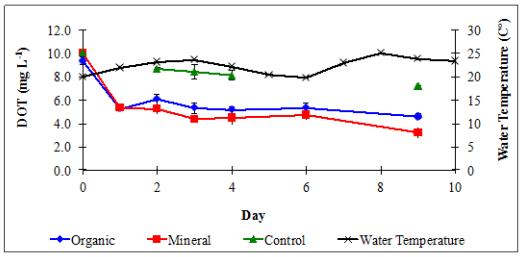

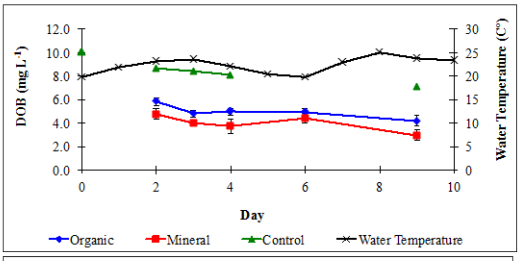

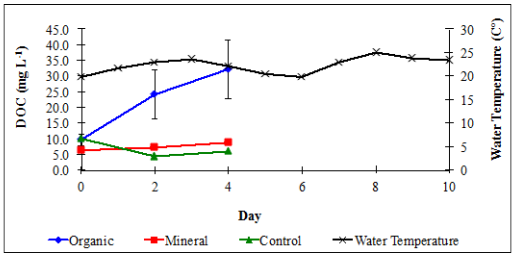

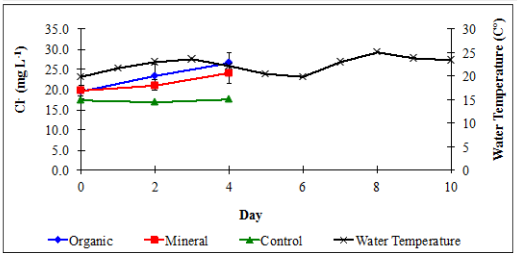

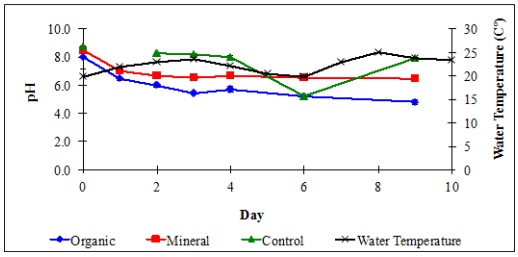

Batch Run 2

Run:	2
Date:	10/16/12 - 10/26/2012
Depth of Water:	7 in
Target NO_3-N (mg L^{-1}) Concentration:	5
Water Recirculation:	1 turnover per day
Antecedent Conditions:	1.5 in

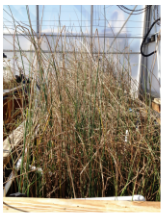

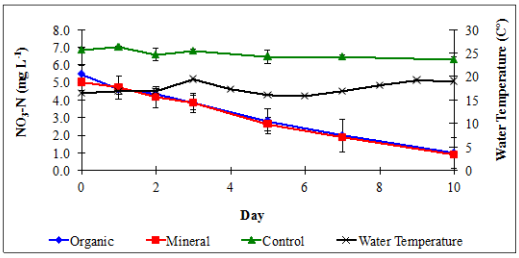

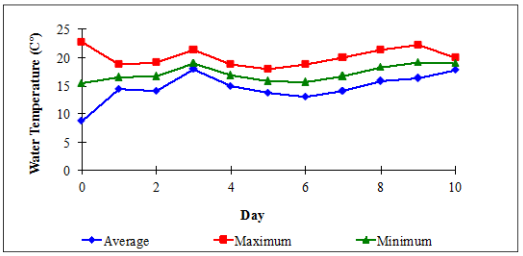

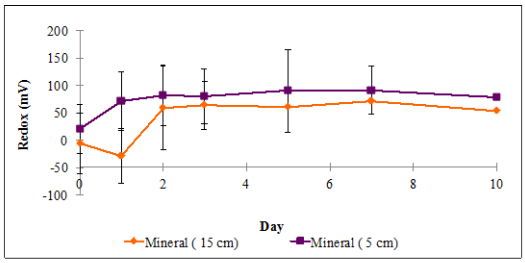

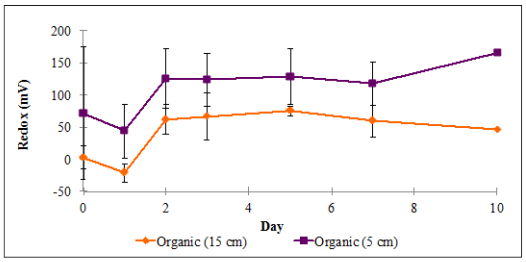

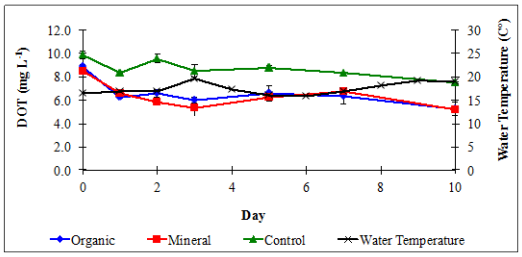

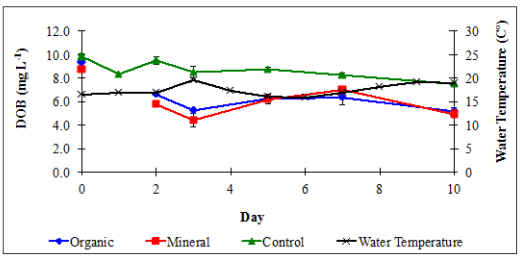

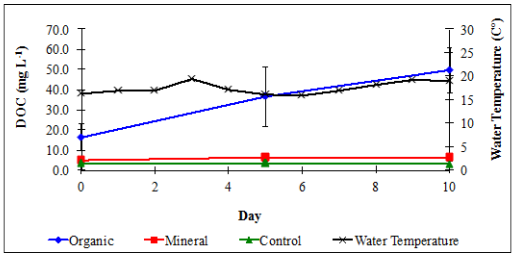

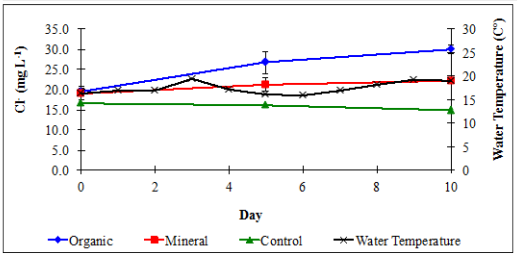

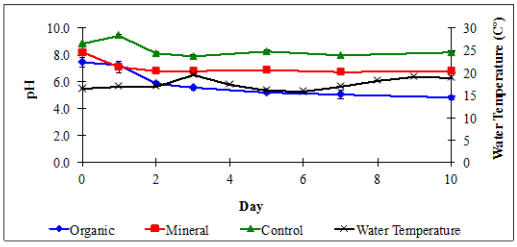

Batch Run 3

Run:	3
Date:	11/5/2012 - 11/15/2012
Depth of Water:	12 in
Target NO_3-N (mg L^{-1}) Concentration:	10
Water Recirculation:	1 turnover per day
Antecedent Conditions:	5 in

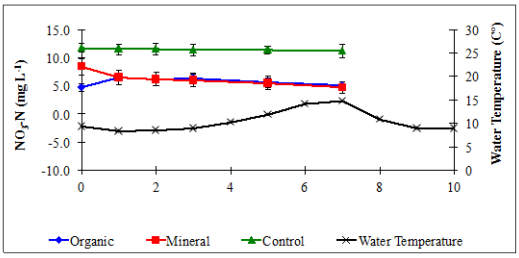

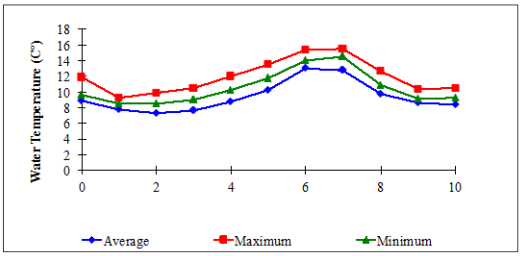

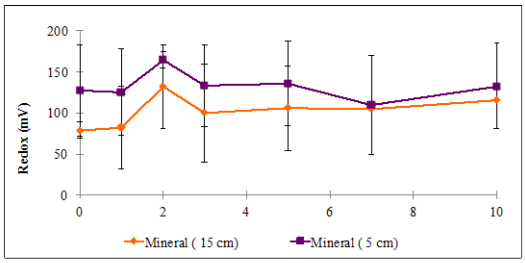

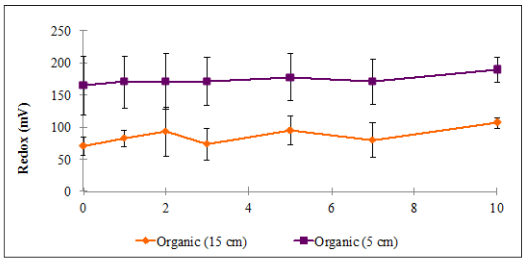

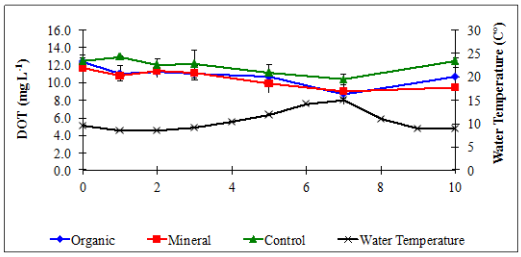

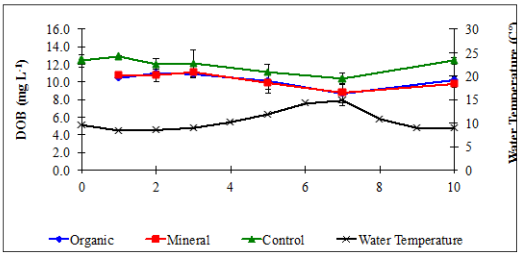

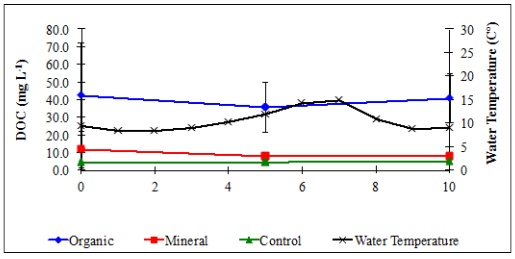

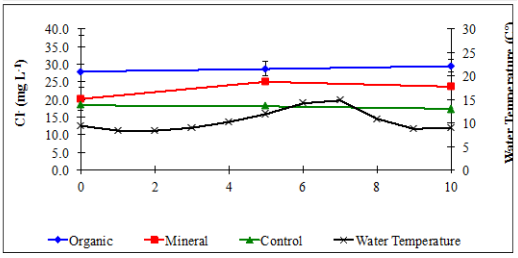

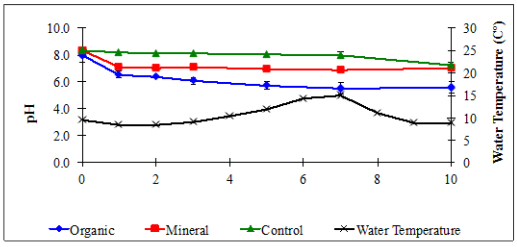

Batch Run 4

Run:	4
Date:	1/22/2013 - 2/1/2013
Depth of Water:	6 in
Target NO_3-N (mg L^{-1}) Concentration:	2.5
Water Recirculation:	1 turnover per day
Antecedent Conditions:	1.5 in

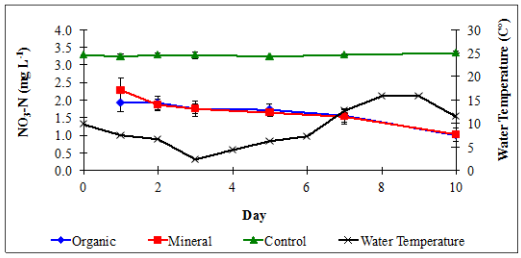

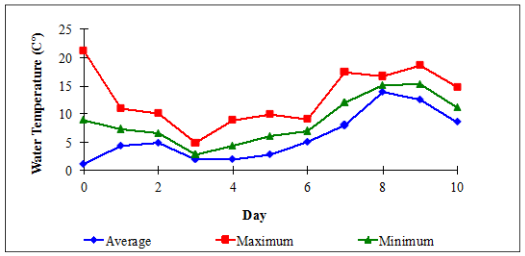

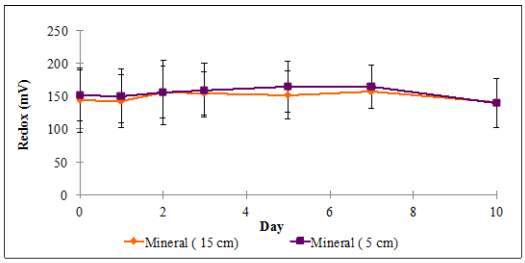

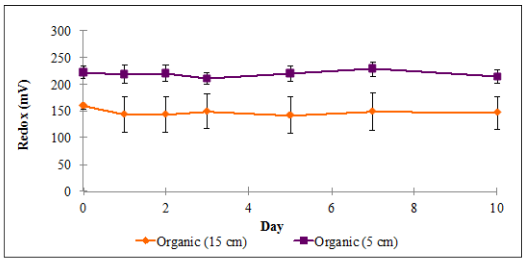

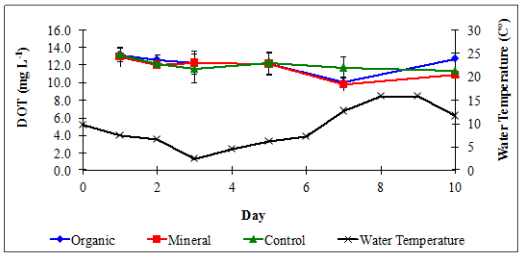

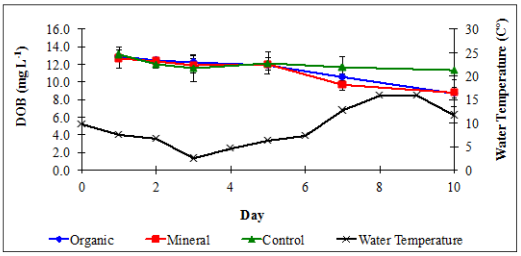

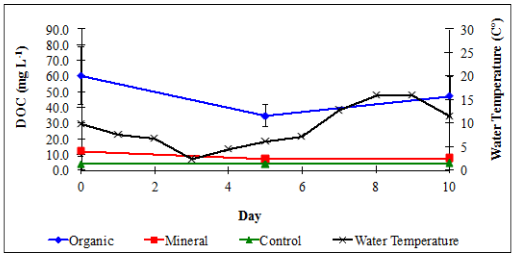

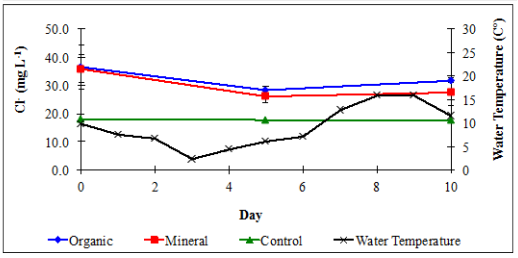

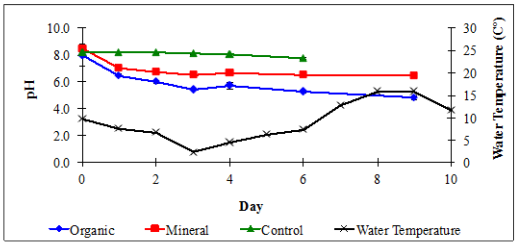

Batch Run 5

Run:	4
Date:	1/22/2013 - 2/1/2013
Depth of Water:	6 in
Target NO_3-N (mg L^{-1}) Concentration:	2.5
Water Recirculation:	1 turnover per day
Antecedent Conditions:	1.5 in

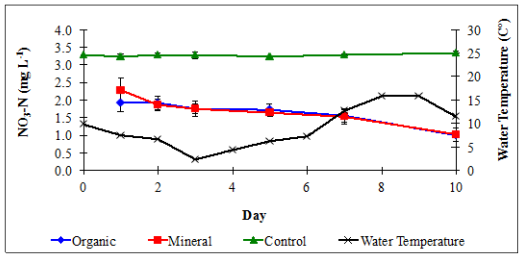

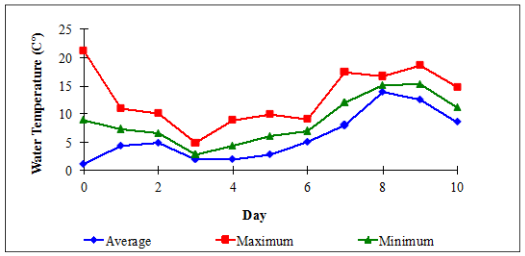

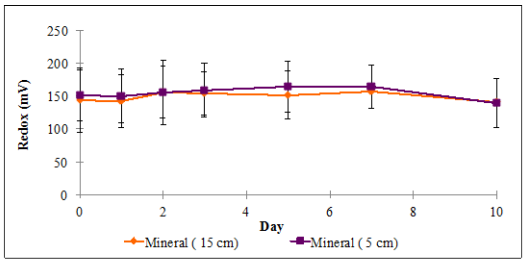

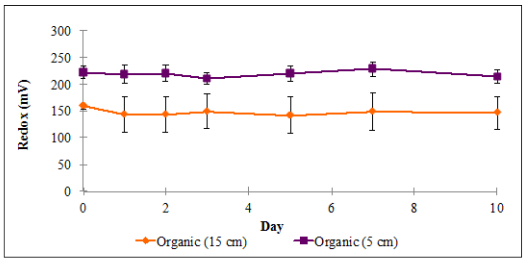

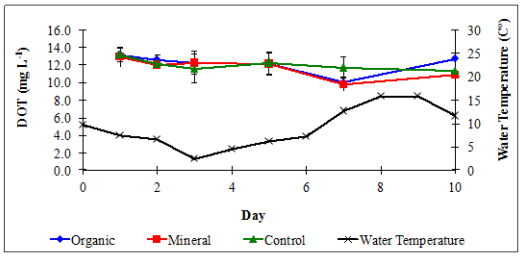

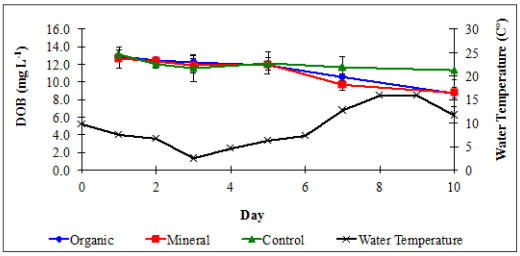

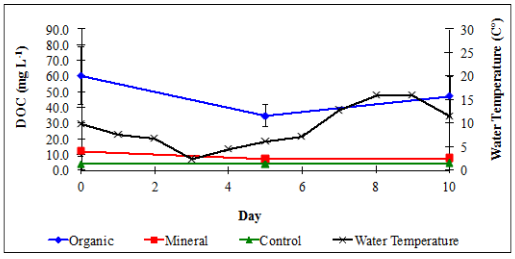

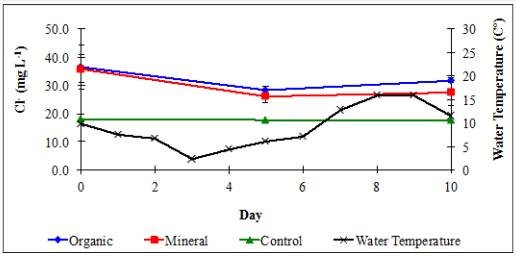

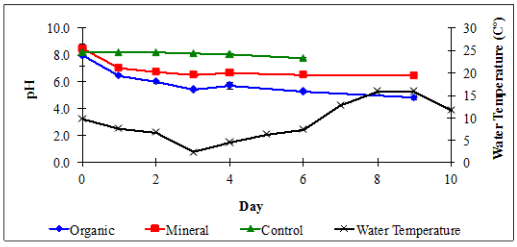

Batch Run 6

Run:	6
Date:	5/28/2013 to 6/7/2013
Depth of Water:	7 in
Target NO_3-N (mg L^{-1}) Concentration:	2.5
Water Recirculation:	1 turnover per day
Antecedent Conditions:	1 in

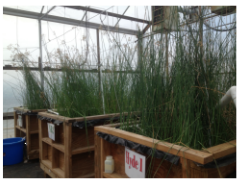

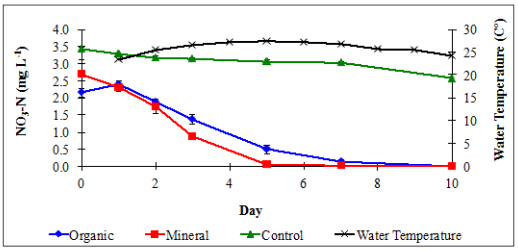

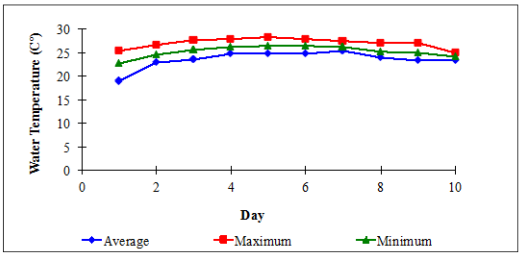

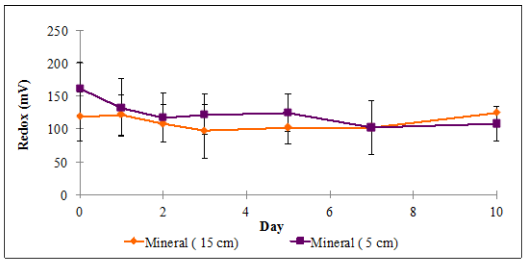

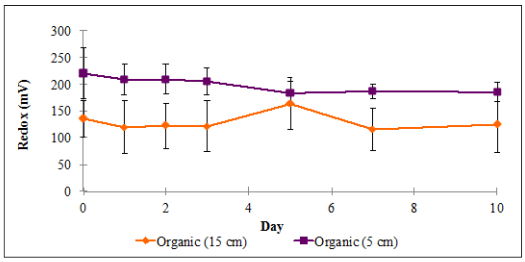

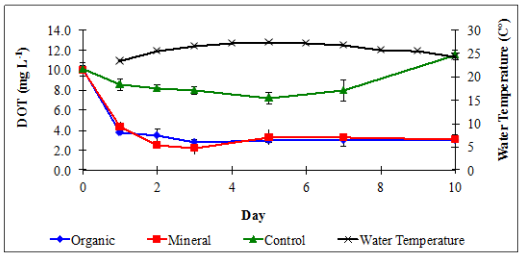

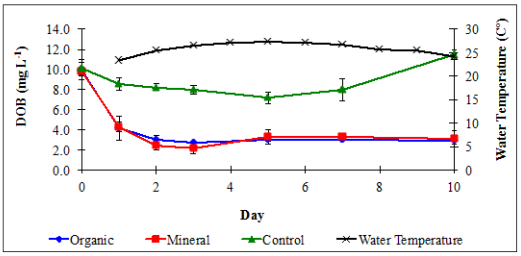

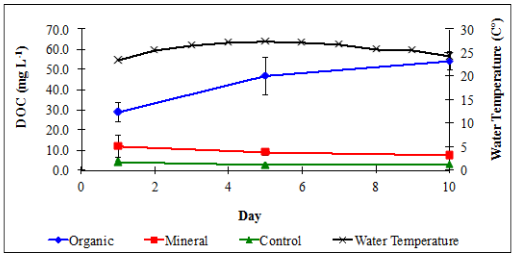

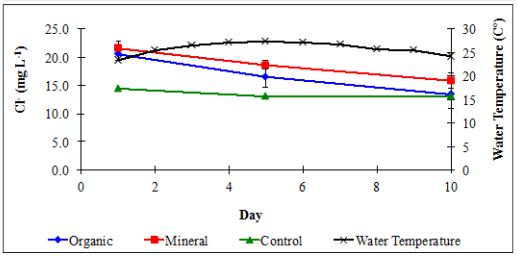

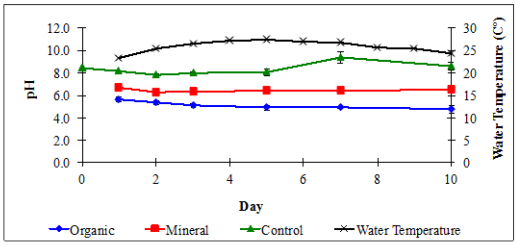

Batch Run 7

Run:	7
Date:	7/2/2013 to 7/12/2013
Depth of Water:	12 in
Target NO_3-N (mg L^{-1}) Concentration:	2.5
Water Recirculation:	1 turnover per day
Antecedent Conditions:	2 in

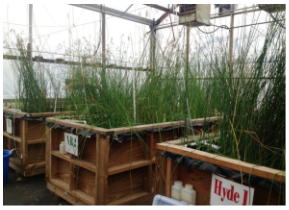

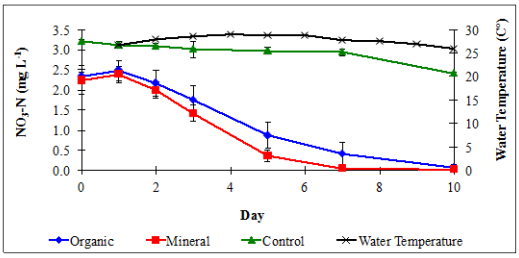

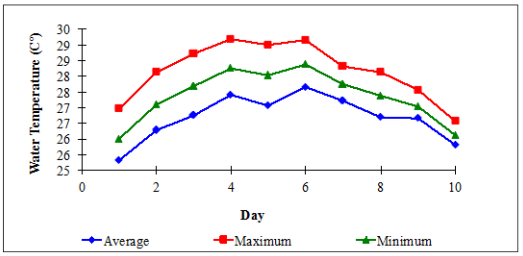

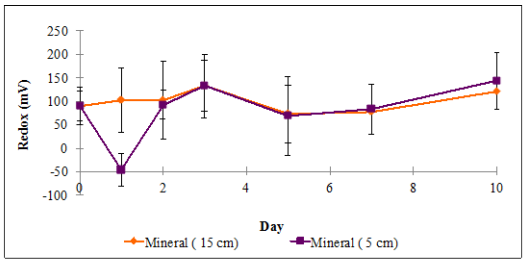

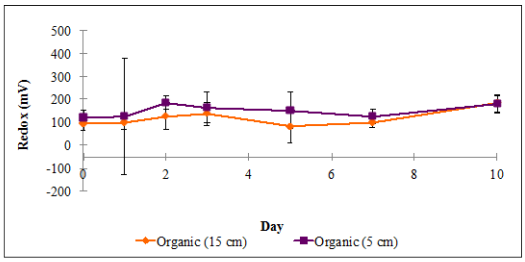

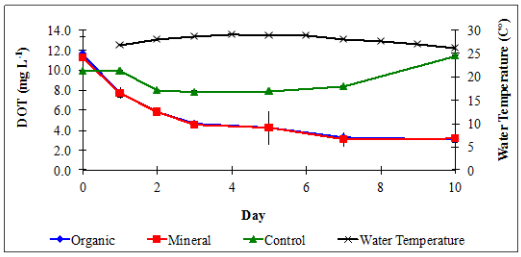

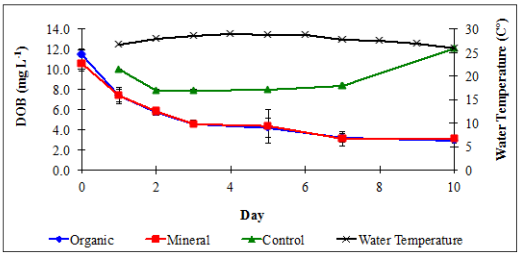

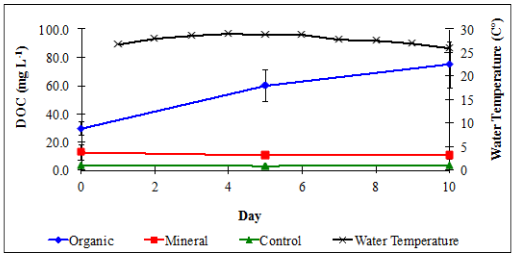

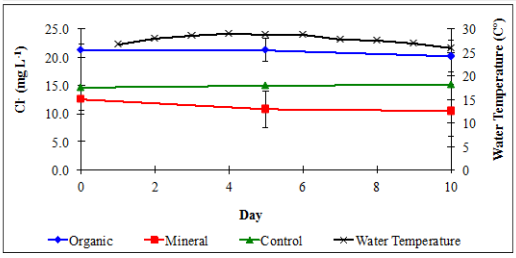

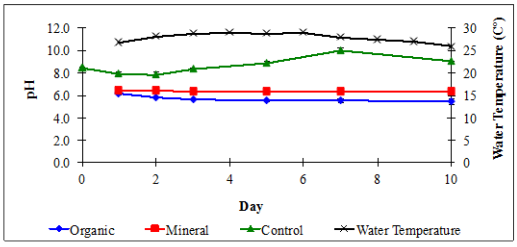

Batch Run 8

Run:	8
Date:	8/6/2013 to 8/16/2013
Depth of Water:	12 in
Target NO_3-N (mg L^{-1}) Concentration:	5
Water Recirculation:	1 turnover per day
Antecedent Conditions:	2 in Argon Study

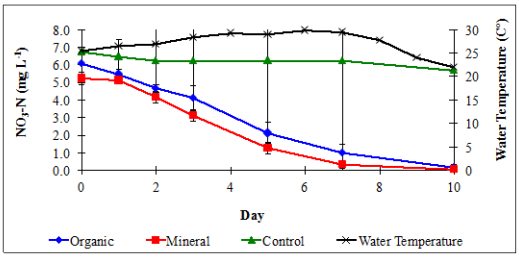

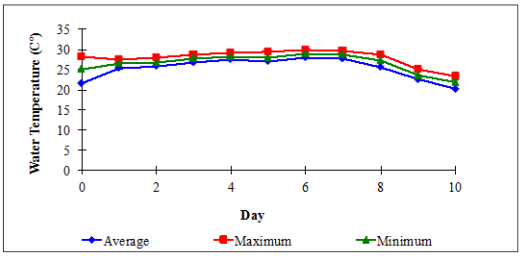

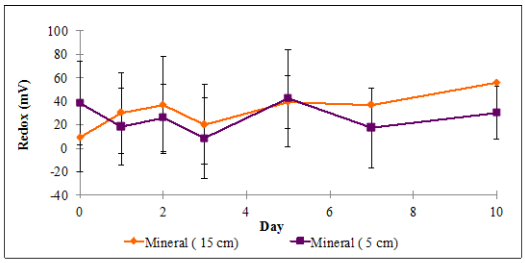

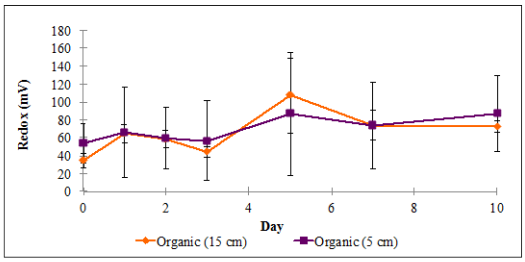

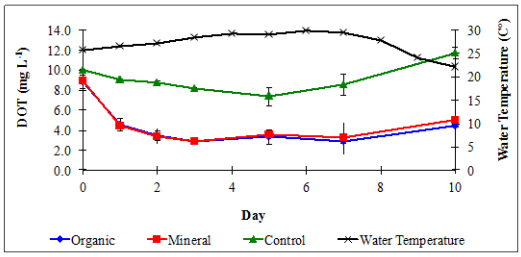

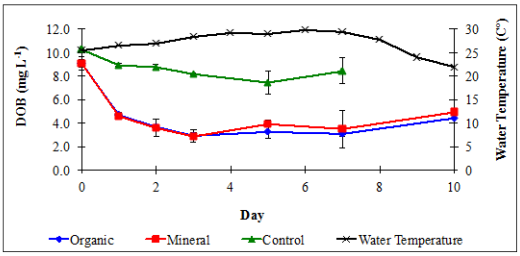

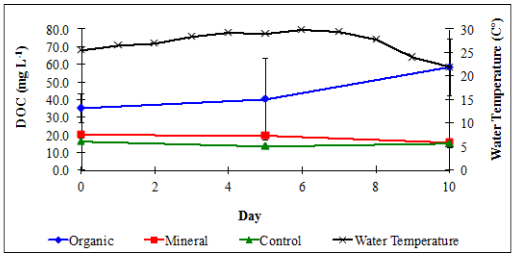

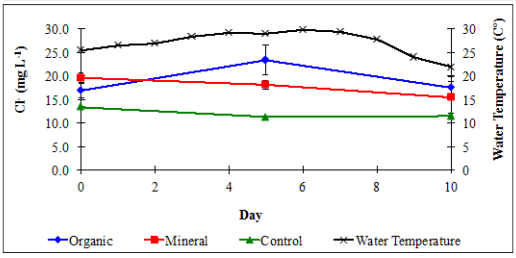

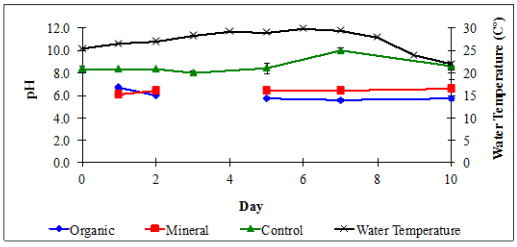

Batch Run 9

Run:	9
Date:	8/20/2013 to 8/29/2013
Depth of Water:	12 in
Target NO_3-N (mg L^{-1}) Concentration:	2.5
Water Recirculation:	1 turnover per day
Antecedent Conditions:	1.5 in 15N Tracer Study

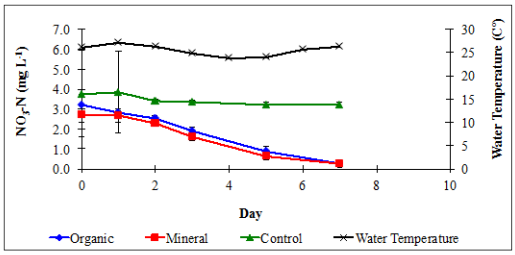

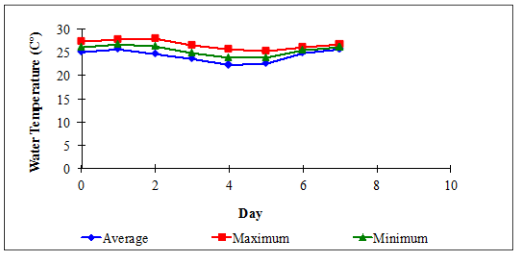

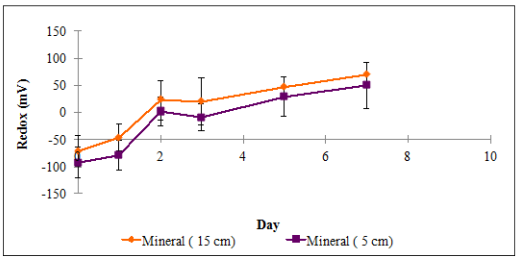

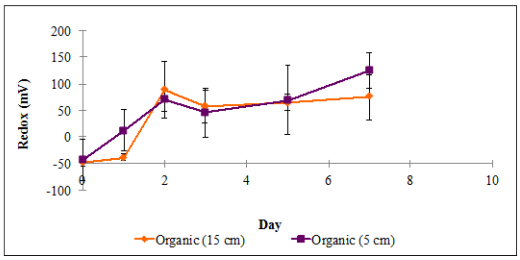

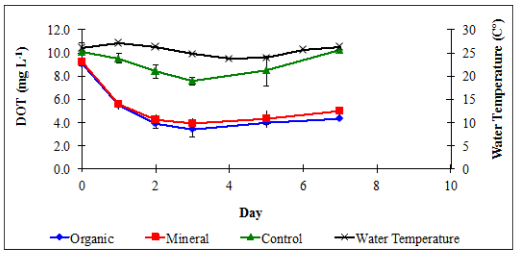

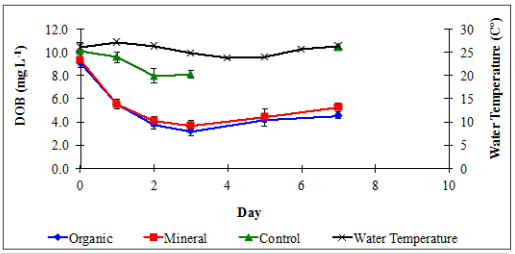

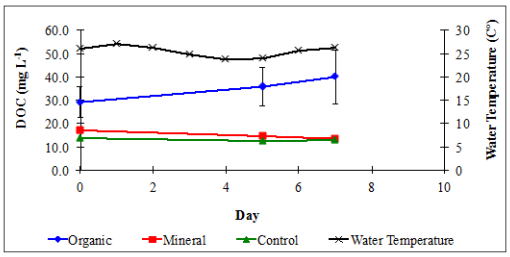

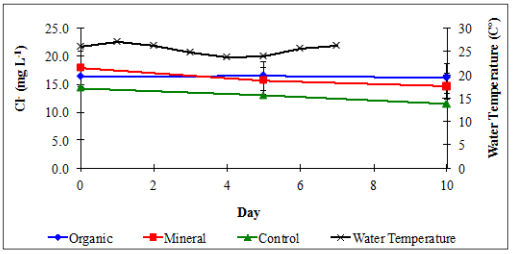

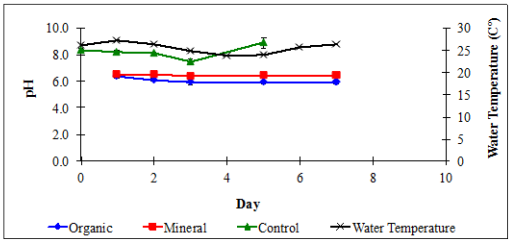

Batch Run 10

Run:	10
Date:	9/24 to 10/4/13
Depth of Water:	12
Target NO_3-N (mg L^{-1}) Concentration:	10
Water Recirculation:	1 turnover per day
Antecedent Conditions:	1.5 in

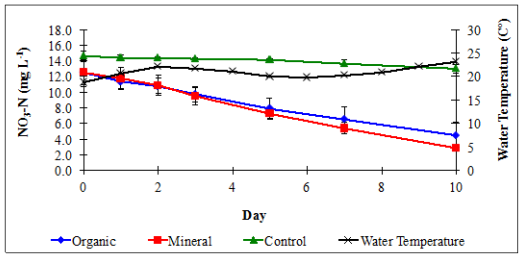

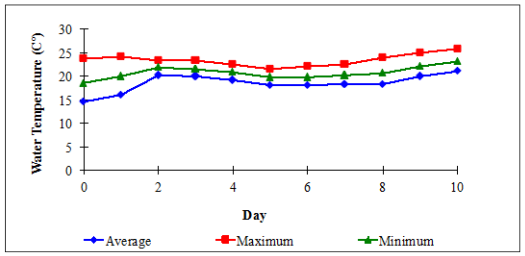

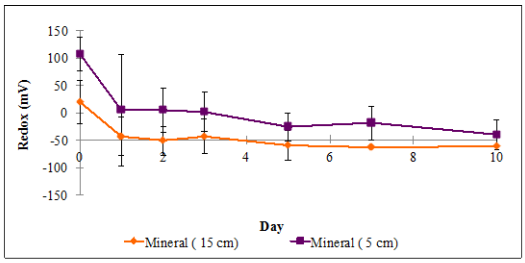

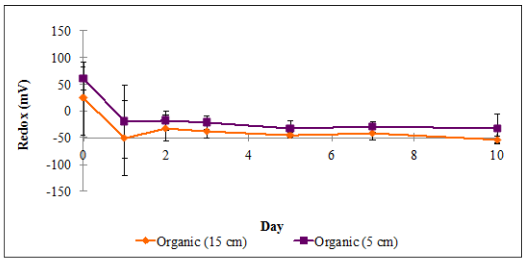

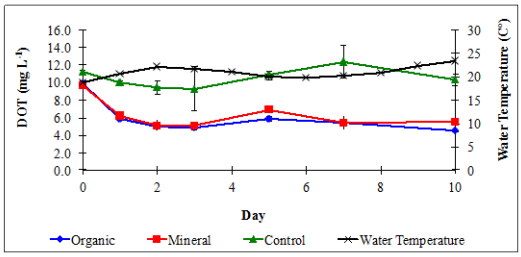

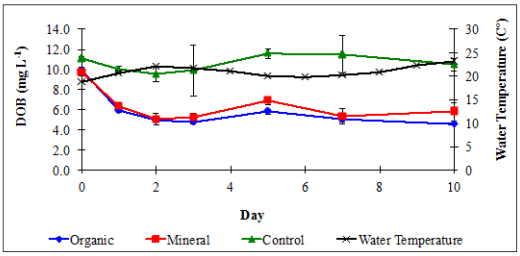

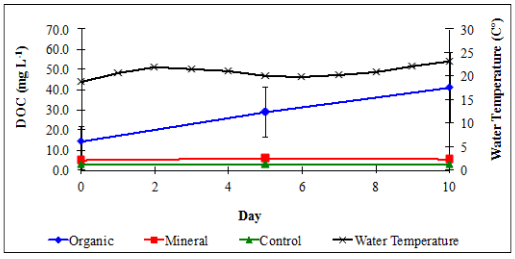

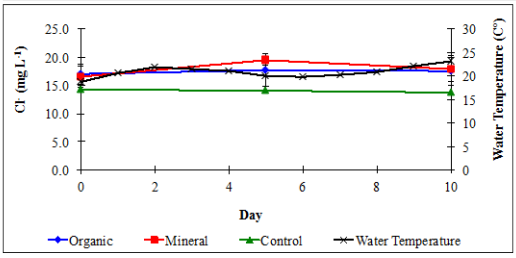

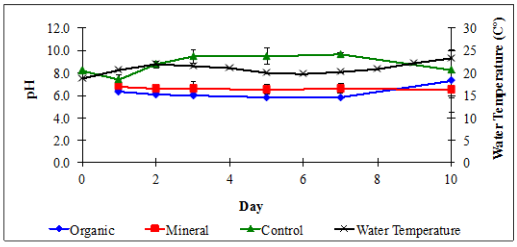

Batch Run 11

Run:	**11**
Date:	**10/15 to 10/25/13**
Depth of Water:	**7 in**
Target NO_3-N (mg L^{-1}) Concentration:	**2.5**
Water Recirculation:	**3 turnover per day**
Antecedent Conditions:	**1.5 in**

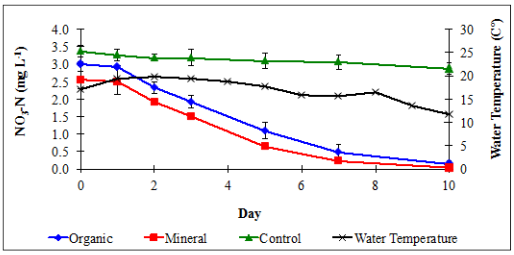

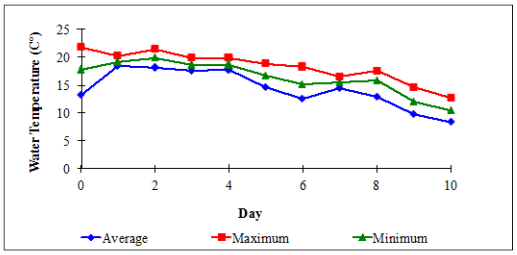

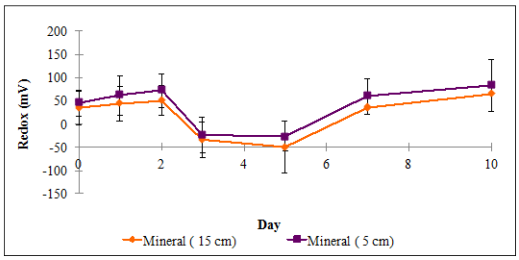

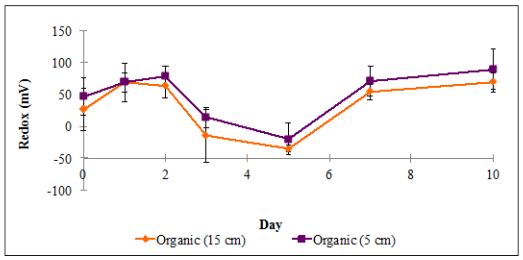

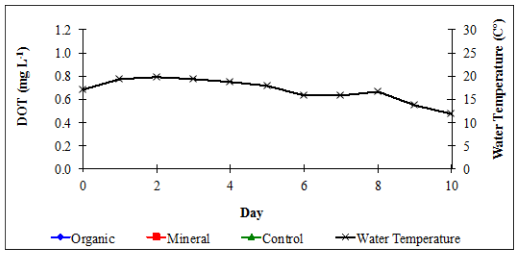

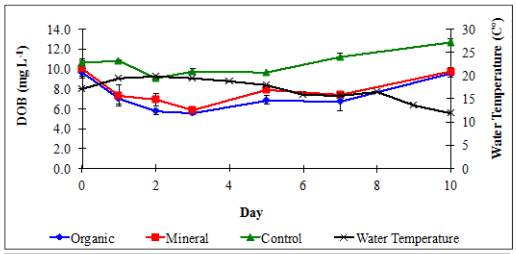

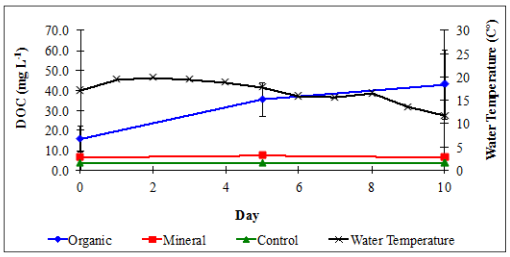

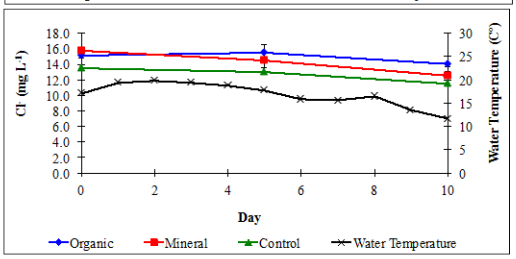

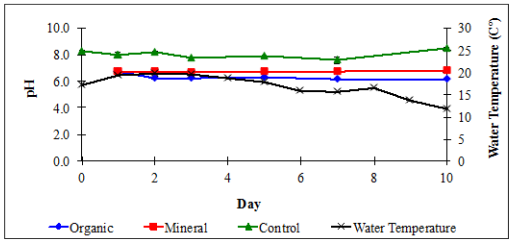

Batch Run 12

Run:	12
Date:	4/8-4/18
Depth of Water:	7 in
Target NO_3-N (mg L^{-1}) Concentration:	5
Water Recirculation:	1 turnover per day
Antecedent Conditions:	1.5 in

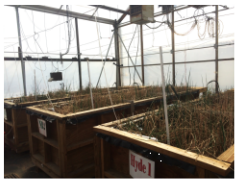

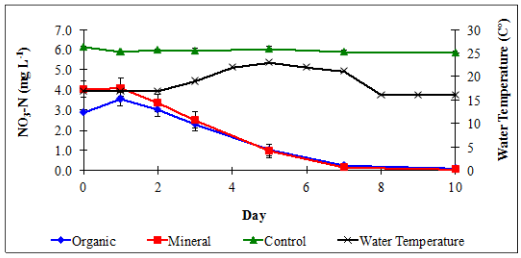

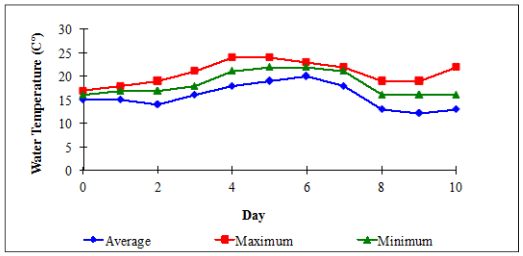

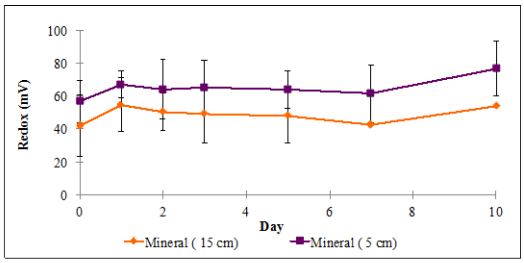

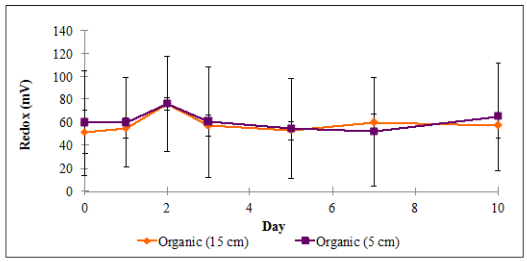

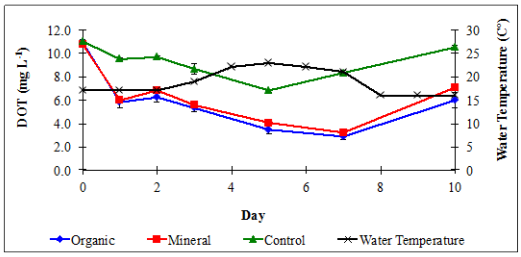

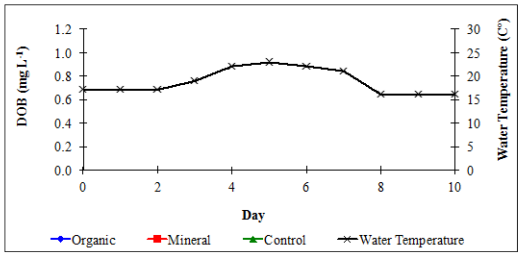

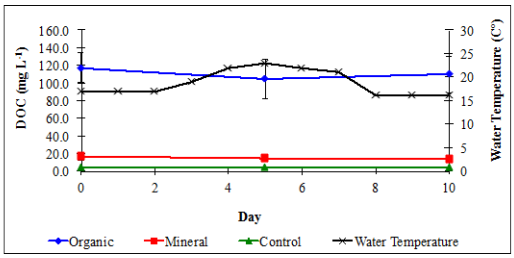

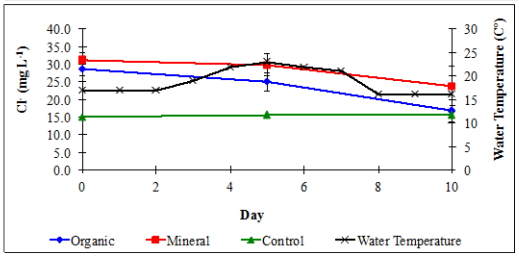

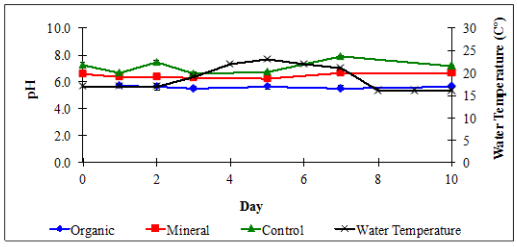

Batch Run 13

Run:	12
Date:	4/8-4/18
Depth of Water:	7 in
Target NO_3-N (mg L^{-1}) Concentration:	5
Water Recirculation:	1 turnover per day
Antecedent Conditions:	1.5 in

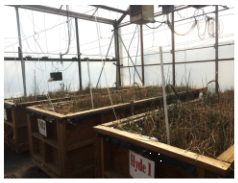

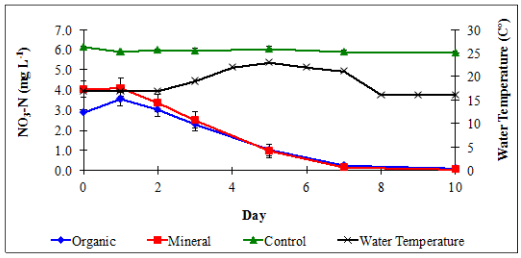

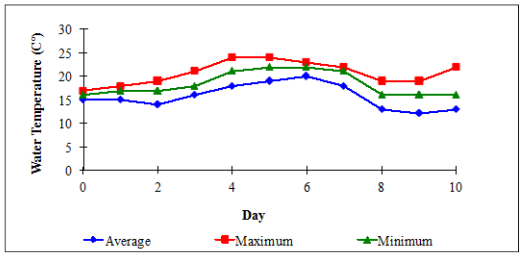

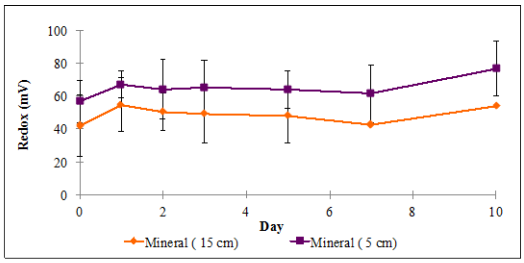

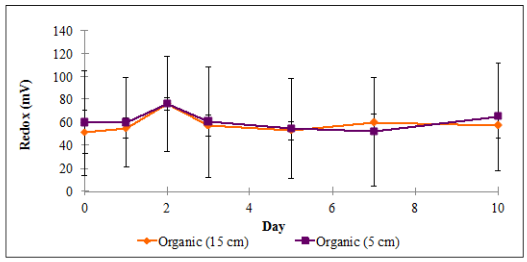

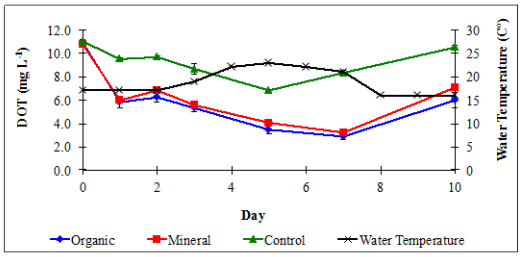

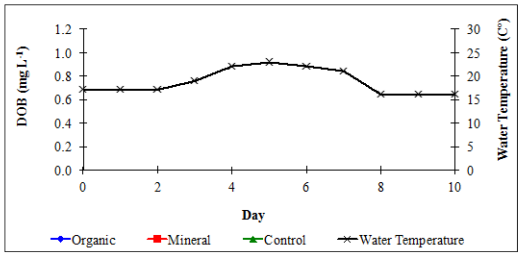

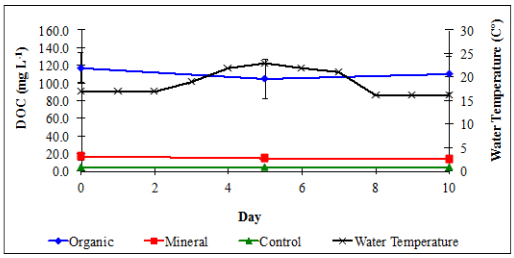

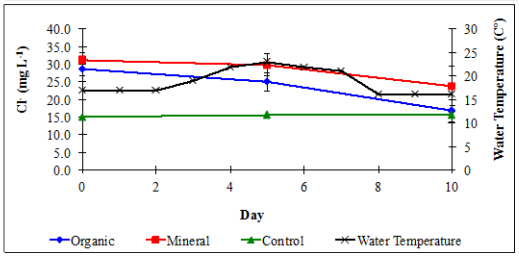

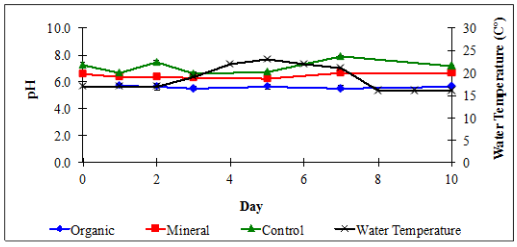

Batch Run 14

Run:	13
Date:	4/21-5/1
Depth of Water:	12 in
Target NO_3-N (mg L^{-1}) Concentration:	10
Water Recirculation:	1 turnover per day
Antecedent Conditions:	1.5 in

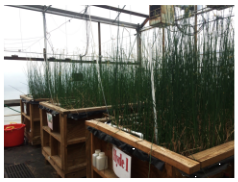

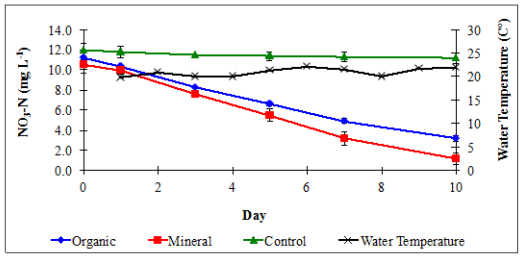

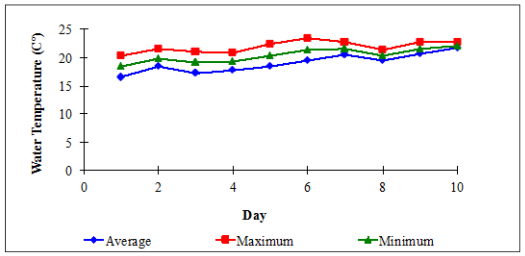

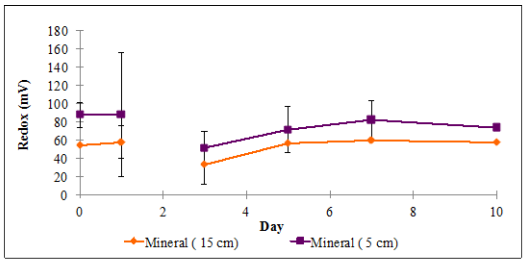

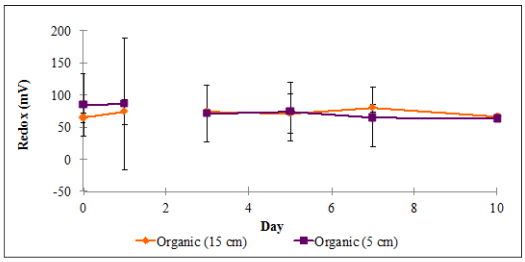

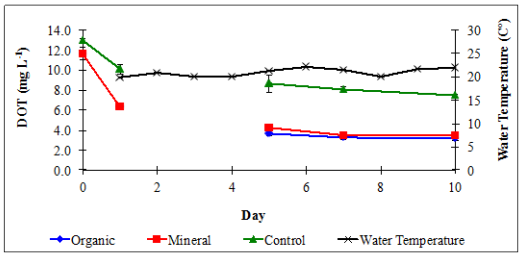

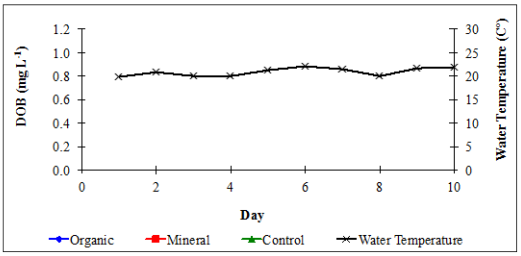

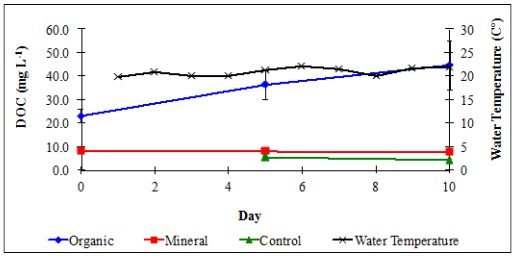

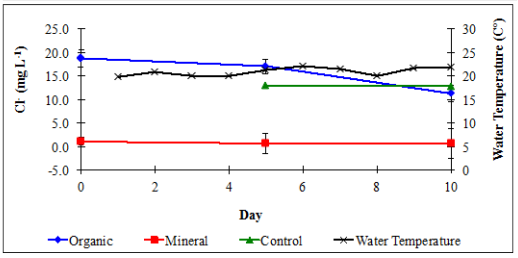

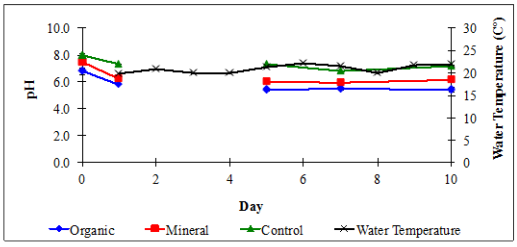

Batch Run 15

Run:	**15**
Date:	**6/12-6/22**
Depth of Water:	**7 in**
Target NO_3-N (mg L^{-1}) Concentration:	**2.5**
Water Recirculation:	**1 turnover per day**
Antecedent Conditions:	**1.5 in**

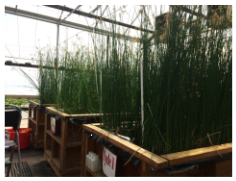

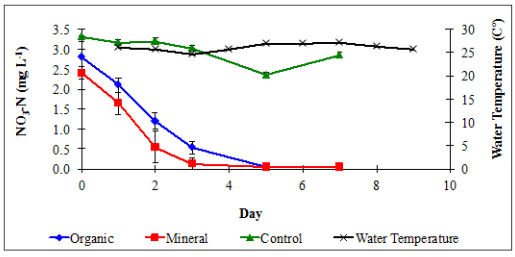

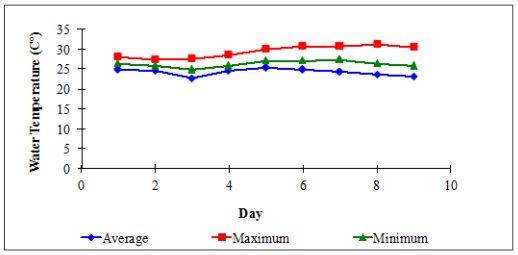

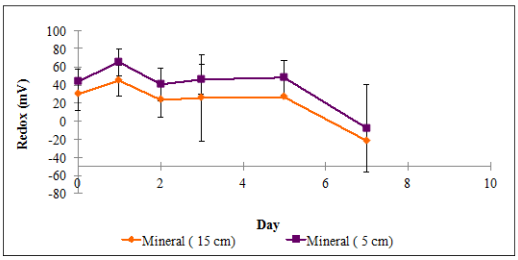

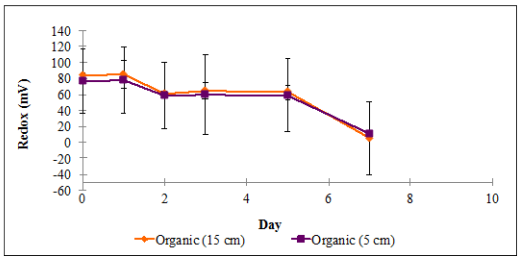

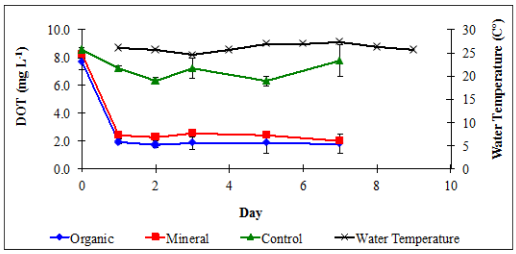

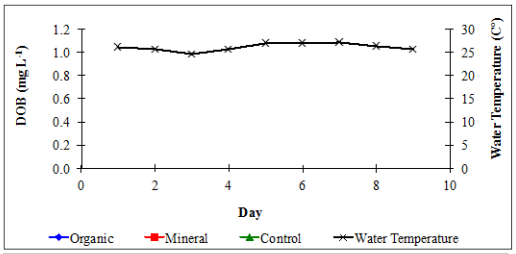

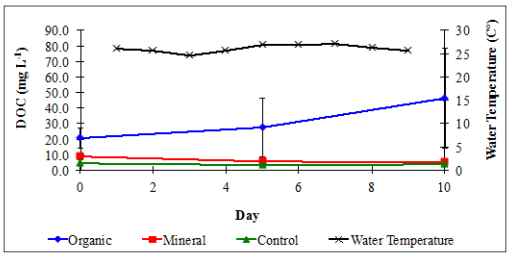

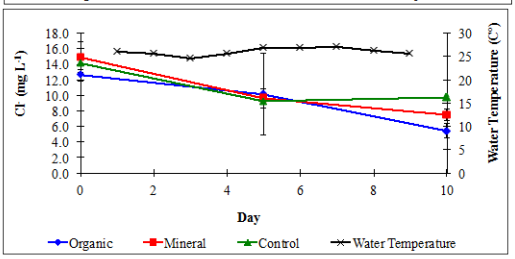

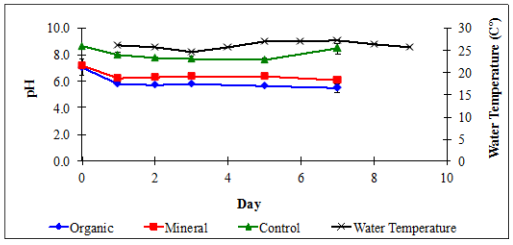

Batch Run 16

Run:	**16**
Date:	**7/22-8/1**
Depth of Water:	**12 in**
Target NO_x-N (mg L^{-1}) Concentration:	**10**
Water Recirculation:	**1 turnover per day**
Antecedent Conditions:	**1.5 in**
	Tracer Study

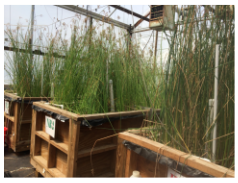

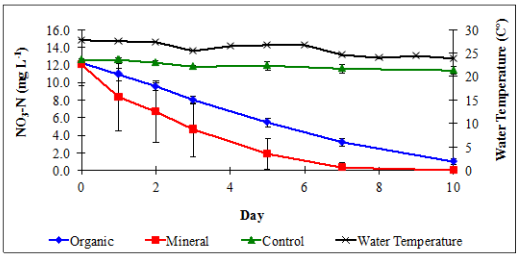

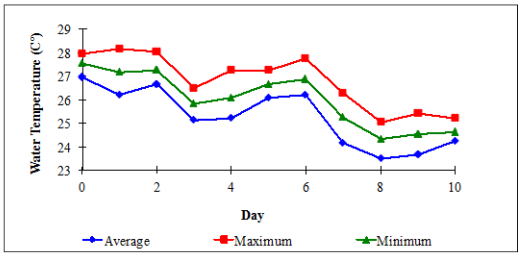

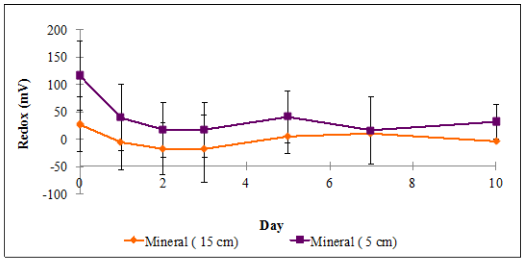

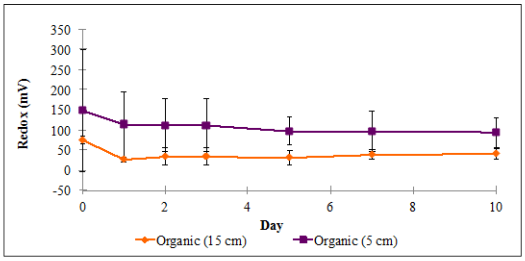

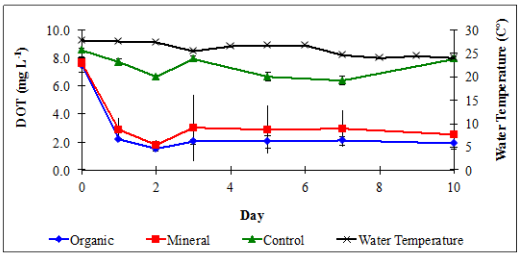

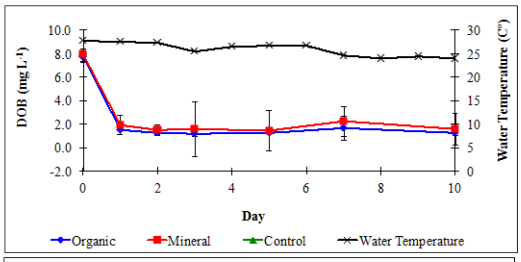

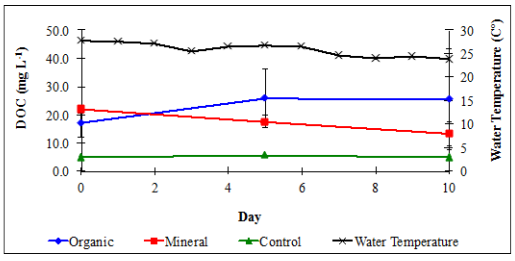

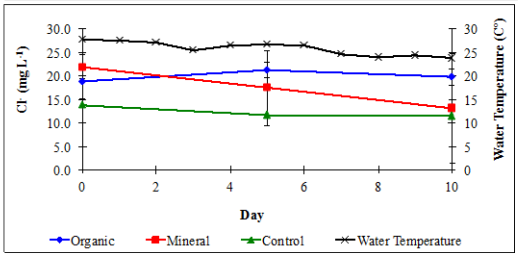

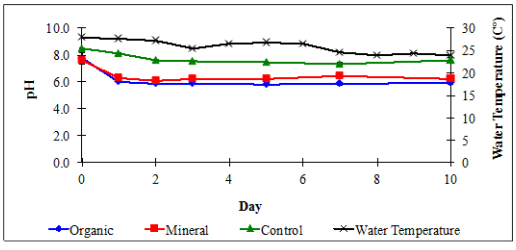

Batch Run 17

Run:	17
Date:	8/12-8/22
Depth of Water:	7 in
Target NO_3-N (mg L^{-1}) Concentration:	5
Water Recirculation:	1 turnover per day
Antecedent Conditions:	1.5 in

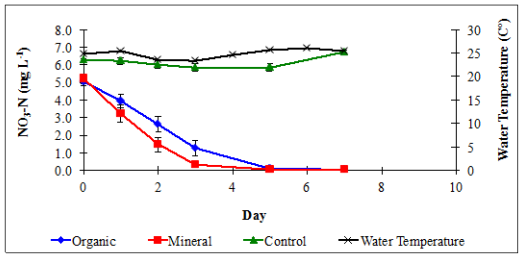

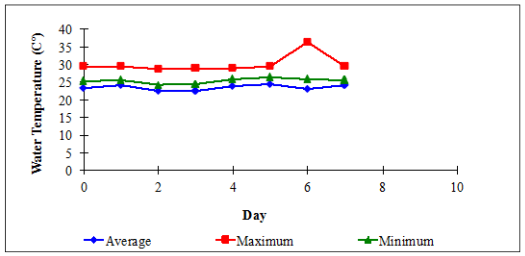

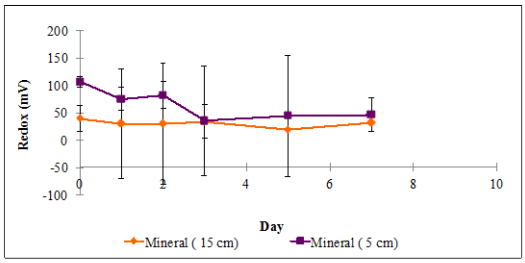

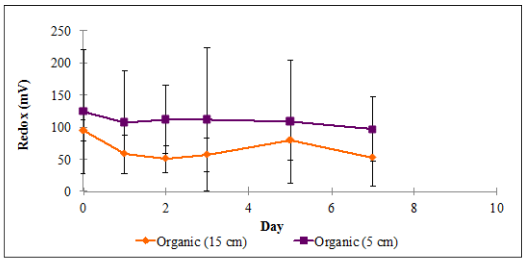

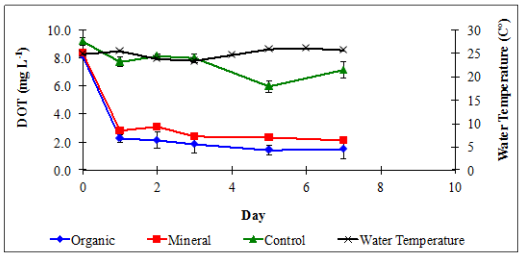

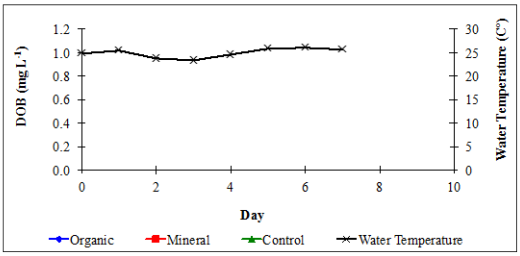

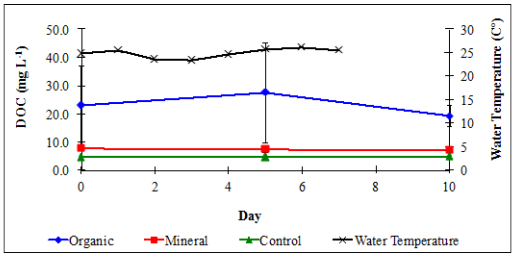

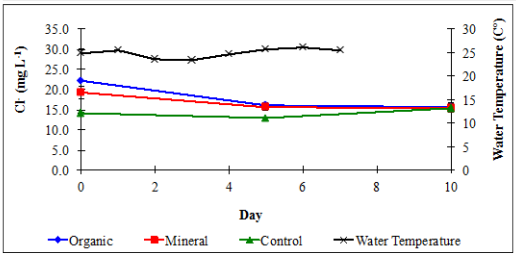

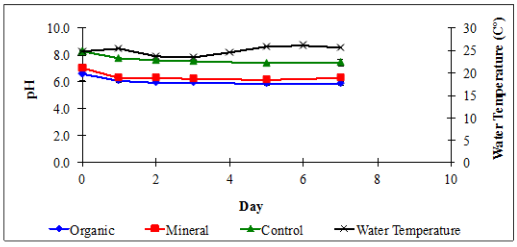

Batch Run 18

Run:	**18**
Date:	**9/2-9/12**
Depth of Water:	**9-10.5 in**
Target NO_3-N (mg L^{-1}) Concentration:	**2.5**
Water Recirculation:	**1 turnover per day**
Antecedent Conditions:	**-2 in**

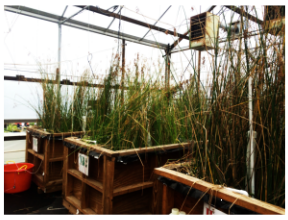

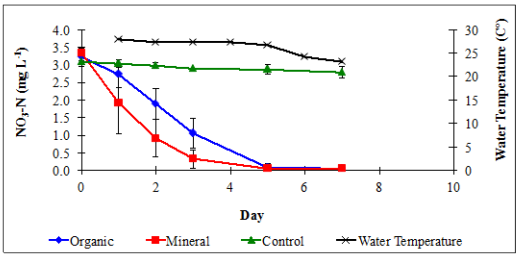

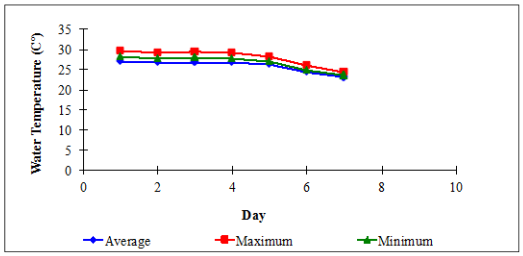

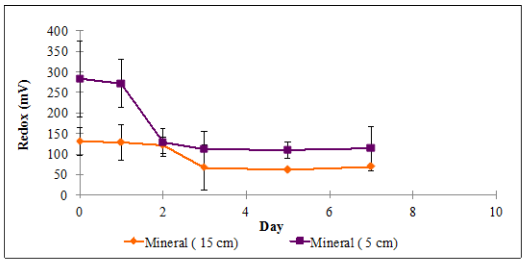

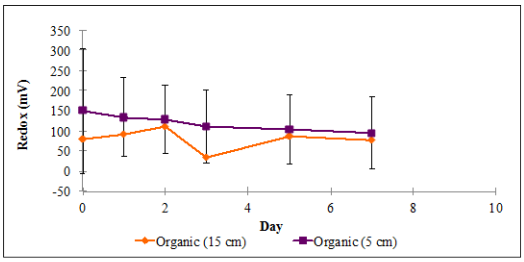

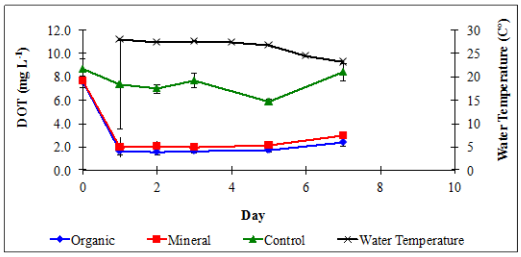

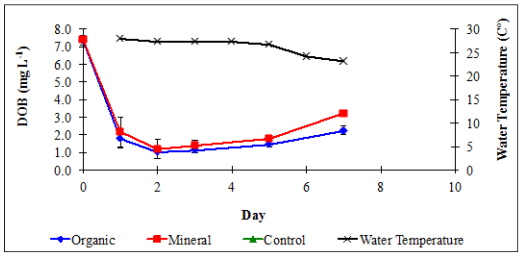

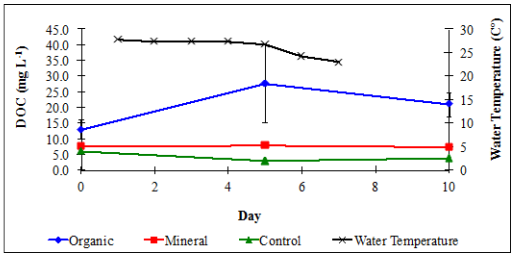

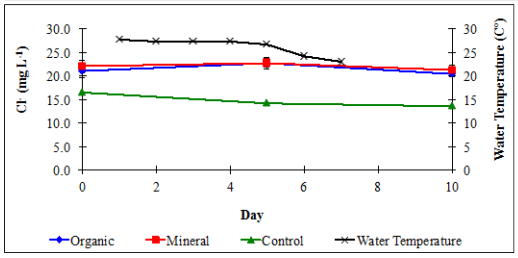

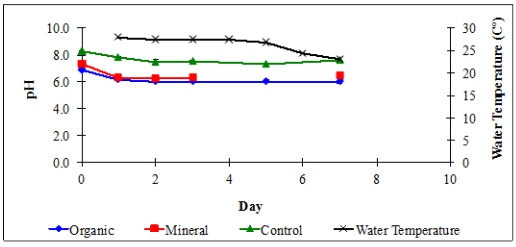

Appendix 4 – SCAN calibration results

Table A4.1: Mineral Mesocosm UV-Vis Spectrometer Fits for NO_3-N

Mineral Mesocosms			
Run	**Comps**	**adjCV**	**% variance**
1		Multiplexor Malfunctioned	
2	2	0.621	87.43
3		Frozen Line	
4		Multiplexor Malfunctioned	
5		Frozen Line	
6	8	0.2212	99.88
7	3	0.1891	98.14
8	5	0.1152	99.86
9	7	0.1799	99.59
10	4	1.023	98.66
11	5	0.3458	97.81
12		Pump Malfunctioned	
13		Pump Malfunctioned	
14	2	0.2537	97.29
15	3	0.06114	99.84
16	4	0.3531	99.72
17	2	0.684	90.71
18	2	0.3569	94.58

Table A4.2: Organic Mesocosm UV-Vis Spectrometer Fits for NO_3-N

Organic Mesocosms			
Run	**Comps**	**adjCV**	**% variance**
1		Multiplexor Malfunctioned	
2	2	0.6406	89.34
3		Frozen Line	
4		Multiplexor Malfunctioned	
5		Frozen Line	
6	1	0.543	62.87
7	10	0.2807	99.74
8	3	0.3415	98.04
9	7	0.1916	99.7
10	6	0.9314	97.21
11	4	95.55	95.55
12		Pump Malfunctioned	
13		Pump Malfunctioned	
14	8	0.8501	99.3
15	4	0.3077	99.2
16	3	0.823	94.61
17	5	0.2936	99.04
18	3	0.2786	97.77

Table A4.3: Control Mesocosm UV-Vis Spectrometer Fits for NO_3-N

Control Mesocosms			
Run	**Comps**	**adjCV**	**% variance**
1		Multiplexor Malfunctioned	
2	6	0.2404	89.6
3		Frozen Line	
4		Multiplexor Malfunctioned	
5		Frozen Line	
6	3	0.0467	97.23
7	7	0.3008	91.82
8	6	0.2861	73.27
9	5	0.1025	90.01
10	3	0.2774	59.11
11	1	0.05189	59.36
12		Pump Malfunctioned	
13		Pump Malfunctioned	
14	6	0.06276	91.15
15	4	0.3128	64.07
16	12	0.2947	99.98
17	2	0.2143	51.15
18	2	0.111	32.45

Table A4.4: Mesocosm UV-Vis Spectrometer Fits for DOC

Mesocosm	**Comps**	**adjCV**	**% variance**
N1	5	0.7846	96.4
N2	5	0.7659	97.6
N3	8	0.6648	98.99
C1	4	0.9718	94.19
C2	15	0.9293	99.7
C3	5	1.176	93.82
H1	9	3.464	95.32
H2	6	1.257	97.32
H3	11	2.308	95.89

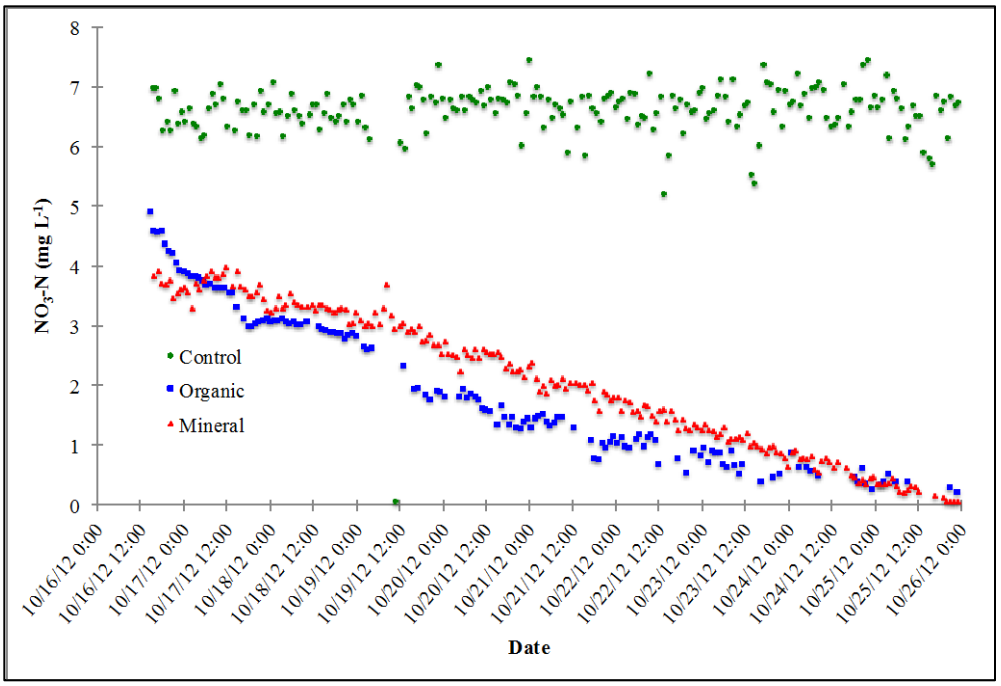

Figure A4.1: UV-Vis Spectrometer NO_3-N readings from 1 of 3 mesocosms from each treatment (Organic, Mineral, and Control) during Batch Run 2.

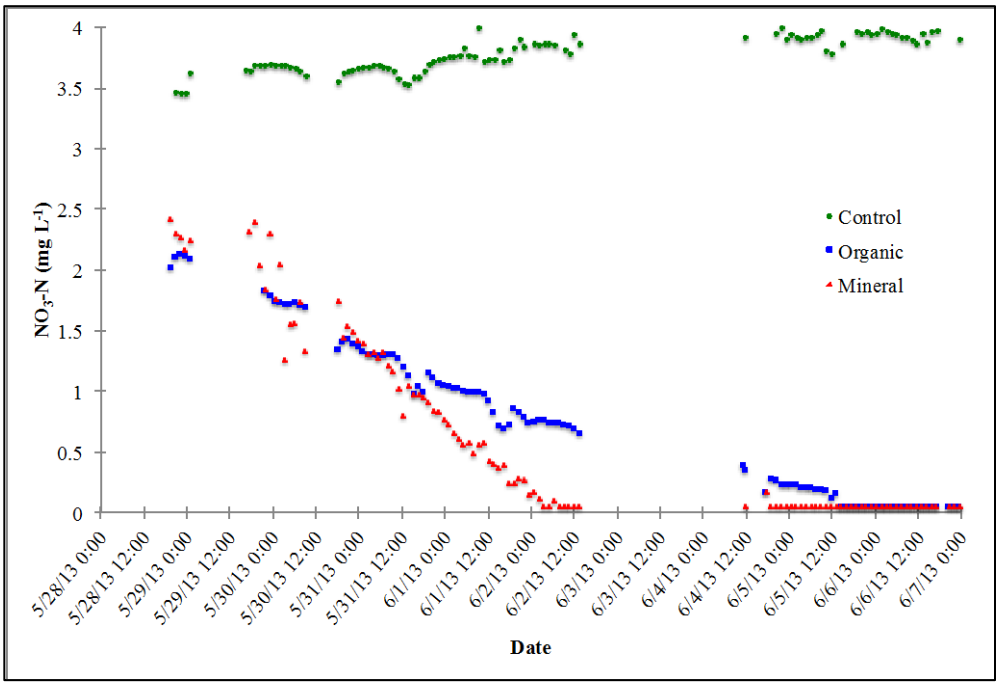

Figure A4.2: UV-Vis Spectrometer NO_3-N readings from 1 of 3 mesocosms from each treatment (Organic, Mineral, and Control) during Batch Run 6.

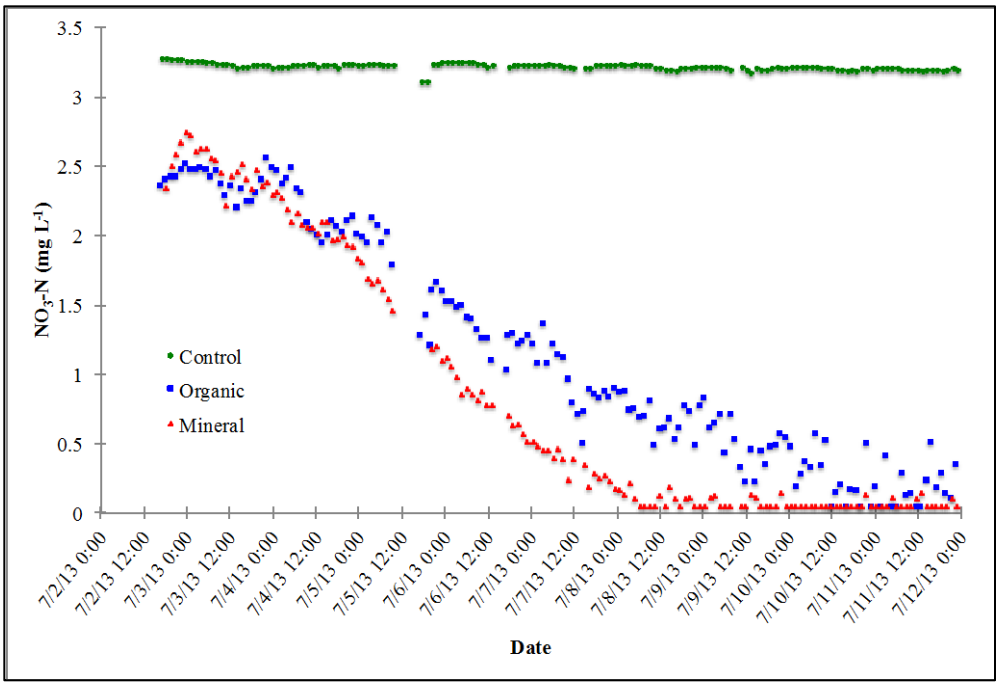

Figure A4.3: UV-Vis Spectrometer NO_3-N readings from 1 of 3 mesocosms from each treatment (Organic, Mineral, and Control) during Batch Run 7.

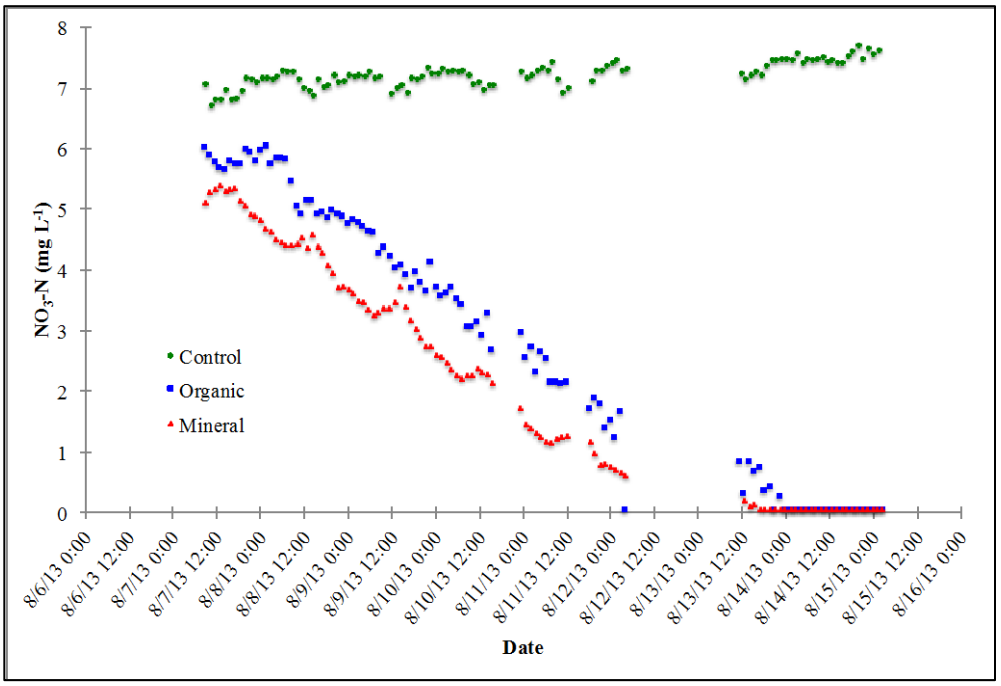

Figure A4.4: UV-Vis Spectrometer NO_3-N readings from 1 of 3 mesocosms from each treatment (Organic, Mineral, and Control) during Batch Run 8.

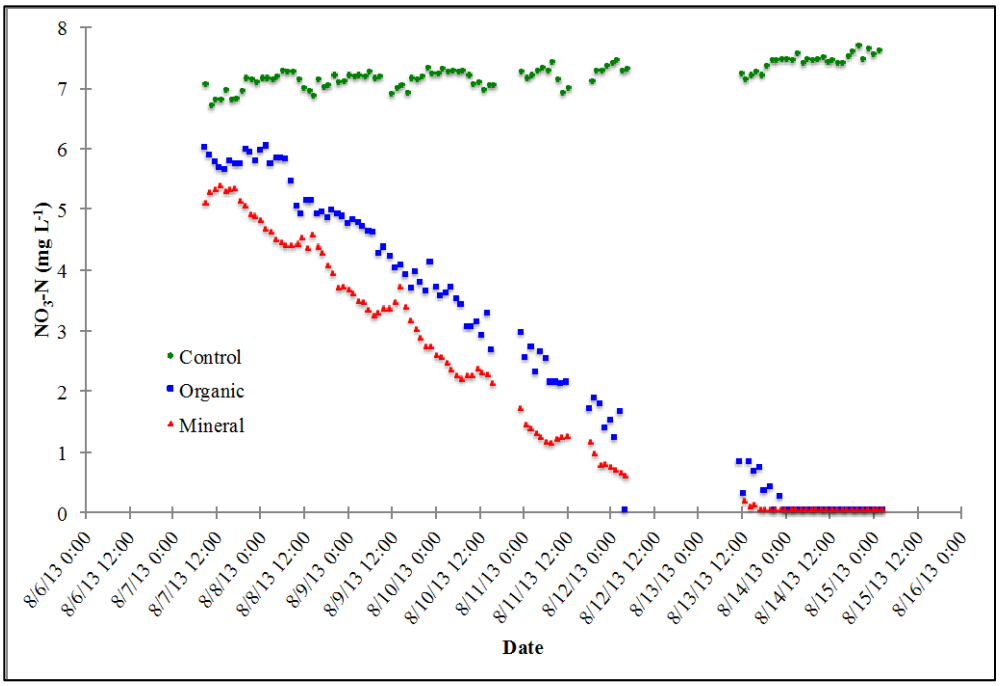

Figure A4.5: UV-Vis Spectrometer NO_3-N readings from 1 of 3 mesocosms from each treatment (Organic, Mineral, and Control) during Batch Run 9.

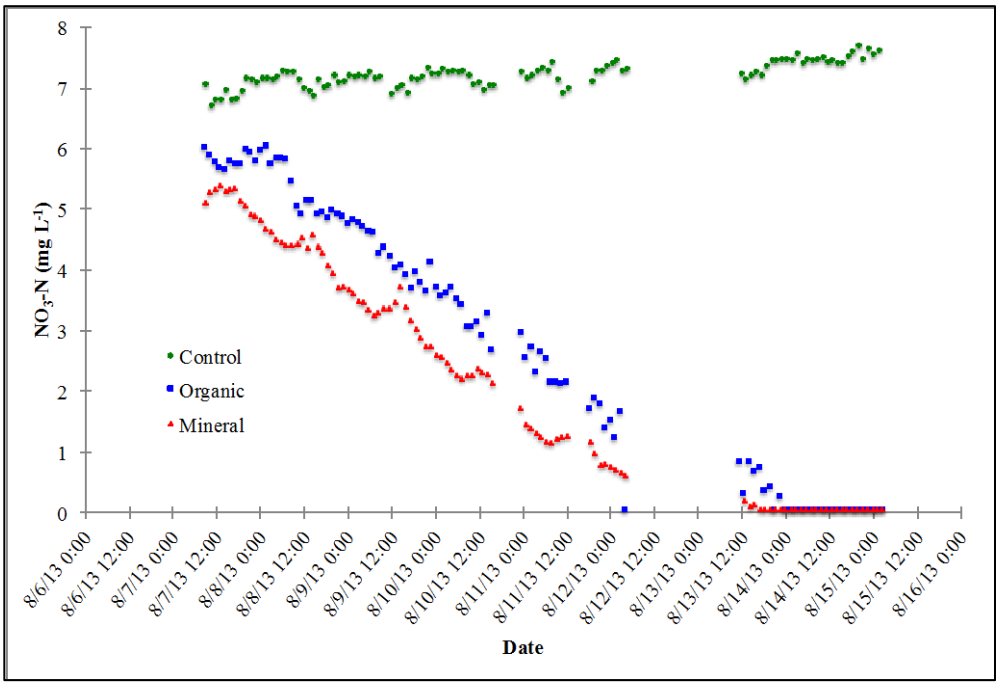

Figure A4.6: UV-Vis Spectrometer NO_3-N readings from 1 of 3 mesocosms from each treatment (Organic, Mineral, and Control) during Batch Run 10.

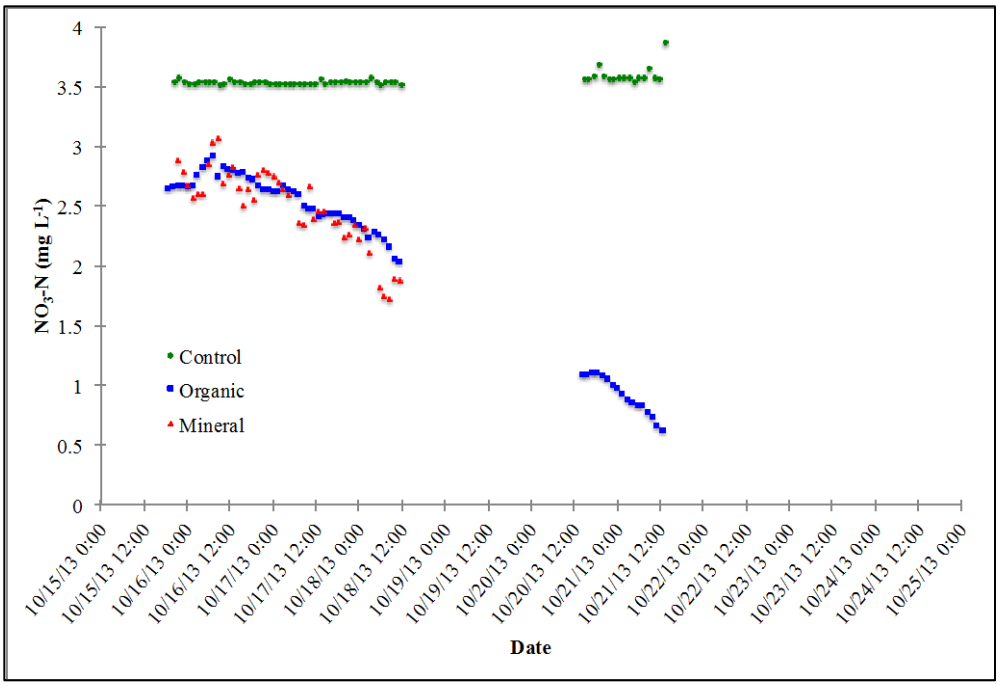

Figure A4.7: UV-Vis Spectrometer NO_3-N readings from 1 of 3 mesocosms from each treatment (Organic, Mineral, and Control) during Batch Run 11.

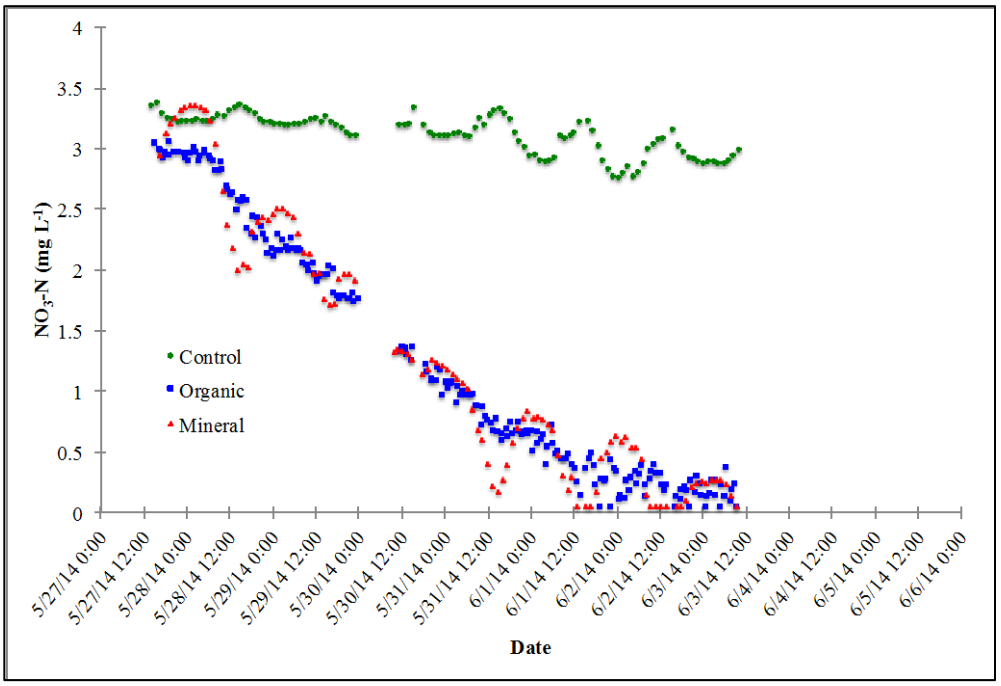

Figure A4.8: UV-Vis Spectrometer NO_3-N readings from 1 of 3 mesocosms from each treatment (Organic, Mineral, and Control) during Batch Run 14.

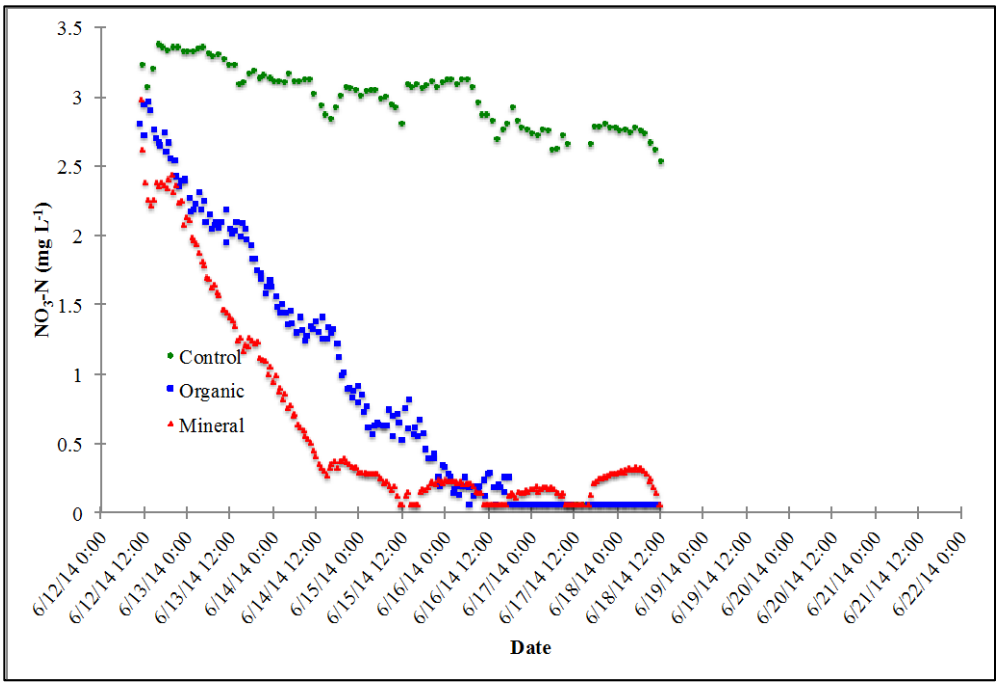

Figure A4.9: UV-Vis Spectrometer NO_3-N readings from 1 of 3 mesocosms from each treatment (Organic, Mineral, and Control) during Batch Run 15.

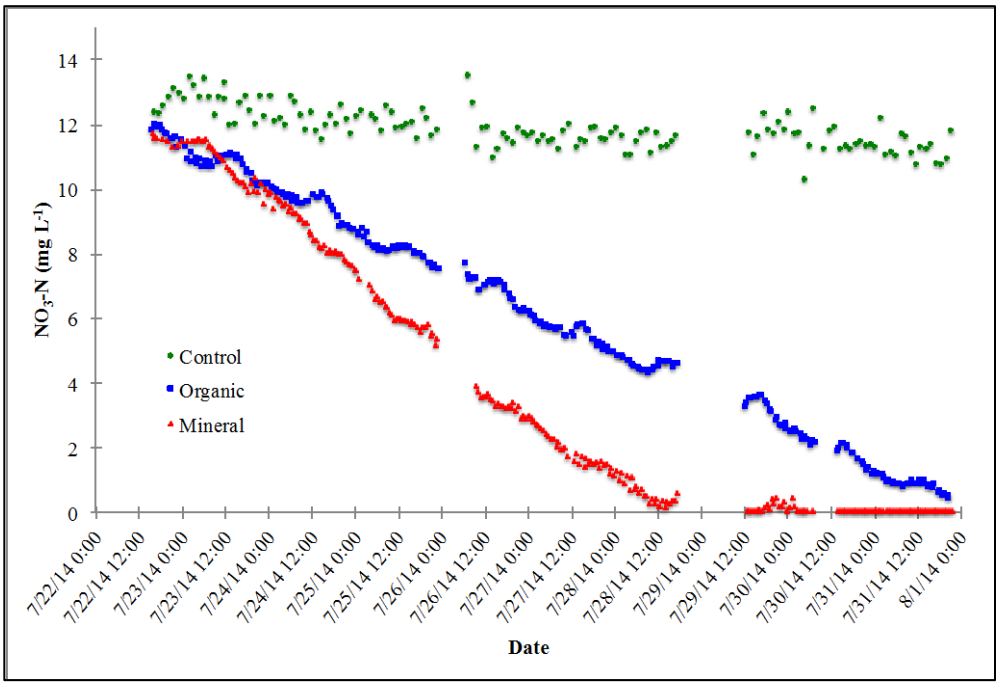

Figure A4.10: UV-Vis Spectrometer NO_3-N readings from 1 of 3 mesocosms from each treatment (Organic, Mineral, and Control) during Batch Run 16.

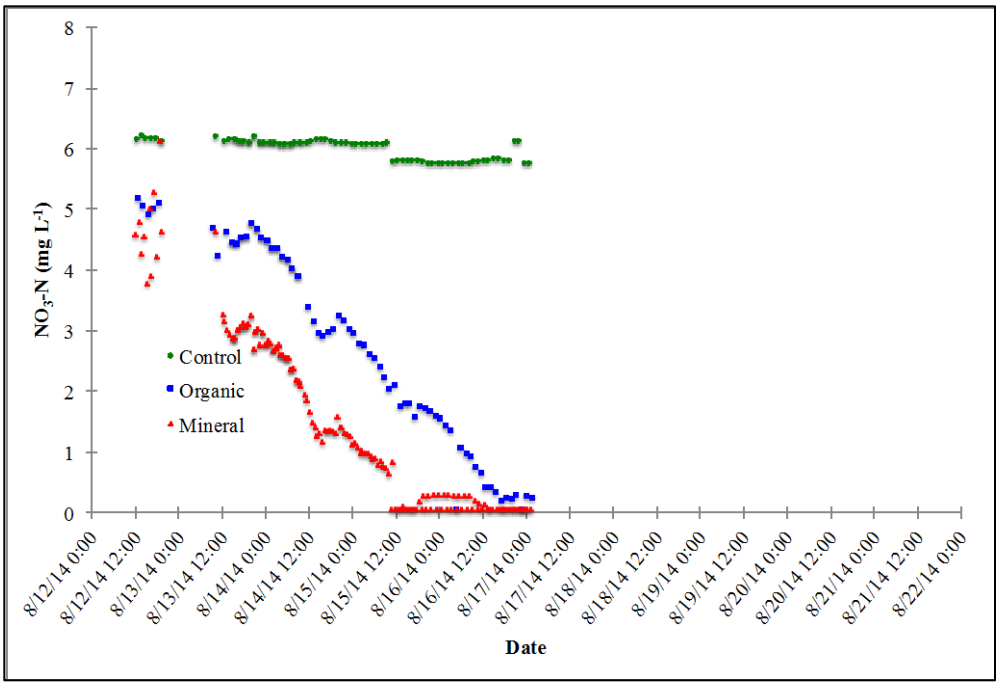

Figure A4.11: UV-Vis Spectrometer NO_3-N readings from 1 of 3 mesocosms from each treatment (Organic, Mineral, and Control) during Batch Run 17.

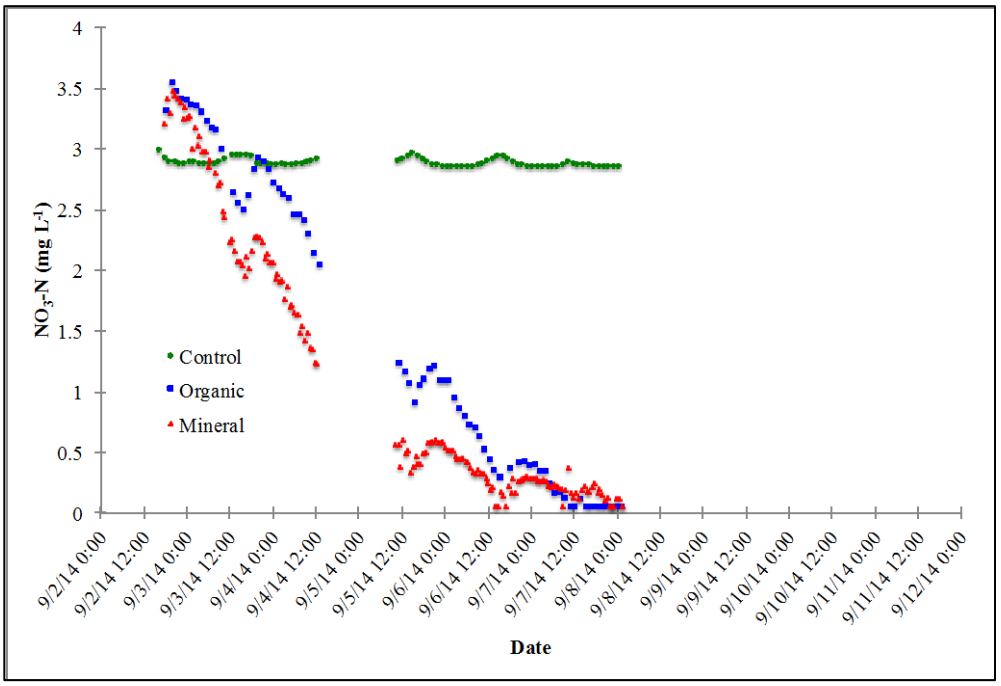

Figure A4.12: UV-Vis Spectrometer NO_3-N readings from 1 of 3 mesocosms from each treatment (Organic, Mineral, and Control) during Batch Run 18.

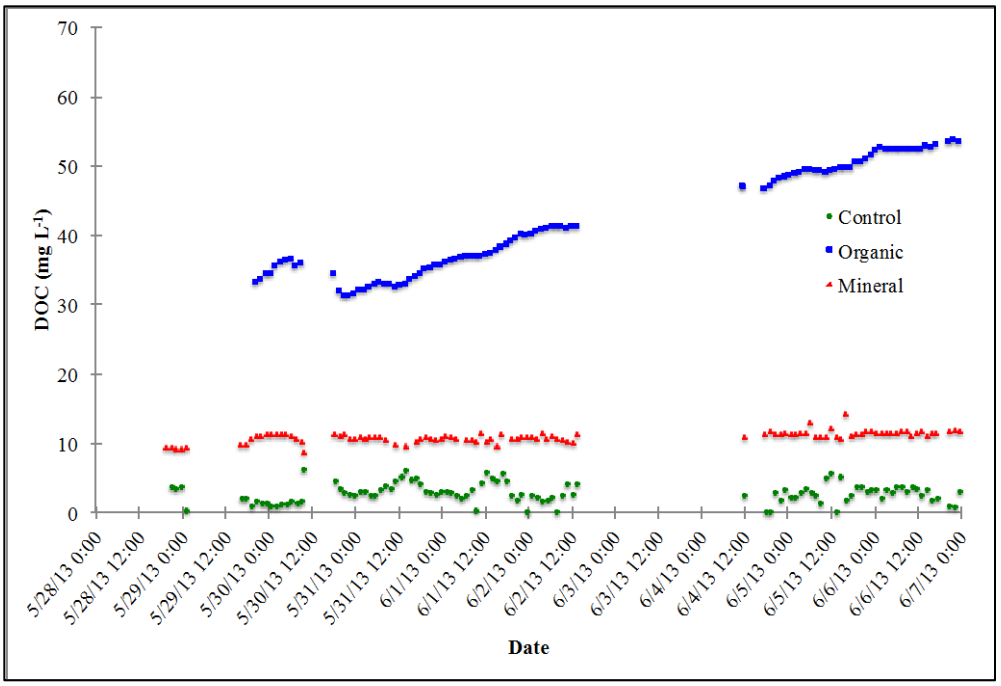

Figure A4.13: UV-Vis Spectrometer DOC readings from 1 of 3 mesocosms from each treatment (Organic, Mineral, and Control) during Batch Run 6.

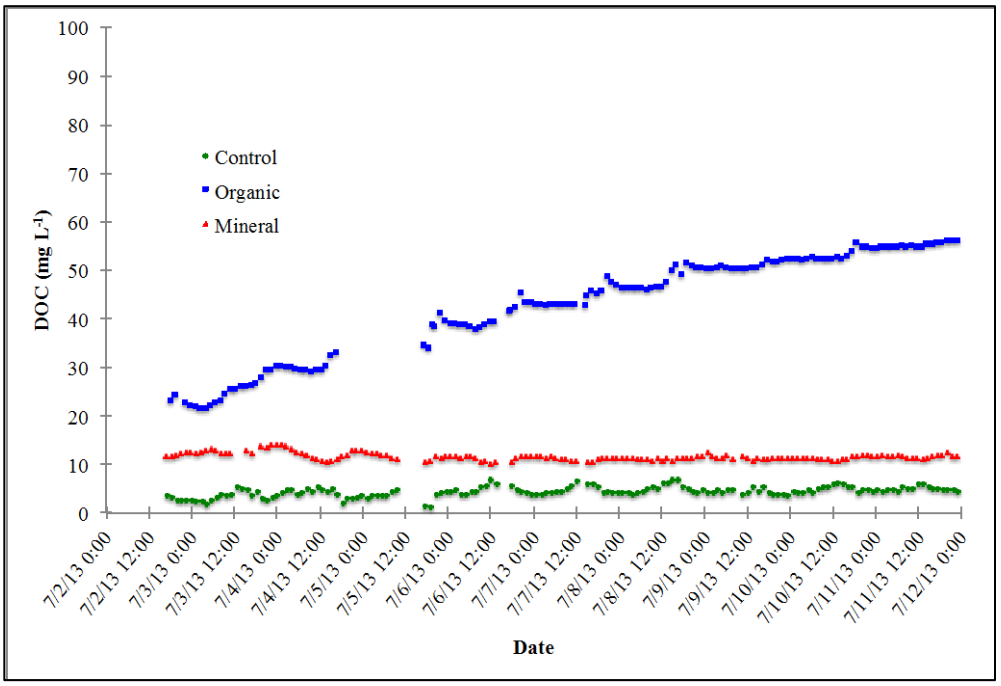

Figure A4.14: UV-Vis Spectrometer DOC readings from 1 of 3 mesocosms from each treatment (Organic, Mineral, and Control) during Batch Run 7.

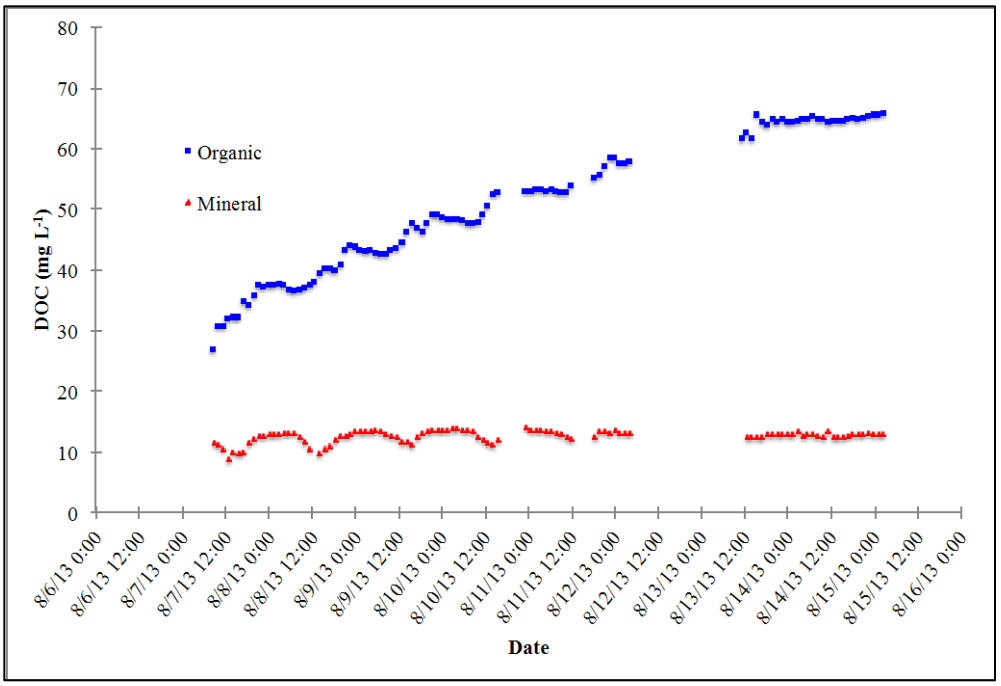

Figure A4.15: UV-Vis Spectrometer DOC readings from 1 of 3 mesocosms from each treatment (Organic, Mineral, and Control) during Batch Run 8.

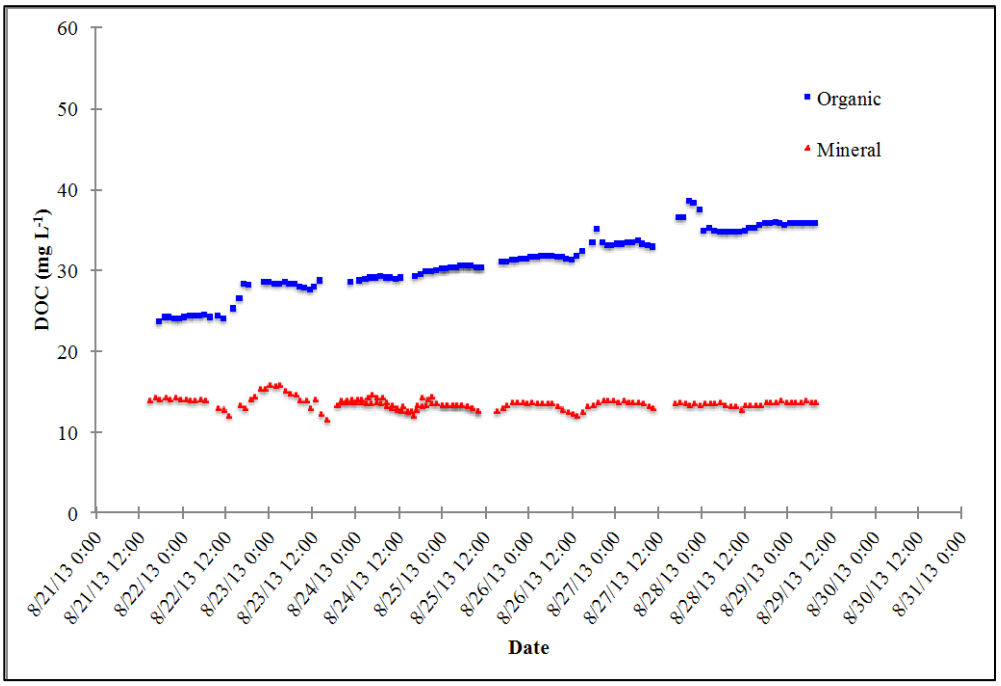

Figure A4.16: UV-Vis Spectrometer DOC readings from 1 of 3 mesocosms from each treatment (Organic, Mineral, and Control) during Batch Run 9.

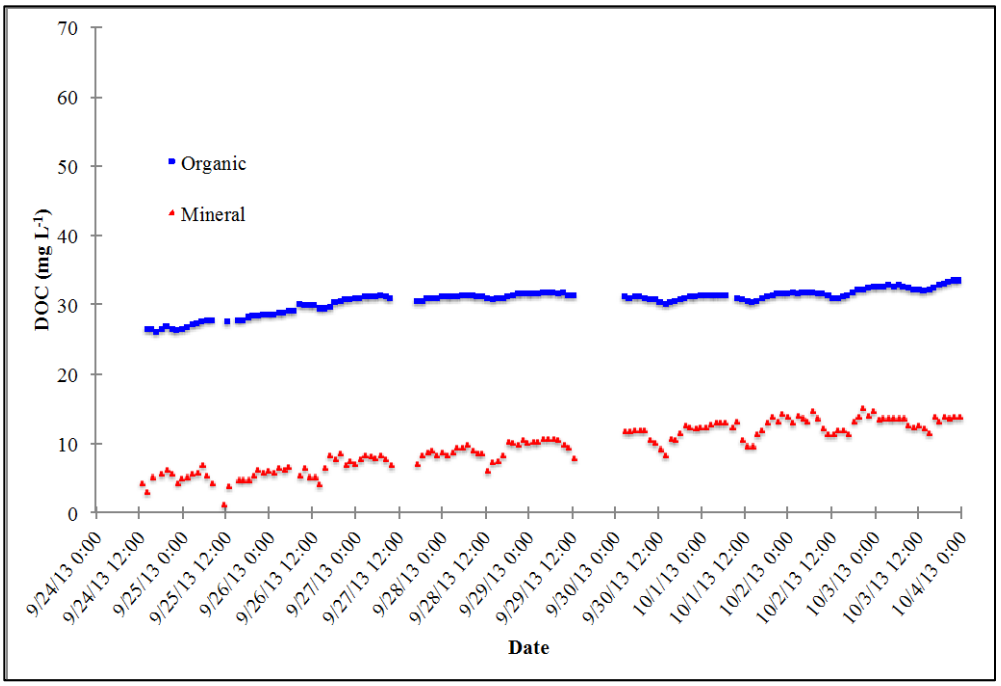

Figure A4.17: UV-Vis Spectrometer DOC readings from 1 of 3 mesocosms from each treatment (Organic, Mineral, and Control) during Batch Run 10.

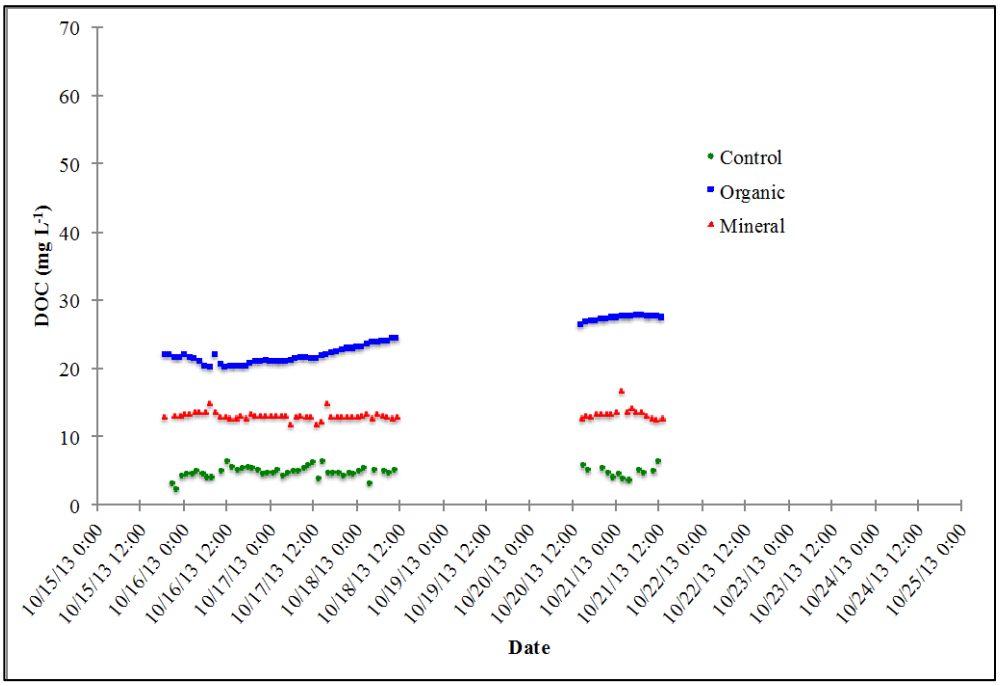

Figure A4.18: UV-Vis Spectrometer DOC readings from 1 of 3 mesocosms from each treatment (Organic, Mineral, and Control) during Batch Run 11.

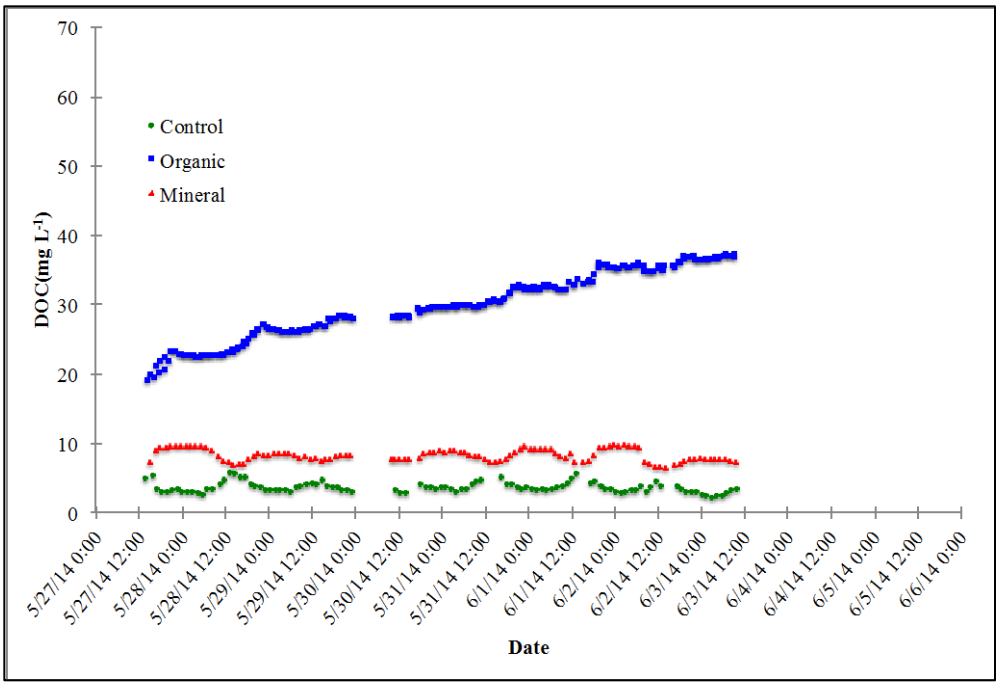

Figure 2I 19: UV-Vis Spectrometer DOC readings from 1 of 3 mesocosms from each treatment (Organic, Mineral, and Control) during Batch Run 14.

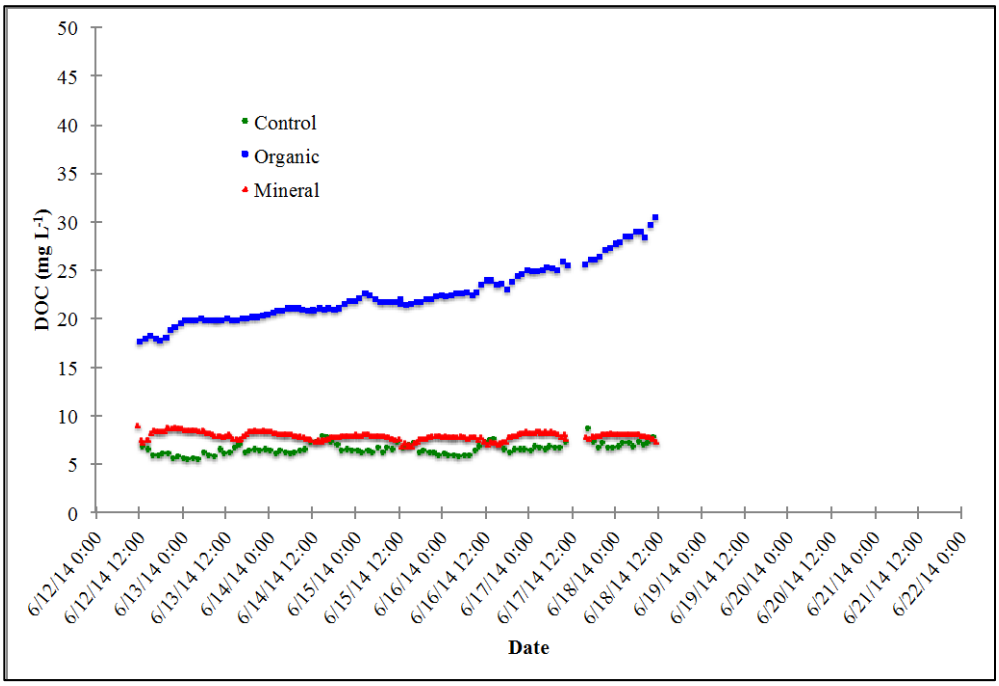

Figure A4.20: UV-Vis Spectrometer DOC readings from 1 of 3 mesocosms from each treatment (Organic, Mineral, and Control) during Batch Run 15.

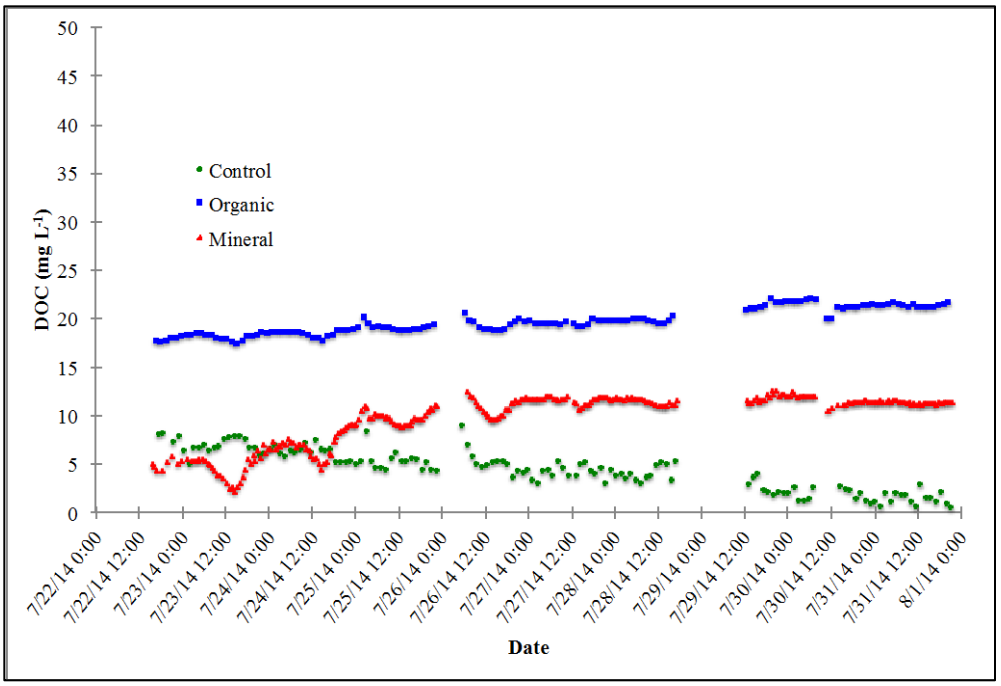

Figure A4.21: UV-Vis Spectrometer DOC readings from 1 of 3 mesocosms from each treatment (Organic, Mineral, and Control) during Batch Run 16.

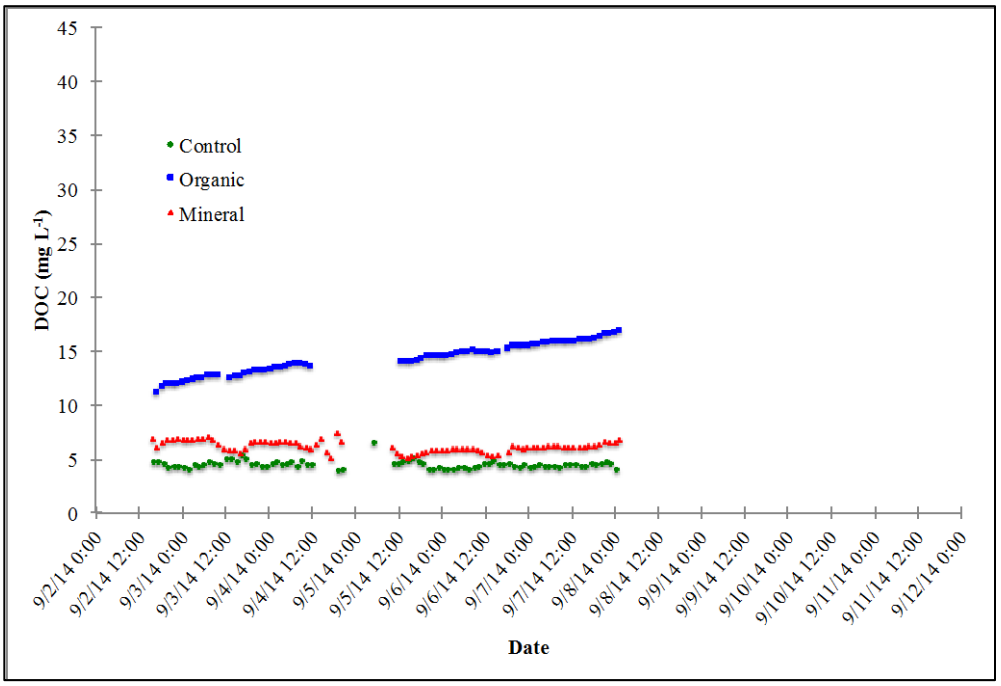

Figure A4.22: UV-Vis Spectrometer DOC readings from 1 of 3 mesocosms from each treatment (Organic, Mineral, and Control) during Batch Run 18.

Appendix 5 – Aeration coefficient results

a.

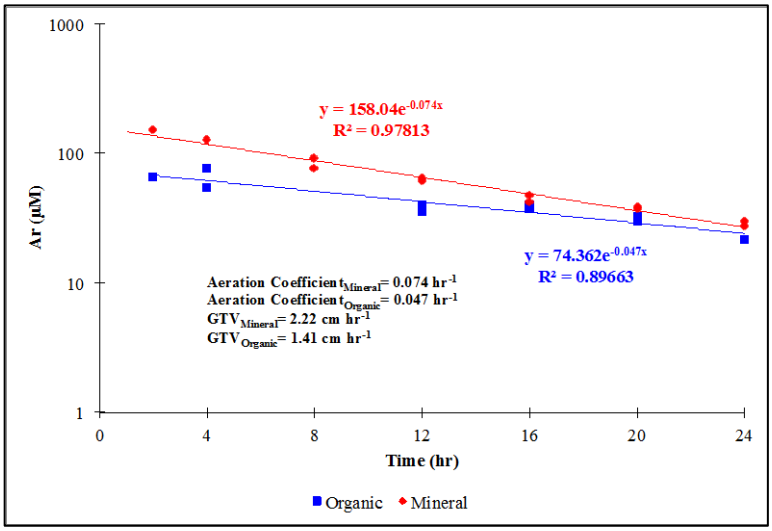

b.

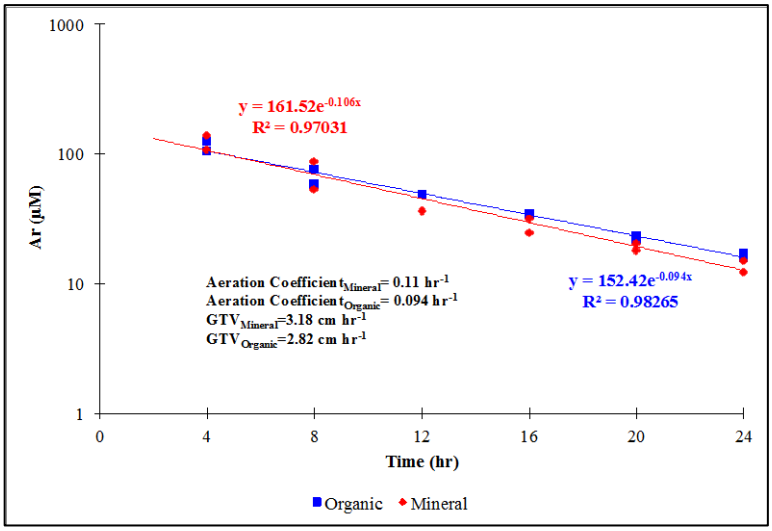

Figure A5. 1: Ar gas transfer velocities (GTV) and aeration coefficient fits for the a. low NO_3-N and b. high NO_3-N loading ^{15}N enrichment experiments. Points indicate argon concentrations adjusted for evapotranspiration with Br^- observed during the experiments as values approached equilibrium with air. The GTVs for Ar were determined by multiplying the Ar aeration coefficients by the water depth in the mesocosms (30 cm).

6. References

Adame, M.F., V. Hermoso, K. Pehans, C.E. Lovelock, and J.A. Herrer-Silveria. 2015. Selecting cost-effective areas for restoration of ecosystem services. Conserv. Biol., 29(2): 495-502.

Ahn, C. and M. J. Mitsch. 2002. Scaling considerations of mesocosm wetlands in simulating large created freshwater marshes. Eco. Eng., 18:327–42.

Ardón, M., J. L. Morse, M.W. Doyle, and E.S. Bernhardt. 2010. The water quality consequences of restoring wetland hydrology to a large agricultural watershed in the southeastern coastal plain. Ecosystems, 13: 1060-1078.

Arheimer, B. and H.B. Wittgren. 2002. Modelling Nitrogen Retention in Potential Wetlands at the Catchment Scale. Eco. Eng., 19(1):63-80.

Aumen, N. (Stream Solute Workshop). 1990. Concepts and methods for assessing solute dynamics in stream ecosystems. J.N. Am. Benthol. Soc., 9:95–119

Bachand, P.A.M. and A.J. Horne. 2000. Denitrification in constructed free-water surface wetlands: I. Very high nitrate removal rates in macrocosm study. Eco. Eng., 14:9-15.

Bardgett, R.D., T.C. Streeter, and R. Bol. 2003. Soil microbes compete effectively with plants for organic-nitrogen inputs to temperate grasslands. Ecology, 84: 1277-1287.

Bekins, B.A., E. Warren, and E.M. Godsy. 1998. A comparison of zero-order, first order, and Monod biotransformation models. Groundwater, 36(20): 261- 268.

Bennett, J.P., and R.E. Rathbun. 1972. Reaeration in open-channel flow: U.S. Geological Survey Professional Paper, 737:75.

Beutel, M.W., C.D. Newton, E.S. Brouillard, and R.J. Watts. 2009. Nitrate removal in surface-flow constructed wetlands treating dilute agricultural runoff in the lower Yakima Basin, Washington. Ecol. Eng., 25: 1538-1546.

Bírgand, F. Quantification and modeling of in-stream processes in agricultural canals of the lower coastal plain, Doctoral thesis, Biological and Agricultural Engineering, North Carolina State University, Raleigh, 2000.

Bírgand, F., R. W. Skaggs, G.M. Chescheir, and J. W. Gilliam. 2007. Nitrogen removal in streams of agricultural catchments – A literature review. Crit. Rev. Env. Sci. Tec., 37(5): 381-487.

Bírgand, F.C., Faucheux, G. Gruau, B. Augeard, F. Moatar and P. Bordenave. 2010. Uncertainties in assessing annual nitrate loads and concentration indicators: Part 1. Impact of sampling frequency and load estimation algorithms. Trans. ASABE, 53(2): 437-446.

Böhkle, J.K., J.W. Harvey, and M.A. Voytek. 2004. Reach-scale isotope tracer experiment to quantify denitrification and related processes in nitrate-rich stream, Midcontinent United States. Amer. Soc. Limnol. Oceanogr., 49(3): 821-838.

Böhlke, J.K., R.C. Antweiler, J.W. Harvey, A.E. Laursen, L.K. Smith, R.L. Smith, and M.A. Voytek. 2009. Multi-scale measurements and modeling of denitrification in streams with varying flow and nitrate concentration in the upper Mississippi River Basin, USA. Biogeochemistry, 93:117-141.

Bollag, J.M. and G. Stotzky, Ed. 2000. Soil Biochem., Vol 10. New York: Marcel Dekker, Inc.

Bowie, G.L., Mills, W.B., Porcella, D.B., et al., 1985. Rates, Constants, and Kinetics Formulations in Surface Water Quality Modeling, 2nd edn. US Environmental Protection Agency, Athens, GA EPA: 600:3-85:040.

Broome, S.W. 1990. Creation and restoration of tidal wetlands of the southeastern United States. Pages 27-72. in. J.A. Kusler and M.A. Kentula, editors. Wetland creation and restoration. Island Press, Washington, D.C., USA.

Bruland, G.L., C.J. Richardson, and S.C. Whalen. 2006. Spatial variability of denitrification potential and related soil properties in created, restored, and paired natural wetland. Wetlands, 26(4): 1042-1056.

Burchell, M.R., R.W. Skaggs, C.R. Lee, S. Broome, G.M. Chescheir, and J. Osborne. 2007. Substrate organic matter to improve nitrate removal in surface flow constructed wetlands. J. Environ. Qual., 36(1):194-207.

Bushaw, K. L., R. G. Zepp, M. A. Tarr, D. Schultz-Jander, R. A. Bourbonniere, R. E. Hodson, W. L. Miller, D. A. Bronk, and M. A. Moran. 1996. Photochemical release of biologically available nitrogen from aquatic dis- solved organic matter. Nature, 381:404–407.

Caffrey, J.M. and W. M. Kemp. 1992. Influence of the submersed plant, Potamogeton perfoliatus, on nitrogen cycling in estuarine sediments. Limnology and Oceanography, 1992. 37(7): 1483-1495.

Caldwell, P.V., M. J. Vepraskas, R.W. Skaggs, and J.D. Gregory. 2007. Simulating the water budgets of natural Carolina Bay wetlands. Wetlands, 27(4): 112-1123.

Carnicer, J., J. Sardans, C. steganescu, A. Ubach, M. Bartrons, D. Asensio, and J. Penuelas. 2015. Global biodiversity, stoichemetry, and ecosystem function responses to human-induced C-N-P imbalances. J. Plant Physiol.,172:82-91.

Cey, E.E., D.L. Rudolph, R. Aravena, and G. Parkin. 1999. Role of the riparian zone in controlling the distribution and fate of agricultural nitrogen near a small stream in southern Ontario. J. Contam. Hydrol., 37: 45-67.

Chanton, J.P., C.S. Martens, and C.A. Kelley. 1989. Gas transport from methane-saturated, tidal freshwater and wetland sediment. Limnol. Oceanogr. 34(5): 807-819.

Chapman, M. G. and Underwood, A. J. 2000. The need for a practical scientific protocol to measure successful restoration. Wetlands (Australia), 19: 28-48.

Chescheir, G.M., J.W. Gilliam, R.W. Skaggs, and R.G. Broadhead. 1991. Nutrient and sediment removal in forested wetlands receiving pumped agricultural drainage water. Wetlands, 11(1): 87-103.

Comín, F.A., R. Sorando, N. Darwiche-Criado, M. Garvia, and A. Masip. A protocol to prioritize wetland restoration and creation for water quality improvement in agricultural watersheds. Ecol. Eng., 66:19-18.

Costanza, R., d'Arge, R., de Groot, R., Farber, S., Grasso, M., Hannon, B., Limburg, K., Naeem, S., O'Neill, R. V., Paruelo, J., Raskin, R. G., Sutton, R., and van der Belt, M. 1997. The value of the world's ecosystem services and natural capital. Nature, 387(6630), 253-260.

Crumpton, W.G. and R. Phipps. 1992. Fate of nitrogen loads in experimental wetlands. In: The Des Plaines River Wetlands Demonstration Project. Wetlands Research, Inc., Chicago, IL.

Dahl, T.E. and G.J. Allord. 1996.Technical Aspects of Wetlands: History of wetlands in the conterminous United States. In: National Water Summary of Wetland Resources Paper 2425, Reston, VA: USGS.

De Groot, R., 2006. Function-analysis and valuation as a tool to assess land use conflicts in planning for sustainable, multifunctional landscapes. Landscape Urban Plan. 75, 175-186.

DeBusk, W.F. and K.R. Reddy. 1987. Removal of floodwater nitrogen in cypress swamp receiving primary wastewater effluent. Hydrobiologia, 153: 79-86.

Dobson, A.P., A.D. Bradshaw, and A.J.M. Baker. 1997. Hopes for the future: Restoration ecology and conservation biology. Science, 277(5325): 515-522.

Dzakpasu, M., O. Hofmann, M. Scholz, R. Harrington, S.N. Jordan, and V. McCarthy. 2011. Nitrogen removal in an integrated constructed wetland treating domestic wastewater. J. Environ. Sci. Heal. A., 46: 742-750.

Engles C. and H. Marschner. 1995. Plant uptake and utilization of nitrogen. In: Bacon PE, ed. Nitrogen fertilization in the environment. New York: Marcel Dekker Inc., 41-81.

Etheridge, J.R., R. Birgand, J.A. Osborne, C.L. Osburn, M.R. Burchell, and J. Irving. 2014. Using in situ ultraviolet-visual spectroscopy to measure nitrogen, carbon, phosphorus, and suspended solids concentrations at a high frequency in a brackish tidal marsh. Limnol. Oceanogr.- Meth., 12: 10-22.

Evans, E. 2003. Action Mode, Deficiency and Toxicity Symptoms of the 17 Essential Nutrients. NCSU Consumer Horticulture. Available at: http://www.ces.ncsu.edu/depts/hort/consumer/quickref/fertilizer/nutri_def.html. Assessed Jan. 9, 2013.

Ewing, J.W., M. J. Vepraskas, S.W. Broome, and J.G. White. 2012. Changes in wetland soil morphological and chemical properties after 15, 20, and 30 years of agricultural production. Geoderma, 179-180: 73-80.

Fleishman, E., D.E. Blockstein, J.A Hall, M.B. Mascia, M.A. Rudd, J.M. Scott, W.J. Sutherland, A.M. Bartuska, A.G. Brown, C.A. Christen, J.R. Clement, D. Dellasala, C.S. Duke, M. Eaton, S.J. Fiske, H. Gosnell, J.C. Haney, M. Hutchins, M.L. Klein, J. Marqusee, B.R. Noon, J.R. Nordgren, P.M. Orbuch, J. Powell, S.P. Quarles, K.A. Saterson, C.C. Savitt, B.A. Stein, M.S. Webster, and A. Vedder. 2011. Top 40 priorities in science to inform US conservation and management policy. BioScience, 61(4): 290-300.

Gebremariam, S.Y. and M.W. Beutel. 2008. Nitrate removal and DO levels in batch wetland mesocosms: Cattail (Typha spp.) versus bulrush (Scirpus spp.). Eco. Eng., 34: 1-6.

Hardison, A., C. Tobias, J. Stanhope, E. Canuel, and Iris Anderson. 2011. An experimental approach for laboratory and field-based perfusion of sediment porewater with dissolved tracers. Estuaries and Coasts, 34: 243-255.

Harrison, K.A., R. Bol, and R.D. Bardgett, R.D. 2007. Preferences for different nitrogen forms by coexisting plant species and soil microbes. Ecology, 88: 989-999.

Harrison, K.A., R. Bol, and R.D. Bardgett, R.D. 2008. Do plant species with different growth strategies vary in their ability to compete with soil microbes for chemical forms of nitrogen? Soil Biol. Biochem., 40: 228-237.

Harrison, M.D., P.M. Groffman, P.M. Mayer and S.S. Kaushal. 2012. Nitrate removal in two relict oxbow urban wetlands: a 15N mass-balance approach. Biogeochemistry, 111:647-660.

Hefting, M. M., J. Clement, P. Bienkowski, D. Dowrick, C. Guenat, A. Butturini, S. Topa, G.Pinay and J. T. A. Verhoeven. 2005. The role of vegetation and litter in the nitrogen dynamics of riparian buffer zones in Europe. Ecol. Eng., 24(5): 465-482.

Hesslein, R. H. 1976. Sediment pore water sampler. Limnol. Oceanogr. 21: 912-914.

Hodge, A., D. Robinson, and A. Fitter. 2000. Are microorganisms more effective than plants at competing for nitrogen? Trends Plant Sci., 5: 304-308.

Hong, Bongghi, D.P. Swaney, and R.W. Howarth. 2013. Estimating net anthropogenic nitrogen inputs to U.S. watersheds: Comparison of methodologies. Environ. Sci. Tech., 47: 5199-5207.

Horne, A.J. 1995. Nitrogen removal from waste treatment pond or activated sludge plan effluents with free-surface wetlands. Water Sci. Tech., 31(12):341-351.

Huang, L., X. Gao, J. Guo, X. Ma, and M. Liu. 2013. A review on the mechanism and affecting factors of nitrous oxide emission in constructed wetlands. Environmental Earth Sciences, 68:2171-2180.

Hunt, P.G., J.O. Miller, T.F. Ducey, M.W. Lang, A.A. Szogi, and G. McCarty. 2014. Denitrification in soils of hydrologically restored wetlands relative to natural and converted wetlands in the mid-Atlantic coastal plain of the USA. Ecol. Eng, 71:438-447.

Hunter, R.G., D.L. Combs, D.L., and D.B. George. 2000. Growth of softstem bulrush (Scirpus validus) in microcosms with different hydrologic regimes and media depths. Wetlands, 20: 15–22.

Hunter, R.G. and S.P. Faulkner. 2001. Denitrification potentials in restored and natural bottomland hardwood wetlands. Soil Sci. Soc. Am. J., 65:1865-1872.

Ishida, C.K. , J.J Kelly, and K.A. Gray. 2006. Effects of variable hydroperiods and water level fluctuations on denitrification capacity, nitrate removal, and benthic-microbial community structure in constructed wetlands. Ecol. Eng., 28: 363-373.

Jackson, L.E., J.P. Schimel, and M.K. Firestone. 1989. Short-term partitioning of ammonium and nitrate between plants and microbes in an annual grassland. Soil Biol. Biochem., 21: 409-415.

Janssen, P.H.M. and P.S.C. Heuberger. 1995. Calibration of process-oriented models. Ecol. Model., 83:55-66.

Jarzemsky, R., M.R. Burchell, and R.O. Evans. 2013. The impact of manipulating surface topography on the hydrologic restoration of a forested coastal wetland. Eco. Eng., 58: 35-43.

Jollymore, A., M.S. Johnson, and I. Hawthorne. 2012. Submersible UV-Vis spectroscopy for quantifying streamwater organic carbon dynamics: Implementation and challenges before and after forest harvest in a headwater stream. Sensors, 12:3798-3813.

Jørgenson, C.J. and B. Elberling. 2012. Effects of flooding-induced N2O production, consumption and emission dynamics on the annual N2O emission budget in wetland soils. Soil of Biology and Biochemistry, 53:9-17.

Kadlec, R.H. 2010. Nitrate dynamics in event-driven wetlands. Ecol. Eng., 36:503-516.

Kadlec, R.H. 2000. The inadequacy of first-order treatment wetland model. Ecol. Eng.,15: 105-119.

Kadlec, R.H., C.C. Tanner, V.M. Hally, and M.M. Gibbs. 2005. Nitrogen spiraling in subsurface-flow constructed wetlands: Implications for treatment response. Ecol. Eng., 25: 365-381.

Kadlec, R. H. and S.D. Wallace. 2009. Treatment Wetlands, 2nd ed. CRC Press, Boca Raton, FL, USA. 182, 395, 472 p.

Kangas, P. and W. Aday. 1996. Mesocosms and ecological engineering. Ecol. Eng., 6:1-5.

Karpuzcu, M.E., and W.T. Stringfellow. 2012. Kinetics of nitrate removal in wetlands receiving agricultural drainage water. Eco. Eng., 42: 295-303.

Kaštovská , E. and H. Šantrůčková. 2011. Comparison of uptake of different N forms by soil microorganisms and two wet-grassland plants: A pot study. Soil Biol. Biochem. 43: 1285-1291.

Knies, S.V., 2009. Riparian Buffer Effectiveness at Removal of NO3-N from Groundwater in the Middle Coastal Plain of North Carolina. M.S. Thesis, North Carolina State University, Raleigh, NC.

Knowles, R. 1982. Denitrification. MicroBiology Reviews, 46(1): 43-70.

Koop-Jacobson, K. and A.E. Giblin. 2009. New approach for measuring denitrification in the rhizosphere of vegetated marsh sediments. Limnology and Oceanography: Methods, 7: 626-637.

Korom, S.F. 1992. Natural denitrification in saturated zone: A review. Water Resources Research, 28(6): 1657-1668.

Kumar, J.L.G. and Y.Q. Zhao. 2011. A review of numerous modeling approaches for effective, economical and ecological treatment wetlands. J. Environ. Manage., 92: 400-406.

Lee, C., T. Fletcher, and G. Sun. 2009. Nitrogen removal in constructed wetland systems. Eng. Life Sci., 9(1): 11-22

Li, Y.H., H.B. Li, T.H Sun, and X. Wang. 2011. Effects of hydraulic loading rate on pollutants removal by a deep subsurface wastewater infiltration system. Eco. Eng., 37:1425-1429.

Lineweaver, H. and D. Burk. 1934. The Determination of Enzyme Dissociation Constants. J. Am. Chem. Soc., 56 (3): 658–666.

Lipson, D. and T. Näsholm. 2001. The unexpected versatility of plants: organic nitrogen use and availability in terrestrial ecosystems. Oceologia ,128: 305-316.

Liu, G., Wilson, J., Qi, J., Ying, J. 2007. Green neighborhoods, food retail and childhood overweight: differences by population density. American Journal of Health Promotion, 21(4 Supplement): 317-325.

Liu, W.J., Y.Z. Su, R. Yang, X.F. Wang, and X. Yang. 2010. Land use effects on soil organic carbon, nitrogen, and salinity in saline-alkaline wetland. Scienc. Cold Arid Regions, 2(3): 263-270.

Lowrance, R. and D. Smittle. 1988. Nitrogen Cycling in a Multiple-Crop Vegetable Production System. Journal of Environmental Quality. 17(1): 158-162.

Matson, P.A., W.J. Parton, A.G. Power, and M.J. Swift. 1997. Agricultural Intensification and Ecosystem Properties. Science, 277:504-509.

Messer, J.J. and P.L. Brezonik. 1984. Laboratory evaluation of kinetic parameters for lake sediment denitrification models. Ecol. Model., 21:277-286.

Messer, T.L. 2015. Predicting Impacts of Rerouting Drainage Water from the Pamlico Sound to Restored Wetlands: A Hydraulic and Water Quality Assessment. Ph.D. Dissertation. N.C. State University, Raleigh, N.C. http://www.lib.ncsu.edu/resolver/1840.16/10634

Min, K., H. Kang, and D. Lee. 2011. Effects of ammonium and nitrate additions on carbon mineralization in wetland soils. Soil Biol. Biochem., 43: 2461-2469.

Mitsch W.J., and J.G. Gosselink. 2007. Wetlands, 4th edn. John Wiley & Sons, New York. 354 p.

Mitsch, W.J., J.W. Day, Jr. , L. Zhang, and R.R. Lane. 2005. Nitrate-nitrogen retention by wetlands in the Mississippi River Basin. Ecol. Eng., 24: 267–278.

Moore, T.L.C. and W.F. Hunt. 2012. Ecosystem service provision by stormwater wetlands and ponds – A means for evaluation? Water Res., 46(20): 6811-6823.

Mulholland, P.J., H. M. Valett, J.R. Webster, S.A. Thomas, S.K. Hamilton, and B.J. Peterson. 2004. Stream denitrification and total nitrate uptake rates measured using a field 15N tracer approach. Limnol. Oceanogr, 49(3): 809-830.

Mustafa, A. and M. Scholz. 2011. Characterization of microbial communities transforming and removing nitrogen in wetlands. Wetlands, 31:583-592.

Naz, M., S. Uyanik, M.I. Yesilnacar, and E. Sahinkaya. 2009. Side-by-side comparison of horizontal subsurface flow and free water surface flow constructed wetlands and artificial neural network (ANN) modeling approach. Ecol. Eng., 35:1255-1263.

NCDA&CS. North Carolina Agricultural Overview. Raleigh, 2013.

Nishio, T., I. Koike and A. Hattori. 1983. Estimates of Denitrification and Nitrification in Coastal and Estuarine Sediments. Applied and Environmental Microbiology, 45(2): 444-450.

O'Brien, J.M., W.K. Dodds, K.C. Wilson, J.N. Murdock, and J. Eichmiller. 2007. The saturation of N cycling in Central Plains streams: 15N experiments across a broad gradient of nitrate concentrations. Biogeochemistry, 84:31-49.

Obenhuber, D.C. and R. Lowrance. 1991. Reduction of Nitrate in Aquifer Microcosms by Carbon Additions. Journal of Environmental Quality. 20(1): 255-258.

Ottosen, L., N. Risgaard-Petersen and L. Nielsen. 1999. Direct and indirect measurements of nitrification and denitrification in the rhizosphere of aquatic macrophytes. Aquatic Microbial Ecology, 19(1): 81-91.

Patrick, Wm.H, Jr. 1960. Nitrate Reduction in a Submerged Soil as Affected by Redox Potential. Trans. Seventh International Congressional Soil Science II. 494-500.

Penton, C.R. J.L. Deenik, B.N. Popp, G.L. Bruland, P. Engstrom, D. St. Louis, and J. Tiedje. 2013. Importance of sub-surface rhizosphere-mediated coupled nitrification-denitrification in a flooded agroecosystem in Hawaii. Soil Bio. Biochem., 57:362-373.

Peterson, B.J., M. Bahr, and G.W. King. 1997. A tracer investigation of nitrogen cycling in a pristine tundra river. Canadian Journal of Fisheries ad Aquatic Science, 54: 2361-2367.

Petru, B.J., G.M. Chescheir, and C. Ahn. 2014. Assessment of water budgets and the hydrologic performance created mitigation wetland – A modeling approach. Ecol. Eng., 71: 667-676.

Petrucio, M.M. and F.A. Esteves. 2000. Uptake rates of nitrogen and phosphorus in the water by Eichhornia crassipes and Salvinai auriculata. Rev. Brasil. Biol., 60(2): 229-236.

Puckett, L.J. 2004. Hydrogeologic controls on the transport and fate of nitrate in groundwater beneath riparian buffer zones: results from thirteen studies across the United States. Water Sci. and Technol., 49(3): 47-53.

Reddy, K. R., W. H., Jr. Patrick, and R.E. Phillips. 1978. The role of nitrate diffusion in determining the order and rate of denitrification in flooded soil. I. Experimental results. Soil Sci. Soc. Am. J., 42: 268-272.

Reddy, K.R., W.H. Patrick, Jr., and C.W. Lindau. 1989. Nitrification-denitrification at the plant root-sediment interface in wetlands. Limnol. Oceanogr., 34(6):1004-1013.

Reddy, K.R. and R.D. DeLaune. 2008. Biogeochemistry of Wetlands: Science and Applications. CRC Press, Baco Raton, FL. 320, 525 p.

Redfield AC. The biological control of chemical factors in the environment. Amer. Scientist. 1958; 46:205– 22.

Reed, S.C. and Brown D. 1995. Subsurface flow wetlands—a performance evaluation. Water Environ. Res., 67(2): 244–8.

Ribaudo, Marc, Jorge Delgado, LeRoy Hansen, Michael Livingston, Roberto Mosheim, and James Williamson. Nitrogen In Agricultural Systems: Implications For Conservation Policy. ERR-127. U.S. Dept. of Agriculture, Econ. Res. Serv. September 2011.

Richardson, J.L. and M.J. Vepraskas. 2001. Wetland Soils. Boca Raton, FL.: CRC Press LLC.

Rivett, M.O., S.R. Buss, P. Morgan, J.W. Smith, and C.D. Bemment. 2008. Nitrate attenuation in groundwater: A review of biogeochemical controlling process. Water Res., 42(16): 4215-4232.

Rudd, M.A. and E. Fleishman. 2014. Policymakers' and scientists' ranks of research priorities for resource-management policy. Bioscience, 64(3):219-228.

Rust, C.M., C.M. Aelion, and J.R.V. Flora. 2000. Control of pH during denitrification in subsurface sediment microcosms using encapsulated phosphate buffer. Water Res., 34:1447-1454.

Rysgaard, S., P.B. Christensen, and L.P. Nielsen. 1995. Seasonal variation in nitrification and denitrification in estuarine sediment colonized by benthic microalgae and bioturbating infauna. Mar. Ecol.-Prog. Ser., 126:111-121.

Saeed, T. and G. Sun. 2011. Kinetic modeling of nitrogen and organics removal in vertical and horizontal flow wetlands. Water Res., 45:3137-3152.

Saeed, T. and G. Sun. 2012. A review on nitrogen and organics removal mechanisms in subsurface flow constructed wetlands: Dependency on environmental parameters, operating conditions, and supporting media. J. Environ. Manage., 112: 429-448.

Seitzinger, S.P., S.W. Nielssen, J. Caffrey, and P.B. Christensen. 1993. Denitrification measurements in aquatic sediments: A comparison of three methods. Biogeochemistry, 23:147-167.

Sloan, A .J., J. W. Gilliam, J. E. Parsons, R. L. Mikkelsen, and R. C. Riley. 1999. Groundwater nitrate depletion in a swine lagoon effluent-irrigated pasture and adjacent riparian zone. Journal of Soil & Water Conservation. 54(4): 651-656.

Smith, L.K., M.A. Voytek, J.K. Böhlke, and J.W. Harvey. 2006. Denitrification in nitrate-rich streams: Application of N2: Ar and 15N-tracer methods in intact cores. Ecol. Appl., 16(6): 2191-2207.

Sparks, E.L., J. Cebrian, C.R. Tobias, and C.A. May. 2015. Groundwater nitrogen processing in North Gulf of Mexico restored marshes. J. Env. Manag., 150: 206-215.

Spruill, T.B., Eimers, J.L., Morey, A.E., 1997. Nitrate-Nitrogen Concentrations in Shallow Ground water of the Coastal Plain of the Albemarle-Pamlico Drainage Study Unit, North Carolina and Virginia. USGS-FS-241-96, Raleigh, NC.

Stringfellow, W.T., M.E. Karpuzcu, C.Speir, J.S. Hanlon, and J. Graham. 2013. Sizing mitigation wetlands in agricultural watersheds. Water Sci. Tech., 67(1): 40- 46.

Suding, K.N., 2011. Toward an era of restoration in ecology: successes, failures and opportunities ahead. Annu. Rev. Ecol. Evol. Syst. 42, 465–487.

Svengsouk, L.M. and W.J. Mitsch. 2001. Dynamics of mixtures of Typha latifolia and Schoenoplectus tabernamontani in nutrient-enrichment wetland experiments. Am. Midl. Nat., 145: 309-324.

Sylvia, D.M., J.J. Fuhrmann, P.G. Hortel, and D.A. Zuberer. 1998. Principles and Applications of Soil Microbiology. Prentice-Hall, Inc. Upper Saddle River. NJ. 550 p.

Tanner, C.C. 2001. Plants as ecosystem engineers in subsurface flow treatment wetlands. Water Sci. Tech., 44(11): 9-17.

Taro, I. and J. Csiszár. 2003. Effects of NO-2 and NO-3 supply on polyamine accumulation and ethylene production of wheat roots at acidic and neutral pH: implications for root growth. Plant Growth Regul., 40: 121-128.

Templer, P.H., M.C. Mack, F.S. Chapin, L.M. Christenson, J.E. Compton, H.D. Crook, W.S. Currie, C.J. Curtis, D.B. Dail, and C.M. D'Antonio CM et al.. 2012. Sinks for nitrogen inputs in terrestrial ecosystems: a meta-analysis of 15N tracer field studies. Ecology, 93: 1816–1829.

Teskey, R.O. and T.M. Hinckley. 1977. Impact of Water Level Changes on Woody Riparian and Wetland Communities. Volume 2: Southern Forest Region. U.S. Fish and Wildlife Service, Biological Services Program, Washington, DC (FWS/OBS-77/59).

Tobias, C.R., S.A. Macko, I.C. Anderson, E.A. Canuel, and J.W. Harvey. 2001. Tracking a fate of a high concentration groundwater nitrate plume through a fringing marsh: A combined groundwater tracer and in situ isotope enrichment study. Limnology and Oceanography, 46(8): 1977-1989.

Tobias, C.R., J.K. Böhlke, J.W. Harvey, and E. Busenber. 2009. A simple technique for continuous measurement of time-variable gas transfer in surface waters. Limnology and Oceanography: Methods, 7: 185-195.

Tobias, C.R. Personal Communication. 17 April 2014

Trevors, J.T., 1985. The influence of oxygen concentrations on denitrification in soil. Appl. Microbiol. Biotech., 23: 152-155.

Trulan, T., F. Birgand, and P. Marmonier. 2007. Comparative use of field and laboratory mesocosms for in-stream nitrate uptake measurement. Ann. Limnol. – Int. J. Lim., 43(1): 51-51.

Tweedy, K. L., E. Scherrer, R. O. Evans, and T. H. Shear. 2001. Influence of microtopography on restored hydrology and other wetland functions (Meeting Paper No. 01-2061) in 2001. American Society of Agricultural Engineers Annual International Meeting. ASAE, St. Joseph, Michigan.

US EPA. 2007. National estuary program Costal Condition Report – NEP CCR Factsheet: Chapt. 4. Virginia Engle EPA Office of Research and Development. Report EPA-842-B-06-001.

U.S. EPA. Nonpoint source pollution: The nation's largest water quality problem. Available at: http://www.epa.gov/nps/facts/point1.htm. Assessed Jan. 12. 2010.

US EPA. Nutrient Policy and Data: Commercial Fertilizer Purchased. Washington: Government Printing Office, 2012.

Vähätalo, A.V. and R.G. Wetzel. 2008. Long-term photochemical and microbial decomposition of wetland-derived dissolved organic matter with alteration of 13C: 12C mass ratio. Limnol. Oceanogr., 53(4): 1387:1392.

Van Cleemput, O., W.H Patrick Jr., and R.C. McClhenny. 1975. Formation of chemical and biological denitrification products in flooded soil at controlled pH and redox potential. Soil Biol. Biochem., 7:329-332.

Van Hale, C.E., D. Barth, and V.A. Stenger. 1965. Elimination of carbonates from aqueous solutions prior to organic carbon determination. Anal. Chem., 37:769-771.

Vitousek, P.M., J.D. Aber, R.W. Howarth, G.E. Likens, P.A. Matson, D.W. Schindler, W.H. Schlesinger, and D.G. Tilman. 1997. Human Alteration of the Global Nitrogen Cycle: Sources and Consequences. Ecol. Appl., 73(3):737-750.

Wafer, C.C., J.B. Richards, and D.L. Osmond. 2004. Construction of platinum-tipped redox probes for determining soil redox potential. J. Environ. Qual., 33(6):2375-2379.

Walbridge, M.R. and B.G. Lockaby. 1994. Effects of forest management on biogeochemical functions in southern forested wetland. Wetlands, 14:10-17.

Wallace, K. 2007. Classification of ecosystem services: Problems and solutions. Biological Conservation, 139(3-4): 235-246.

Wang, W., M.A. Tarr, T.S. Bianchi, and E. Engelhaupt. 2000. Ammonium photoproduction from aquatic humic and colloidal matter. Aquat. Geochem., 6: 275-292.

Wanninkhof, R. 1992. Relationship between wind speed and gas exchange over the ocean. J. Geophys. Res. 97: 7373–7382.

Warneke, S., L.A. Schipper, M.G. Matiasek, K.M. Scow, S. Cameron, D.A. Bruesewitz, and I.R. McDonald. 2011. Nitrate removal, communities of denitrifiers, and adverse effects in different carbon substrates for use in denitrification beds. Water Res., 45: 5463-5475.

Welsh, D., M. Bartoli, D. Nizzoli, G. Castaldelli, S. Riou and P. Viaroli. 2000. Denitrification, nitrogen fixation, community primary productivity and inorganic-N and oxygen fluxes in an intertidal Zostera noltii meadow. Marine Ecology-Progress Series 20865-77.

Wollheim, W.M., T.K. Harms, B.J. Peterson, K. Morkeski, C.S. Hopkinson, R.J. Stewart, Gooseff, M.N. and M.A. Briggs. 2014. Nitrate uptake dynamics of surface transient storage in stream channels and fluvial wetlands. Biogeochemistry, 120:239-257.

Woltermade C.J. 2000. Ability of Restored Wetlands to Reduce Nitrogen and Phosphorus Concentrations in Agricultural Drainage Water. J. Soil Water Conserv., 55(3): 303-308.

Young, R. G. and A. D. Huryn. 1999. Effects of land use on stream metabolism and organic matter turnover. Ecol. Appl. 9: 1359-1376.

Youssef, M.A., R.W. Skaggs, G.M. Chescheir, and J.W. Gilliam. 2006. Field evaluation of a model for predicting nitrogen losses from drained lands. J. Environ. Qual., 35(6): 2026-2042.

Zedler, J. B. 2003. Wetlands at your service: reducing impacts of agriculture at the watershed scale. Front. Eco. Environ., 1(2)65-72.

Zepp, T V. ,C.A.L. Aghan, AND D. J. Erickson. 1995. Effects of increased solar ultraviolet radiation on biogeochemical cycles. Ambio, 24: 181-187.